INFORMATION TO USERS

This manuscript has been reproduced from the microfilm master. UMI films the text directly from the original or copy submitted. Thus, some thesis and dissertation copies are in typewriter face, while others may be from any type of computer printer.

The quality of this reproduction is dependent upon the quality of the copy submitted. Broken or indistinct print, colored or poor quality illustrations and photographs, print bleedthrough, substandard margins, and improper alignment can adversely affect reproduction.

In the unlikely event that the author did not send UMI a complete manuscript and there are missing pages, these will be noted. Also, if unauthorized copyright material had to be removed, a note will indicate the deletion.

Oversize materials (e.g., maps, drawings, charts) are reproduced by sectioning the original, beginning at the upper left-hand corner and continuing from left to right in equal sections with small overlaps.

Photographs included in the original manuscript have been reproduced xerographically in this copy. Higher quality 6" x 9" black and white photographic prints are available for any photographs or illustrations appearing in this copy for an additional charge. Contact UMI directly to order.

UMI®

University of Alberta

Two Landslides and their Dams, Peace River Lowlands, Alberta

by

Brendan G. N. Miller ©

A thesis submitted to the Faculty of Graduate Studies and Research in partial fulfillment of the requirements for a degree of Master of Science.

Department of Earth and Atmospheric Sciences

Edmonton, Alberta

Fall 2000

The author has granted a non-exclusive licence allowing the National Library of Canada to reproduce, loan, distribute or sell copies of this thesis in microform, paper or electronic formats.

The author retains ownership of the copyright in this thesis. Neither the thesis nor substantial extracts from it may be printed or otherwise reproduced without the author's permission.

L'auteur a accordé une licence non exclusive permettant à la Bibliothèque nationale du Canada de reproduire, prêter, distribuer ou vendre des copies de cette thèse sous la forme de microfiche/film, de reproduction sur papier ou sur format électronique.

L'auteur conserve la propriété du droit d'auteur qui protège cette thèse. Ni la thèse ni des extraits substantiels de celle-ci ne doivent être imprimés ou autrement reproduits sans son autorisation.

0-612-59848-9

Canada

University of Alberta

Library Release Form

Name of Author: Brendan G. N. Miller

Title of Thesis: Two Landslides and their Dams, Peace River Lowlands, Alberta

Degree: Master of Science

Year this Degree Granted: 2000

Permission is hereby granted to the University of Alberta Library to reproduce single copies of this thesis and to lend or sell such copies for private, scholarly, or scientific research purposes only.

The author reserves all other publication and other rights in association with the copyright in the thesis, and except as hereinbefore provided, neither the thesis nor any substantial portion thereof may be printed or otherwise reproduced in any material form whatever without the author's prior written permission.

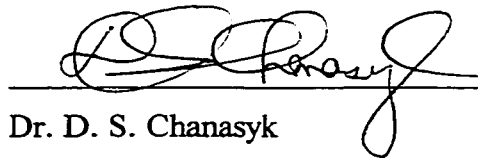August 24, 2000

P.O. Box 29

Lions Bay

British Columbia

University of Alberta

Faculty of Graduate Studies and Research

The undersigned certify that they have read, and recommend to the Faculty of Graduate Studies and Research for acceptance, a thesis entitled Two Landsides and their Dams, Peace River Lowlands, Alberta by Brendan G. N. Miller in partial fulfillment of the requirements for the degree of Master of Science.

Dr. D. M. Cruden

Dr. D. S. Chanasyk

Dr. R. B. Rains

August 20, 2000

Abstract

The 1990 Eureka River landslide was an enlarged earth slide, in preglacial lacustrine sediment, with a volume of approximately 40 Mm^3, and a friction angle of 13.1 to 22.2°. The riverbed was thrust upwards by 20 to 23 m, forming a reservoir 8 km long. The 1995 Spirit River landslide was a reactivated and retrogressive earth slide, in till, with a volume of approximately 20 Mm^3, and a friction angle of 7.9 to 15.9°. A 9 m pressure ridge formed a reservoir 2 km long. Valley gradients increase and channel gradients decrease upstream of both landslides. Precipitation was the likely trigger of the landslides. Increased streamflow due to land clearing was not apparent. Both landslides occurred within preglacial valley sediment; glaciolacustrine sediments overlie and underlie till. Each deposit is prone to slide. Landslides in or below the till form dams. Both landslides broke the streambed armour thus the streambeds are susceptible to erosion.

Acknowledgements

Table of Contents

List of Tables

List of Figures

1.0 Introduction

Slope instability on tributaries of the Peace River, in the Peace River Lowlands of Alberta, has likely been a recurring phenomenon since regional deglaciation (circa 11,000 to 13,500 years before present (Catto et al., 1996)). In the last 60 years, at least six major landslides have occurred, in natural settings (i.e. where no major anthropogenic manipulation of the topography has occurred), within the Peace River Lowlands. These landslides rank by volume as some of the largest recorded in Alberta, and include: the 1995 Spirit River landslide (Section 2), the 1990 Eureka River landslide (Section 3), the 1990 Hines Creek landslide (Lu et al., 1998), the 1939 Montagneuse River landslide (Cruden et al., 1997), the 1990 Saddle River landslide (Cruden et al., 1997; Keegan, 1992), and the Vessall Creek landslide (October 1993 to September 1997) (Figure 1.1). Each of the above landslides obstructed their associated stream and created a reservoir.

Other recent landslides within the Peace River Lowlands include the 1959 Dunvegan Creek landslide (Brooker, 1959; Hardy et al., 1962), the Meikle River landslide (active in 1961) (Nasmith 1964), and the Little Smoky Landslide (Thomson and Hayley, 1975; Hardy et al., 1962). These landslides were likely partially induced by transportation corridor placement and as such, are not being considered. The Vessall Creek landslide is also not being considered due to a lack of detailed information.

This research describes the Spirit River (Section 2) and Eureka River (Section 3) landslides in a manner consistent with Cruden and Varnes (1996), and classifies the landslide dams according to Costa and Schuster (1988). Possible causes for the landslides are also examined, with emphasis on investigating the relationship between agricultural land area and streamflow, following the work of Laycock (1990) (Section 4). The significance of the landslides in the evolution of tributary watershed within the Peace River Lowlands is also examined (Section 5). This thesis is in paper format so there is some duplication of information between Sections 2 and 3.
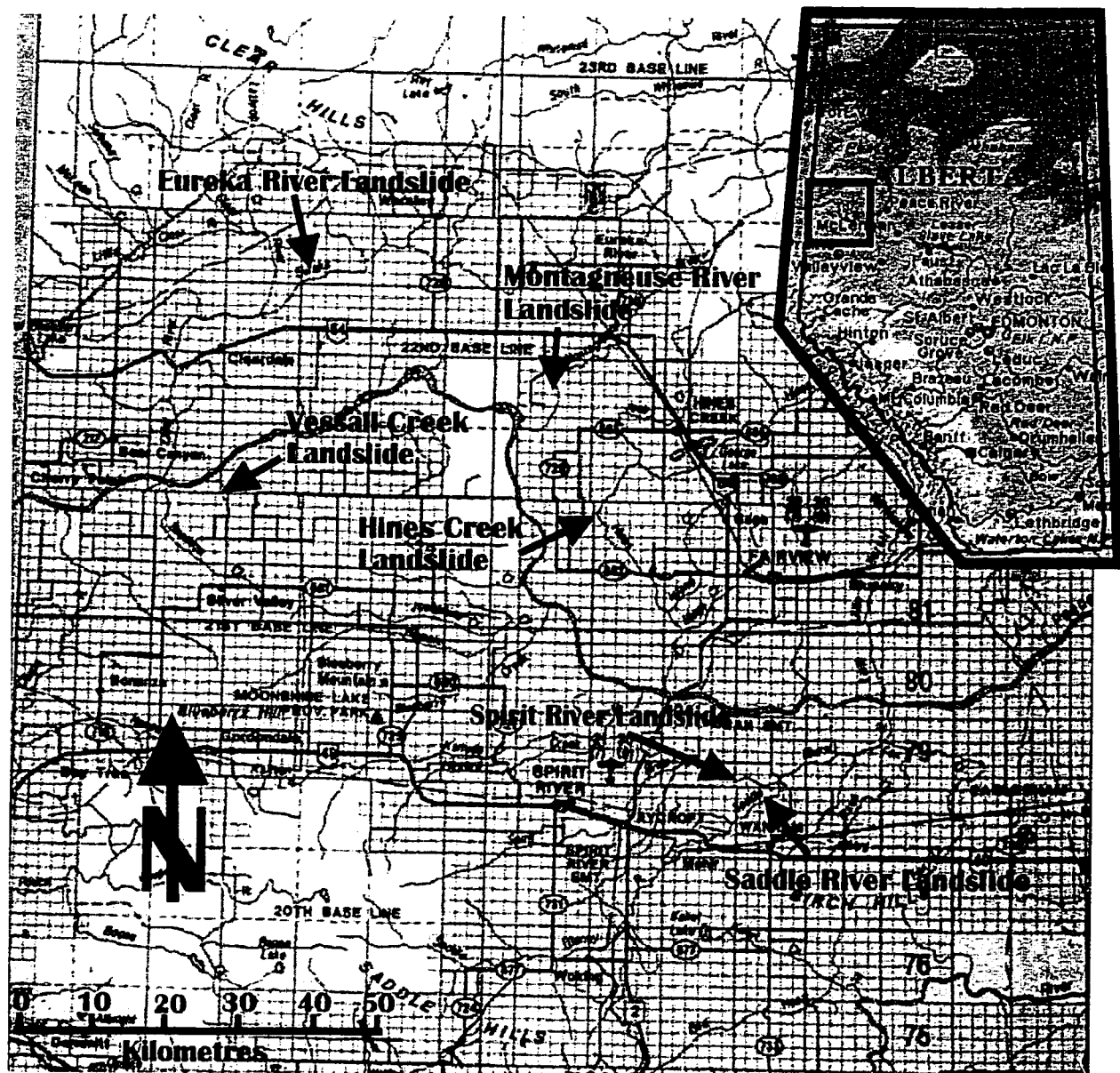
Figure 1.1: The Peace River Lowlands, Alberta, with recent landslides indicated (scale 1:1,000,000; Alberta, 1991).

References

Alberta, Forests, Lands and Wildlife. 1991. Forest Management Unit Map Area, 1:1,000,000, Edmonton.

Brooker, E.W. 1959. Dunvegan Landslide. Alberta Research Council, Edmonton, Open file Report 1959-6.

Catto, N.R., Liverman, D.G.E., Bobrowsky, P.T., and Rutter, N. 1996. Laurentide, Cordilleran and montane glaciation in the western Peace River – Grande Prairie Region, Alberta and British Columbia, Canada. Quaternary International, 32: 21-32.

Costa, J.E. and Schuster, R.L. 1988. The formation and failure of natural dams. Geological Society of America, Bulletin 100: 1054-1068.

Cruden, D.M., Keegan, T.R., and Thomson, S. 1993. The landslide dam on the Saddle River near Rycroft, Alberta. Canadian Geotechnical Journal, 30: 1003-1015.

Cruden, D.M., Lu, Z-Y., and Thomson, S. 1997. The 1939 Montagneuse River landslide, Alberta. Canadian Geotechnical Journal, 34: 799-810.

Cruden, D.M. and Varnes, D.J. 1996. Landslides Types and Processes. In Landslides: Investigation and Mitigation. Transportation Research Board, National Academy of Science, Special Report 247, Washington, D.C.

Hardy, R.M., Brooker, E.W., and Curtis, W.E. 1962. Landslides in over-consolidated clays. Engineering Journal, 45.6: 81-89.

Keegan, T.R. 1992. The Rycroft landslide dam on the Saddle River, Alberta. Master of Science thesis, Department of Civil Engineering, University of Alberta, Edmonton.

Laycock, A.H. 1990. Integrated Land Use and Water Management to Limit Erosion in the Peace River Region. A World of Real Places, Studies in Geography, University of Alberta, Edmonton: 115-132.

Lu, Z.Y., Cruden, D.M., and Thomson, S. 1998. Landslides and Preglacial Channels in the Western Peace River Lowland. Proceedings, 51st Canadian Geotechnical Conference, Edmonton, Alberta, 4-7 October, 1: 267-274.

Thomson, S. and Hayley, D.W. 1975. The Little Smoky Landslide. Canadian Geotechnical Journal, 12: 379-392.

2.0 Spirit River Watershed

2.1 Introduction

In mid-July, 1995 (Signal, 1995), an estimated 10.4 Mm^3 to 31.1 Mm^3 of surficial material slid southwards, and dammed the Spirit River in four locations. The Spirit River watershed is within the Peace River Lowlands, Alberta. The most upstream of the four dams was approximately 9 m in height, creating a reservoir of approximately 2100 m in length.

Of the land involved in the landslide, approximately 4.0 ha was farmland (Figure 2.1) owned by the Shmyr family, and operated by Paul Nedohin. Mr. Nedohin was the first person to notice the landslide, while checking his grain crops on July 22, 1995 (P. Nedohin, personal communication, 1999). Despite the Shmyr home being less than 250 m from the landslide main scarp, the Shmyrs were unaware that the landslide had occurred.
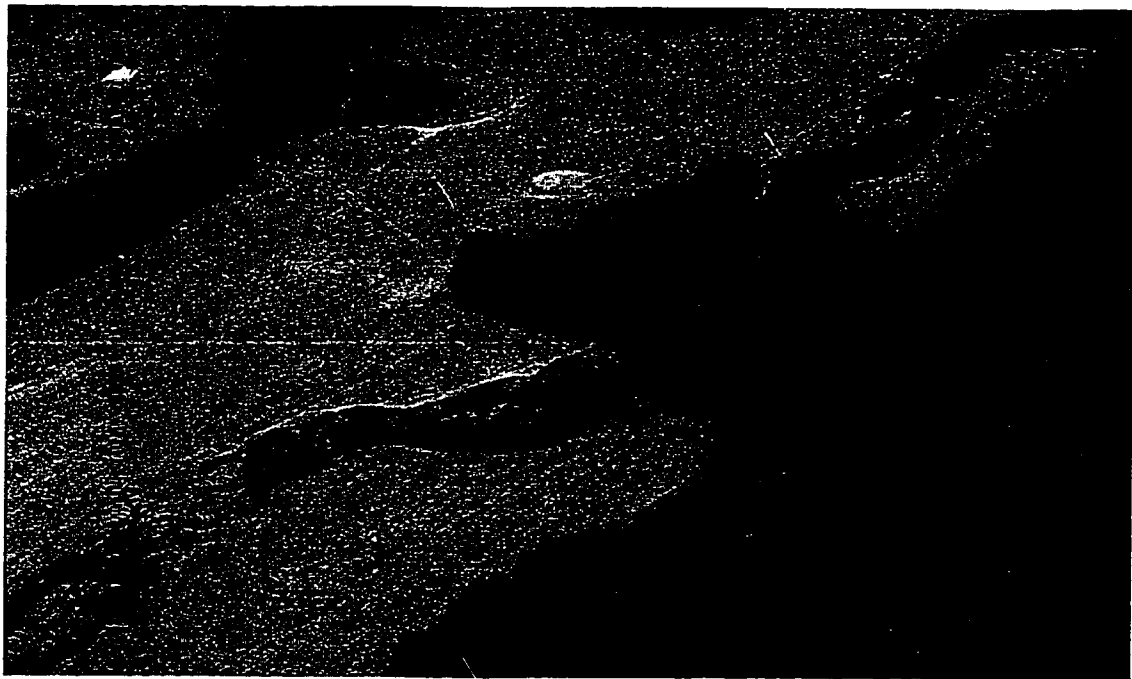
Figure 2.1: Spirit River landslide (photo by J. Gallagher, 1995)

Within this paper, I present background information (2.2), describe the study methodology (2.3), describe the watershed's stratigraphy (2.4), situate the 1995 landslide within a watershed context (2.5), describe the 1995 landslide (2.6) and landslide dams (2.7), and speculate on possible triggers for the landslide (2.8).

4

.

2.2 Background

2.2.1 Introduction

The background information discussed includes landslide location (2.2.2), watershed physiography (2.2.3), channel form (2.2.4), surficial geology (2.2.5), and bedrock geology (2.2.6).

2.2.2 Landslide Location

The Spirit River landslide is at 1 and 2 − 79 − 4 − W 6, on the north bank of the Spirit River, approximately 9 km from the confluence of the Spirit and Saddle Rivers (Figure 2.2). The crown of the landslide is at 55° 49' 15" North, 118° 29' 30" West at an elevation of 560 m.a.s.l. The toe of the landslide is at river level at an elevation of 505 m.a.s.l., 55 m below the crown of the landslide. The National Topographic System (NTS) maps, of this area, are the 1:250,000 Grande Prairie, Alberta (83M), and the 1:50,000 Codesa, Alberta (83M/16) and Rycroft, Alberta (83M/15) maps. Larger scale (1:20,000) Alberta Environment provincial base maps of the area include maps 83M/16SW and 83M/15SE.
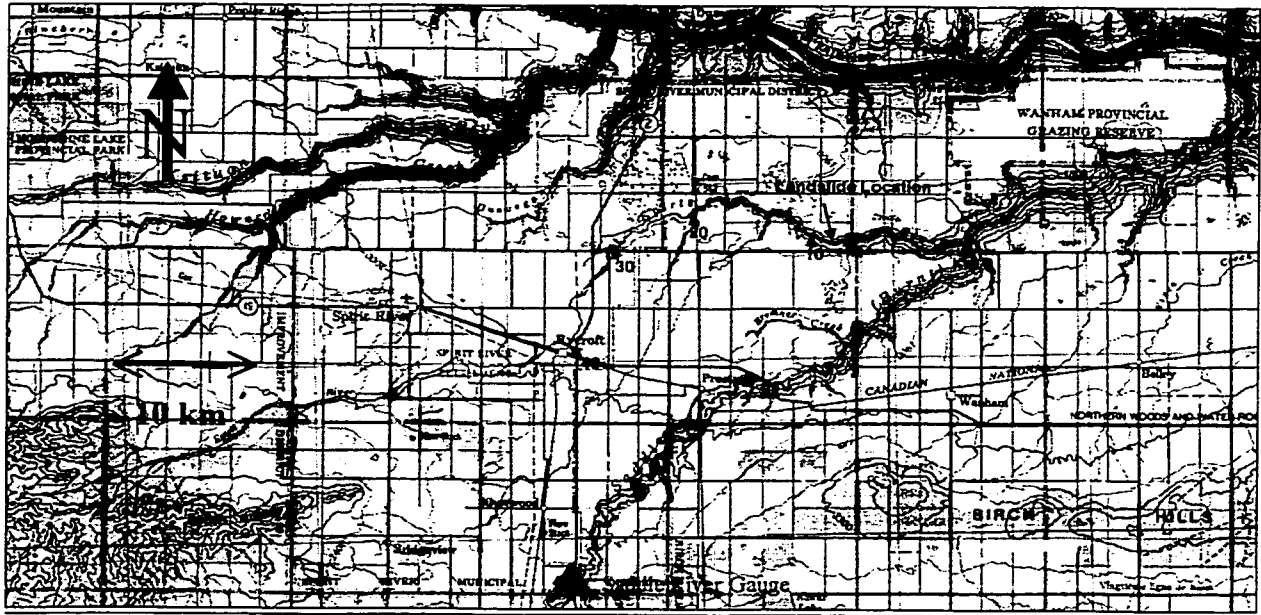
Figure 2.2: Landslide location (scale 1: 430,000)(NTS map 83M).

2.2.3 Watershed Physiography

The Spirit River watershed is within the Peace River Lowlands; a broad, gently-undulating upland plain, dissected by steep gorges. The Spirit River flows within one of these gorges. The river's headwater is the Spirit Ridge (1005 m.a.s.l.); the mouth is at the confluence of the Spirit and Saddle Rivers (440 m.a.s.l.). The Saddle River in turn, flows into the Peace River at 335 m.a.s.l. The vertical drop of the Spirit River, from the headwaters to the mouth is 565 m. The lower reach of the Spirit River is convex (Figure 2.3). Lower-reach, longitudinal profile convexity has been noticed in several rivers in Alberta (Cruden et al., 1993, 1997; Rains and Welsh, 1988; Rains et al., 1994).

2.2.4 Channel Form

From near the confluence of the Spirit and Saddle Rivers to km 13.6 (520 m.a.s.l.), the Spirit River is straight in form (Figure 2.3) (nomenclature following Knighton, 1998). Within this region point bars are rare. From km 13.6 to 26.7 (556 m.a.s.l.) the channel is confined meandering in form. Where the channel begins to meander is roughly coincidental with the upstream extent of large landslides (Section 2.5.3). Valley slopes (from 1:20,000 provincial base maps), also show a gradient increase at about the same location (Figure 2.3). From km 26.7 to 31.6 (571 m.a.s.l.) the Spirit River channel is once again straight in form, and the valley slopes lessen. Beyond km 31.6 the channel was not classified, as sections are meandering, and others are straight.
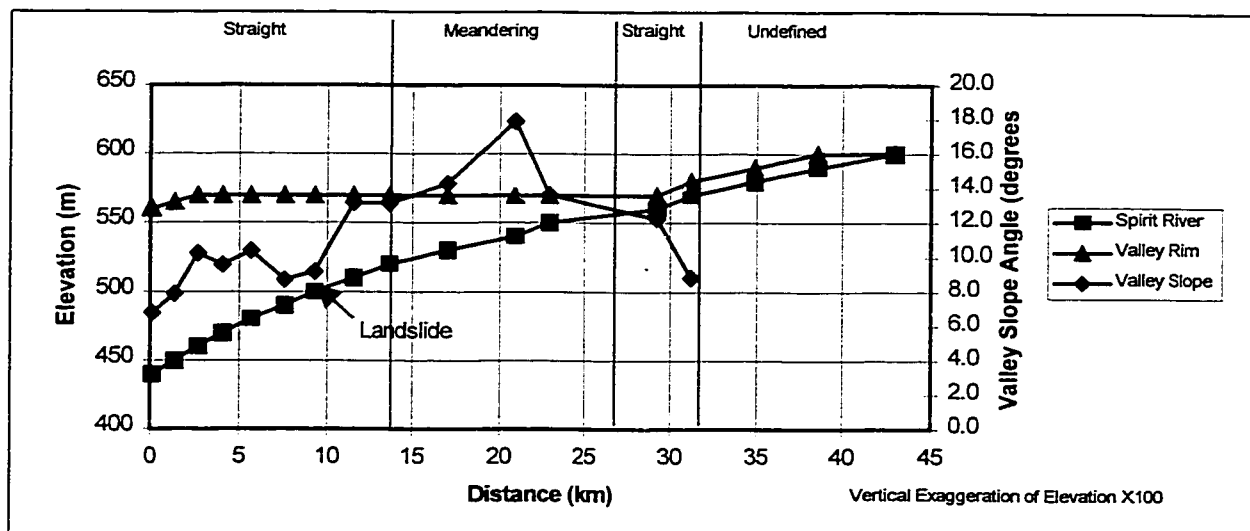
Figure 2.3: Spirit River longitudinal and average valley slope, and channel form.

2.2.5 Surficial Geology

Typically, the thickness of the surficial deposits in the watershed is less than 50 m (Carlson and Hackbarth, 1974). The surficial deposits thin towards the Spirit Ridge. Where the buried preglacial channels exist within the watershed, sediment thickness can be over 75 m (Hackbarth, 1977; Carlson and Hackbarth, 1974; Pawlowicz and Fenton, 1995), filling the preglacial channel in its entirety. The 1995 Spirit River landslide is composed of sediments deposited within the preglacial Peace River valley (Carlson and Hackbarth, 1974), the Shaftsbury buried channel (Pawlowicz and Fenton, 1995). The depth to bedrock at the site of the landslide is between 60 (from field survey) and 76 m (Carlson and Hackbarth, 1974) from the upland plain.

The genesis of the sediments within the preglacial channels is the up-drainage advance of the Laurentide ice sheet followed by the down-drainage ice front retreat. These events deposited preglacial lacustrine, till, and postglacial lacustrine sediments atop the pre-existing fluvial sediments.

2.2.6 Bedrock Geology

The bedrock underlying the surficial deposits, at the site of the 1995 Spirit River landslide, is the Cretaceous, marine, Smoky Group (Hackbarth, 1977). This group includes the Kaskapau, Bad Hart, and Puskwasau Formations (Hackbarth, 1977). The Kaskapau Formation is composed of "dark gray silty shale, ... interbedded with fine-grained quartzose sandstone and thin beds of ferruginous oolitic mudstone" (Ozoray, 1982, p. 5). The Bad Heart Formation is composed of "fine-grained quartzose sandstone, ferruginous oolitic sandstone and mudstone" (Ozoray, 1982, p. 5). The Puskwasau Formation is a "dark gray fossiliferous shale" (Ozoray, 1982, p.5). The bedrock does not outcrop at the site of the 1995 landslide. Beneath the Smoky Group, is the deltaic to marine Dunvegan Formation (Hackbarth, 1977). This formation, also of Cretaceous age, is a "gray, fine grained feldspathic sandstone with hard calcareous beds, laminated siltstone and gray silty shale" (Ozoray, 1982, p.4). The depth to the Dunvegan Formation at the site of the 1995 landslide is approximately 150 m (extrapolated from Rutherford, 1930). Overlying the Smoky Group, to the south of the site of the landslide, is the Wapiti Formation – a non-marine "gray feldspathic clayey sandstone, gray bentonitic mudstone, [and] bentonite [unit with] scattered coal" (Hackbarth, 1977, p.3). The regional bedrock dip is towards the south at greater than 15 m/km (0.9°) (Hackbarth, 1977).

2.3 Methods

2.3.1 Introduction

The methods employed in this study, ordered chronologically, are detailed in the following sections: Preliminary Investigation (2.3.2), Field Investigation (2.3.3), and Post-Field Investigation (2.3.4).

2.3.2 Preliminary Investigation

During my preliminary study, I reviewed topographic maps (2.3.2.1), aerial photographs (2.3.2.2), geotechnical reports (2.3.2.3), and regional physiographic information (2.3.2.4).

2.3.2.1 Topographic Maps

Alberta provincial base maps 83M/16SW, 83M/16SE, 83M/16NE, 83M/15SE (1:20,000) were used to determine the stream's longitudinal profile and valley gradients (Figures 2.3, 5.3, and 5.5). Information was extracted, from the topographic maps, using an Ushikata Computer Co-ordinating Area–Curvimeter X-PLAN 360d. Reference distances, used throughout this chapter, are measured along the stream (stream length), from the confluence of the Spirit and Saddle Rivers. Between km 0.0 and 1.0, the difference between valley length and stream length is 280 m. From km 1.0 to km 13.6, the valley length is approximately equal to stream length. Beyond km 13.6, the valley length is less than stream length due to river meandering.

Valley slope measurements were taken from where the topographic contours crossed the stream. In determining the valley slopes, I measured from one contour interval (10 m) above the stream (to avoid erroneous values due to the flood plain) to the contour just below plains level.

2.3.2.2 Aerial Photographs

Aerial photographs were used to produce a preliminary map of the landslide. In mapping the landslide, I used the most recent (1995) publicly available aerial photographs (Alberta, AS4680 #32, 33), and the most recent (1989) pre-slide aerial photograph (Alberta, AS3895 #97). To facilitate the mapping, I had these photos enlarged to a scale of 1:5000, from scales of 1:40,000 (Alberta, AS4680) and 1:30,000 (Alberta, AS3895). Despite the photographic enlargement, a

preliminary description of the 1995 landslide was severely hampered by thick vegetation (Figure 2.10). With the exception of the main scarp, distinguishing landforms associated with the 1995 event, from earlier landforms caused by landslides prior to 1945, was difficult. To rectify this situation, photo interpretation was performed on a 1945 aerial photograph (Figure 2.7) (Canada A8765 #15). A forest fire prior to 1945 had removed the vegetation, which facilitated photo interpretation. My interpretation of the 1945 photographs was done at the original scale (1:15,840) on a Mylar overlay. The overlay was enlarged to 1:5000, using a photocopier, and then overlaid on the interpretation of the 1995 photos. The interpretation of the 1995 photograph was then modified accordingly (Figure 2.11).

All the preliminary mapping was done on Mylar overlays using a Wild type 392824 stereoscope, with magnification capabilities of between 3 and 15.5 times.

Aerial photographs were also used to determine the periodicity of landslides (of size greater than 1 Mm^2) within the watershed. This involved examining 17 different series of aerial photographs, from 1945 to 1995 (Appendix 1).

2.3.2.3 Geotechnical Reports

Geotechnical reports of other landslides (Bidwell, 1999; Brooker, 1959; Cruden et al., 1990, 1993, 1997; Evans et al., 1996; Hardy et al., 1962; Keegan, 1992; Lu et al., 1998; Nasmith, 1964; Thomson and Hayley, 1975) and landslide dams (Bidwell, 1999; Cruden et al., 1993, 1997; Evans et al., 1996; Hardy et al., 1962; Keegan, 1992; Lu et al., 1998) in the Peace River Lowlands, and further afield (Costa and Schuster, 1988; Evans, 1986; Schuster and Costa, 1986; Thomson and Morgenstern, 1977) were reviewed for possible models for the Spirit River landslide and landslide dam, and for regional physiographic information.

2.3.2.4 Regional Physiographic Information

Regional physiographic information was used to provide pre-field background information. This information included: topographic and land cover information (Canada, Energy Mines and Resources, Rycroft, Alberta, 1990; Canada, Energy Mines and Resources, Codesa, Alberta, 1990), geological information (Hackbarth, 1977; Hamilton et al., 1998; Jones, 1966; Ozoray, 1982; Rutherford, 1930); surficial geology information (Jones, 1966; Bobrowsky et al., 1990;

Catto, 1991; Catto et al., 1996; Liverman, 1991), hydraulic information (Canada, Environment Canada, Water Survey of Canada, 1998), climatic information (Canada, Environment Canada, Climate Services, 1998), and seismic information (Canada, Geological Survey, 2000).

2.3.3 Field Investigation

Susan Shirkoff (field assistant) and I conducted the field investigation between July 1 and 20, 1999. The tasks performed included ground-truthing the preliminary map (2.3.3.1), surveying (2.3.3.2) the length of the landslide to produce a cross-section, gathering information about the landslide's kinematics (2.3.3.3), determining the classification and status of the landslide dams (2.3.3.4), assessing the geomorphic significance of the landslide and landslide dams (2.3.3.5), and determining the local stratigraphy.

2.3.3.1 Ground-Truthing the Preliminary Map

The preliminary map of the Spirit River landslide, generated by aerial photographic interpretation, was ground-truthed. Substantial augmentation to the initial interpretation was required, as thick vegetation had obscured the landslide features. Initially, a Garmin GPS (Global Positioning System) – 12 was employed for geo-referencing. However, this device proved ineffective, as the position error from the GPS was too great for mapping purposes. Instead, a baseline was established along the main scarp, using a V/R hipchain and Sylva compass, with stations spaced 50 m apart. Mappable features (i.e. tension cracks and scarps) were then referenced to the baseline, using a V/R hipchain, a Sylva compass, and a Suunto clinometer. The feature could then be identified on the aerial photograph and accurately mapped. All mapping revisions were done by myself, after each day's field survey, using a Sokkia MS27 stereoscope with 3-times magnification binoculars.

2.3.3.2 Surveying

A transect, running parallel to the slide's direction of movement and approximately in the region of greatest displacement, was surveyed. For this purpose I used a V/R hipchain and a Brunton compass/clinometer. The placement of the transect was west of the zone of greatest displacement, due to a beaver pond. The locations of breaks in slope, scarps, tension cracks, and other important physiographic information were recorded. The information derived from the survey was plotted that evening, and a preliminary cross-section was produced. The error in

measurement was determined to be less than 5% in the vertical (using base map 83M/16SW) and horizontal (using the 1:5,000 aerial photograph Alberta, AS3895 #97).

2.3.3.3 Landslide Kinematics

Information for determining the kinematics of the landslide was gathered. Primarily, this involved determining the rotation of the upper block. Attempts to quantify the rotation of the upper block proved imprecise. As such, the rotation had to be estimated, based on a shallow pond near the main scarp, which was previously (pre-landslide) drained by a, now redundant, drainage channel.

2.3.3.4 Landslide Dams Classification and Status

The classification of each landslide dam, according to Costa and Schuster (1988), was accomplished in the field by determining where the rupture surface daylighted, in relation to the pre-landslide stream channel. This assessment could not be done remotely as the Spirit River, at the site of the landslide, was obscured by shadow in the 1995 aerial photographs (Alberta, AS4680#32). The statuses of the landslide dams were also determined in the field.

2.3.3.5 Geomorphic Significance of the Landslide and Landslide Dams

The assessment of the geomorphic significance of the Spirit River landslide, and landslide dams, was accomplished by traversing the stream, from upstream of the area inundated by reservoir floodwaters (km 11.3) to 800 m downstream of the eastern margin of the landslide (km 7.7). In addition, the mouth of the Spirit River was visited.

2.3.4 Post-field Investigation

The post-field investigation involved tilt-table tests (2.3.4.1) and determining the Atterberg limits (2.3.4.2), texture (2.3.4.3), and friction angle (2.6.4) of the units bounding the rupture surface, and estimating the landslides volume (2.6.5) and kinematics (2.6.6).

2.3.4.1 Tilt Table Testing

The tilt table tests were performed, by myself, on the day that the sample was collected. The testing involved slowly increasing the inclination of the table, to which the lower rupture surface (plate) was fastened, until the upper rupture surface (slider) completely detached itself from the plate. The plate was attached to the table, so that the surface of the plate roughly paralleled the table. The orientation of plate and slider, with respect to the table, was positioned so the displacement of the slider, relative to the plate, would be the same as had occurred during the landslide events (determined by striations on the rupture surfaces). Adjusting the inclination of the table was done by opening a valve, which allowed oil to flow from a hydraulic piston to a reservoir. This apparatus enabled the table's rate of inclination increase to be carefully controlled. The increase in inclination proceeded at a constant rate until the slider began to move; at this point, the inclination increase rate of the table was reduced until the slider detached from the plate, and the experiment was halted. The inclination of the table was then measured using a Brunton clinometer. I repeated the tilt table tests six consecutive times on the same sample. (Bruce et al., 1989).

2.3.4.2 Atterberg Limits

The Atterberg Limits include the liquid limit, the plastic limit, and plasticity index of one sample from above, and one sample from below the rupture surface. I performed each of the tests to the American Society for Testing and Materials, 1998 (D4318-95a) standards. Christine Hereygers (Department of Civil and Environmental Engineering, University of Alberta) assisted me, by providing equipment, instructions, and reviewing my results.

The liquid limit of the samples was determined using a Casagrande cup. The methods include: partially filling a brass (Casagrande) cup with soil, cutting a groove into the soil using a standard tool, and then raising and dropping the cup by 0.624 cm, by turning a lobed crank at two revolutions per second. The action of dropping the cup causes the groove to close. When a 12-mm section of the groove had closed, the experiment was halted and the number of blows was recorded. This procedure was repeated thrice. Distilled water was then added to the sample and the test was repeated three more times. The intent was to have groove closure with 35 blows for the first three tests, and closure with 15 blows for the next three tests. Soil from each successive test was weighed, then oven dried (at 110°C for 24 hours), then weighed again, in order to determine the moisture content of each sample. The number of blows versus moisture content

12

was plotted on semi-logarithmic graph paper (with number of blows plotted on the logarithmic horizontal axis), and a best-fit line was drawn between the two data clusters. The moisture content at 25 blows is the liquid limit.

Determining the plastic limit involved rolling approximately 0.5 mL of soil, by hand, into a thread 3 mm in diameter. The test soil was then formed back into a ball and then rolled into a thread again. The test was repeated until the soil could no longer be rolled into a 3-mm thread. The sample was weighed, then oven dried (at 110°C for 24 h), and then weighed again, in order to determine the moisture content of the sample. This test was repeated three times. The plastic limit is the average moisture content from the three tests.

The plasticity index is the liquid limit minus the plastic limit.

2.3.4.3 Textural Analyses

The textural analysis, involving wet filtering and hydrometer tests (Appendix 5), was performed on one sample from above the rupture surface (hanging wall), and one sample from below the rupture surface (footwall). I performed the wet filtering. The hydrometer tests were conducted by Christine Hereygers (University of Alberta) with my assistance.

The wet filtering involves oven drying a sample (at 110°C for 24 hours), weighing the sample, breaking up the sample with a mortar and pestle, hydrating the sample with distilled water, and then pouring the sample through a #230 sieve. To facilitate the passage of the fine particles through the sieve, the sample was flushed with tap water. The material caught in the #230 sieve was oven dried (at 110°C for 24 hours), and then poured through sieves 7, 8, 10, 18, 35, 60, 80, 100, 120, 140, 170, 200, and 230. The footwall sample was also poured through sieves 14, 25, and 45. To facilitate particle passage through the sieves, the sieves were mechanically shaken and hammered, using a ROTAP RX-29 (W.S. Tyler Inc.), for 15 minutes. The remaining material in each sieve was then weighed, and the percent of the total sample that that material represents was determined.

The hydrometer tests involved recording the settling velocity of particles finer than fine sand, and were performed to the American Society for Testing and Materials, 1998 (D422-63) standards. The methods are as follows:

13

1. the sample was broken up using a milk shake machine;

2. the sample was then transferred to a graduated cylinder and the cylinder was filled with distilled water (at 20°C) with 0.5% sodium hexametaphosphate to the 1000 ml mark;

3. the cylinder was then sealed, and shaken 25 times in a teeter-totter motion;

4. a type 152H hydrometer was placed within the cylinder;

5. hydrometer and temperature readings were then taken at 0.5, 1, 2, 4, 8, 16, 36, 86, 132, 165, 248, 368, 1393, 1595, 1763, 3364, 4506, and 5714 (95h 14min) minutes;

6. the data were entered into the University of Alberta, hydrometer program, and plotted (Figure 2.9).

2.4 Stratigraphy

2.4.1 Introduction

At the landslide site, two distinct sedimentary units were identified, a postglacial lacustrine deposit (2.4.2), and a diamicton (assumed to be till) (2.4.3). The rupture surface of the 1995 landslide was within the till. In determining of the genesis of the two units, emphasis was placed on stratigraphic analyses of landslides in proximal watersheds (Figure 2.4).
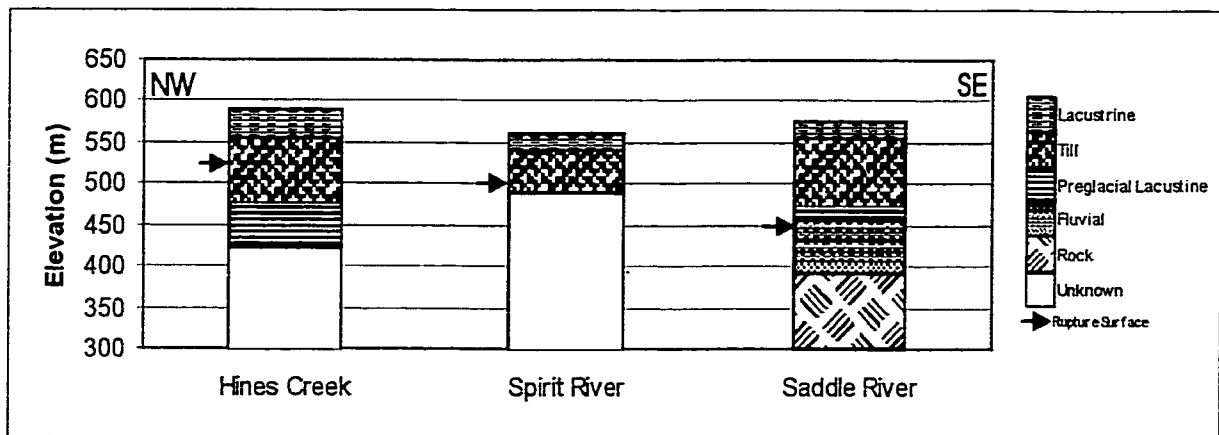
Figure 2.4: Stratigraphy at Spirit River, Saddle River (Cruden et al., 1993), and Hines Creek (Lu et al., 1998).

14

2.4.2 Postglacial Lacustrine Deposit

The postglacial lacustrine deposit could be observed from the top of the valley to close to the bottom of the valley (elevation 515 to 560 m). Translational landslides have displaced blocks of the lacustrine sediment downwards into the valley, thus exaggerating the unit thickness. The true unit thickness is likely comparable to the 20-m thickness found at the Saddle River landslide (Cruden et al., 1993). The unit is a mottled grey to tan coloured, clay and silt, and mostly structureless. The mottling is likely due to postglacial pedogenesis and frost action (Catto, 1991). Occasional well-rounded quartzite pebbles were found within the unit, and presumed to be dropstones. Where structure was observed, it was highly contorted (Figure 2.5). Explanations for the contorted structures can be found in Liverman (1991) and Catto (1991). Liverman (1991) deciphered a complex depositional history within glacial Lake Peace sediments south of the Saddle Hills, near Grande Prairie, Alberta. Specifically, he recognised sub-aqueous sedimentary gravity or debris flow deposits, punctuated by silt and clay laminae, deposited near the ice margin, grading upwards into turbidity current deposits, and eventually into suspension settled deposits, with the progressive northeastward retreat of the Laurentide ice sheet. Catto (1991) found indications of syndepositional or post-depositional mass movement within postglacial lacustrine sediments in the Peace River region, British Columbia.

The surface topography at the landslide is hummocky. Catto (1991) found hummocks were associated with glacial lacustrine sediment of more than 3 m thickness. Mollard (in press) suggests explanations for the hummocks.

Figure 2.5: Contorted postglacial lacustrine sediment (at main scarp, 75 m east of surveyed transect (Figure 2.11)).

15

2.4.3 Till

Beneath the postglacial lacustrine sediment, is a diamicton. The thickness of the diamicton could not be determined as landslides have obscured the upper surface, and the lower surface was beneath the bottom of the valley. The rupture surface daylighted within this diamicton at 505 m.a.s.l. Across the rupture surface, the colour of the diamicton changed, from a light grey below (footwall), to a dark grey above (hanging wall) (Figure 2.6). There is no indication of weathering at the rupture surface. No rhythmitic structures were apparent throughout the diamicton. The diamicton is assumed to be till, for consistency with other proximal landslide studies. Liverman (1991) found diamicton deposits were generated from subaqueous sedimentary gravity or debris flows. Catto (1991) proposed three modes of diamicton genesis; those being, direct from the ice, and directly from the ice and subsequently modified by mass movement either out-of or within a lacustrine environment. Catto (1991) recognised that the latter two depositional modes would preclude the deposit from being morainic, but maintained, for practicality, this classification for all diamicton containing at least 5% coarse clast content. Either successive mass movement deposits, or a mass movement deposit overlying till, would explain the colour change across the rupture surface observed at the Spirit River. The presence of two tills, as an explanation for the colour change, can be rejected (Catto et al., 1996). The Atterberg Limits (Section 2.6.3.2), and textures (Section 2.6.3.3) from the hanging wall and footwall diamicton, are similar to one another, and are also similar to the till at the Saddle River (Cruden et al., 1993), and the Montagneuse River (Cruden et al., 1997). Clast petrology is varied, in both the hanging wall and footwall diamicton, and includes clasts of shield provenance. Some organic matter, including small (1 cm in length) wood fragments, was identified in the footwall diamicton.
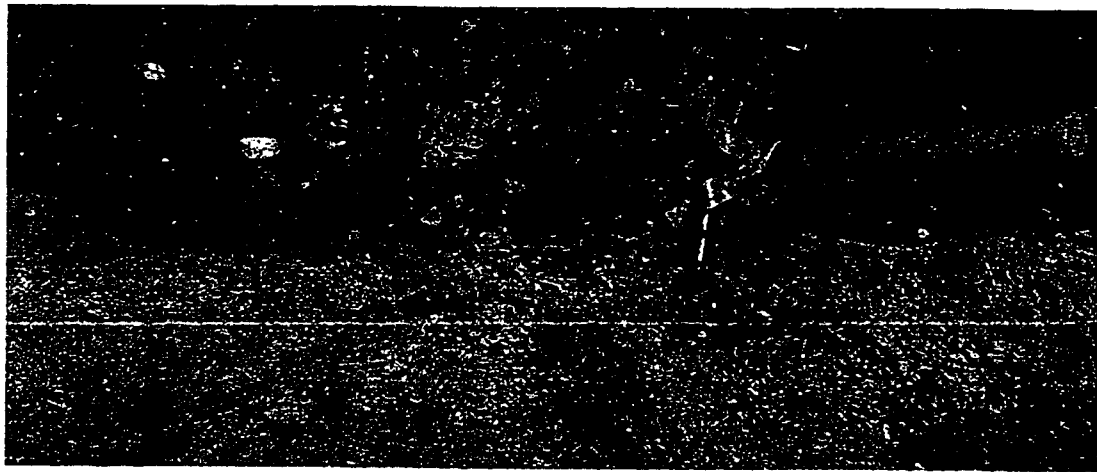
Figure 2.6: Appearance change in till across rupture surface (Figure 2.11).

16

2.5 Landslides in the Spirit River Watershed

2.5.1 Introduction

An analysis of aerial photographs was conducted to determine the frequency of landslides (2.5.2) and the distribution of landslides (2.5.3) within the Spirit River watershed. The objective of this procedure was to situate the 1995 landslide within a temporal and spatial context.

2.5.2 Landslide Frequency

An analysis of 17 different series of aerial photographs, from 1945 to 1995 (appendix 1), has revealed that the July 1995 landslide was the only large landslide (greater than 1 Mm^3) that occurred within the Spirit River watershed during this period. Further, it appears that there have been no large landslides (greater than 1 Mm^3) for several years prior to 1945, as there is an absence of large unvegetated scarps (of length greater than 500 m), in the 1945 aerial photographs.

2.5.3 Distribution of Large Landslides

Aerial photographs show inactive large landslides from the confluence of the Spirit and Saddle Rivers, to km 12.8 on north bank and to km 14.1 on the south bank of the Spirit River. Evidence for these landslides includes sag ponds, irregular (broken) topography, and uphill facing slopes. As these landslides generally involve the entire slope, the volume of the landslides decrease upstream. The mode of instability appears to be primarily translational slides.

The 1995 landslide is located between km 8.8 to km 10.9 on the north (left) bank of the Spirit River. This landslide is a reactivation and retrogression, or enlargement of an earlier slide. The earlier slide, evident in an aerial photograph from 1945 (Canada A8765 #15), likely occurred substantially prior to 1945, as the main scarp of the slide had been extensively modified by 1945 (Figure 2.7).

Figure 2.7: 1945 Aerial photograph (Canada A8765 #15) of the site of the 1995 landslide (scale 1:10,000).

Above km 12.8 and 14.1 (north and south banks respectively) four landslides have been recognized on aerial photographs. Two of the landslides occurred on a tributary of the Spirit River (entering the Spirit River at km 14.1 on the south bank), 0.9 and 1.0 km from the Spirit River. The landslide at 0.9 km dammed the tributary and a small reservoir, visible in 1989 aerial photograph Alberta, AS3895 #97, was created. Two other slides were identified at km 15.4 (north side) and 15.7 (south side) on the Spirit River main channel.

Occurrences of landslides are reflected in valley slope gradients (Figure 2.8). Where there is evidence of past large landslides, valley slope gradients are less than where there is no indication of past landslides. Longitudinal gradients and channel form also reflect the occurrence of landslides (Figure 2.3). In the lower reach (km 0 to 13.6), the longitudinal gradient is steepest (0.34°), the channel is straight, and there is evidence of past large landslides. Within this reach, streambed incision is likely occurring, which is destabilizing the banks, and laterally restricting the channel. Upstream of this reach, longitudinal gradients lessen (0.16° for the following 17.6 km), valley slopes steepen, and the channel meanders.

18

The site of the 1995 landslide is near the upstream extent of the landslide prone lower reach. The pre-landslide gradient at the surveyed transect is 9° (from NTS map 83 M/16 (1:50,000)); the post-landslide slope gradient, as measured in the field, is 6.8°. The Spirit River, at the site of the 1995 landslide, is straight and the longitudinal gradient is 0.33°.
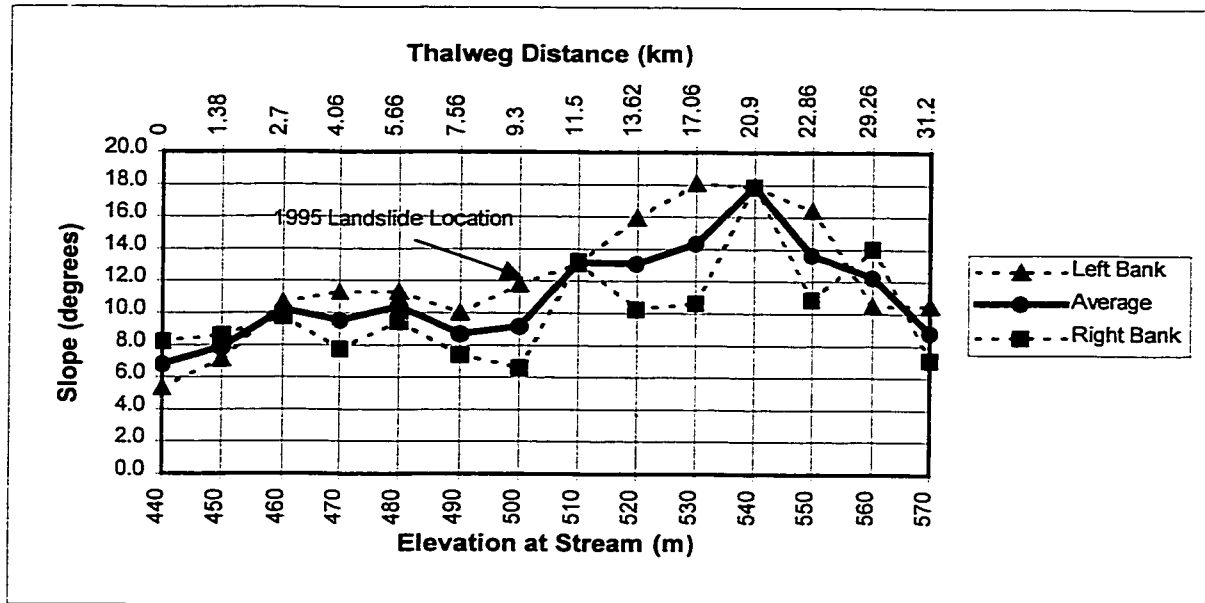
Figure 2.8: Valley slopes of the Spirit River (from base map 83M/15SE and 16SW).

2.6 Description of 1995 Spirit River Landslide

2.6.1 Introduction

The following includes the empirically derived landslide properties (2.6.2), an estimation of the landslide's friction angle (2.6.3) and volume (2.6.4), a description of the 1995 landslide and landslide kinematics (2.6.5), the classification of the landslide (2.6.6), and an analysis of instability associated with the 1995 landslide (2.6.7). The nomenclature used in this section follows Cruden and Varnes (1996).

2.6.2 Empirically Derived Properties

This section includes the results from the tilt table tests (2.6.2.1), and the determined textures (2.6.2.2) and Atterberg Limits (2.6.2.3). These procedures were performed on one sample from the hanging wall, and one from the footwall, collected at the Spirit River at km 9.5.

2.6.3.1 Tilt Table Test Results

The tilt table tests (Table2.1) generated unexpectedly high results. An inferred friction angle based on these results would clearly be the maximum. The high values (Table2.1) generated from this experiment might be caused by the samples being drier and under a lower normal load, than during the landslide event (Section 2.6.3). Of interest are the higher results produced when the movement of slider, with respect to plate, is the same relative direction as during the landslide (tests 1 to 4, Table 2.1), compared to when the relative displacement direction is opposite to that of the landslide (tests 5 and 6); the cause of which is unknown.

Table 2.1: Tilt table test results.

Test #	Tilt of Plate Prior to Test	Tilt of Table after Detachment of Slider from Plate	Final Tilt of Plate after Detachment of Slider	Comments
Equivalent to slider moving southward				
1	1.4	47.9	49.3	
2	1.4	43.3	44.7	Area decrease due to slider breakage
3	1.4	46.3	47.7	
4	1.8	44.5	46.3	
Average			47.0	
Equivalent to slider moving northward			-	
5	-4.6	42.0	37.4	No initial motion
6	-5.4	47.2	41.8	
Average			39.6	

2.6.2.2 Texture of Rupture Surface Bounding Units

Texture analysis was performed on a single sample of the rupture surface footwall diamicton and a single sample of the hanging wall diamicton (Figure 2.9). The samples were collected at the Spirit River, at km 9.5. The soil textures are consistent with the textures of the till at the Montagneuse River (Cruden et al., 1997) and Saddle River (Cruden et al., 1993) landslides, though they are inconsistent with the till at the Little Smoky River landslide (Thomson and Hayley, 1975) (Table2.2).

Table 2.2: Textures of diamicton at the Spirit River, Little Smoky River (Thomson and Hayley, 1975), Montagneuse River (Cruden et al., 1997), and Saddle River (Cruden et al., 1993) landslides (minimum and maximum values in brackets).

Landslide	Spirit River		Little Smoky River		Montagneuse River	Saddle River
	Hanging Wall	Footwall	Upper Till	Lower Till		
Sand %	12	11	24 (23-25)	43 (25-60)	11 (9-12)	12 (3-21)
Silt %	52	55	37 (34-40)	36 (31-40)	62 (59-64)	51 (45-57)
Clay %	33	30	29 (23-35)	22 (09-35)	27 (23-31)	37 (30-45)
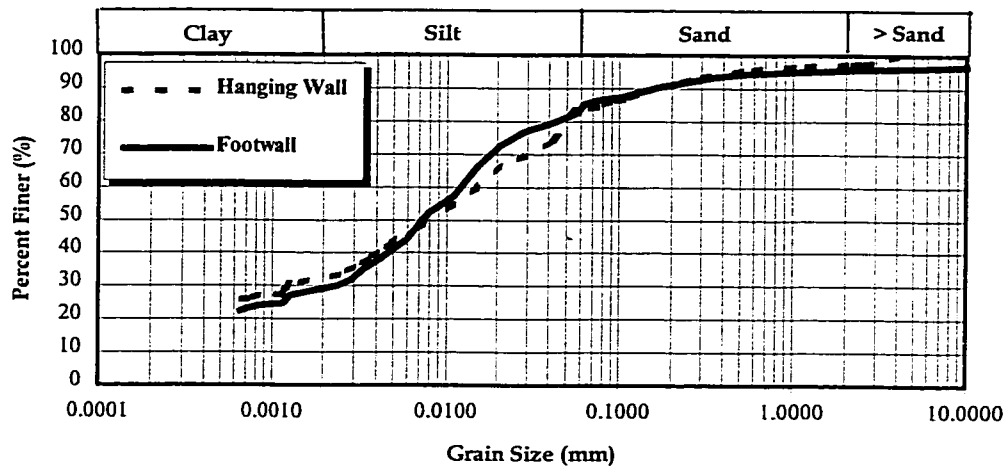
Figure 2.9: Grain size distributions of diamicton from above and below the rupture surface at the Spirit River landslide.

2.6.2.3 Atterberg Limits

The Atterberg limits and activity of diamicton from the Spirit River landslide, and the Atterberg limits, activity, and unit weight of till at Little Smoky River (Thomson and Hayley, 1975), Montagneuse River (Cruden et al., 1997), and Saddle River (Cruden et al., 1993) landslides, are given in Table 2.3. The Atterberg limits and activities of the diamicton from the Spirit River landslide are similar to the limits of the till at the Montagneuse River (Cruden et al., 1997) and Saddle River (Cruden et al., 1993) landslides, though dissimilar to the till at Little Smoky River landslide (Thomson and Hayley, 1975).

Table 2.3: Atterberg limits and activity of diamicton at the Spirit River and the Atterberg limits, activity and unit weight of till at Little Smoky River (Thomson and Hayley, 1975), Montagneuse River (Cruden et al., 1997) and Saddle River (Cruden et al., 1998) (minimum and maximum values in brackets).

Landslide	Spirit River		Little Smoky River		Montagneuse River	Saddle River
	Hanging Wall	Footwall	Upper Till	Lower Till		
Liquid Limit %	38.4	39.6	48	43	34 (31-38)	45 (36-59)
Plastic Limit %	18.4	19.7	18	21	18 (16-20)	18 (14-21)
Plasticity Index %	20.0	19.9	30	22	16 (15-18)	28 (22-38)
Activity	0.61	0.66	1.03	1.00	0.59	0.64
Unit Weight (kN/m³)			19.3	19.6	21.3	20.4

2.6.3 Estimated Friction Angle

The residual friction angle, Φ_r, at the Spirit River landslide was estimated in three ways: using Φ_r values from the Hines Creek (Lu et al., 1998) and Saddle River (Cruden et al., 1993) landslides, using an empirical relationship between clay fraction and friction angle from Skempton (1985), and using models by Norrish and Wyllie (1996, eq. 15.3, p. 399) and Skempton and De Lory (1957) (in Selby, 1993).

Values of Φ_r, peak friction angle (Φ_p), and cohesion (c) from the Hines Creek (Lu et al., 1998) and Saddle River (Cruden et al., 1993) landslides form Table 2.4. Table 2.4 shows consistency between Φ_r values from Hines Creek (Lu et al., 1998) and the Saddle River. The residual friction angle for the Spirit River landslide may be similar to the residual friction angle values from Hines Creek and the Saddle River (10° to 12°), due to the close proximity of the landslides (Saddle River - 4.2 km, Hines Creek - 35 km) to the Spirit River landslide, and the similar textures (Table2.2) and Atterberg limits (Table2.3) of the Spirit and Saddle River diamicton.

Table 2.4: Friction angles (degrees) of till at the Hines Creek (Lu et al., 1998) and Saddle River (Cruden et al., 1993) landslides.

Landslide	Depth (m)	Φp	c(kPa)	Φr	c(kPa)	Test
Hines Creek	76-77	20	0	12	0	reverse direct shear
	85-86	20	0	10	0	reverse direct shear
Saddle River	50-100	15.5	45	10.9	0	reverse direct shear, consolidated undrained triaxial

Skempton's (1985) relationship between clay fraction and Φ_r, for soils with activities between 0.5 and 0.9, produces a non-normalized Φ_r of between 15° and 20° for the Spirit River landslide. Skempton (1985) normalized his data to an effective stress (σ') of 100 kPa, using the following relationship:

σ' (kPa)	25	50	100	150
$\tan\Phi/\tan\Phi_{100}$	1 .12	1.07	1.00	0.96

The pre-landslide σ_n' values at Spirit River range between 340 and 660 kPa (for rupture surface slopes (Ψ_p) of 7° and 0° respectively, with average normal landslide thicknesses (z) of 17 and 33 m respectively) (from Figure 2.13). Using my derived relationship,

$$\tan\Phi/\tan\Phi_{(\sigma n=100)}= -0.20\log \sigma_n'+1.4 \qquad (eq.2.1),$$

Φ_r values between 12.5 and 17.8° are produced. The lower bound of this range of values is consistent with the upper bounds of the Φ_r from the Hines Creek and Saddle River landslides (Table 2.4).

To numerically assess the residual friction angle, equations 2.2 and 2.3 (below) were employed. Equation 2.3 requires near rupture surface slope (Ψ_p) and valley slope (Ψ_f) parallelism, and as such its applicability is limited to the maximum probable rupture surface slope (7°). Equation 2.3 has been included for comparative purposes. Equation 2.2 is a more realistic model for the Spirit River landslide, as different valley (Ψ_f), upland (Ψ_{so}), and rupture surface (Ψ_p) slopes, can be accounted for. Equation 2.2 and 2.3 are as follows:

$$FS = \frac{[cA + (W\cos\Psi_p - U - V\sin\Psi_p)\ \tan\Phi]}{(W\sin\Psi_p + V\cos\Psi_p)} \qquad (eq.\ 2.2)$$

$$\text{(Norrish and Wyllie, 1996, eq. 15.3, p. 399),}$$

and

$$FS = \frac{c + (\gamma_r - m\gamma_w)z\cos^2\Psi_{fp}\tan\Phi}{\gamma_r z\sin\Psi_{fp}\cos\Psi_{fp}} \qquad (eq.\ 2.3)$$

$$\text{(Skempton and De Lory, 1957, in Selby, 1993, p.270).}$$

In the calculations the following assumptions were made:

1. the factor of safety equaled one (FS=1), as the slope had failed;

2. the water table was at the surface ($Z=Z_w$; m=1) (Figure 2.1);

3. the main scarp is at the top of the valley – this assumption is true only for the areas in which there was no retrogression, and was made to simplify calculations;

4. there was no cohesion (c=0) and the friction angle was at residual ($\Phi = \Phi_r$).

The assumptions of no cohesion and the friction angle being at residual are justified as the trace of the main scarp is visible in Alberta aerial photograph AS1996 #223 (1979) and AS3895 #97 (1989), indicating pre-1995 landslide movement. Further, gypsum crystals were found in vertical fractures near the main scarp indicating the fractures had been open for some time.

With the preceding assumptions, equation 2.2 and 2.3, respectively, can be simplified to

$$\tan\Psi_f = \tan(\Phi-\Psi_p)(\gamma_r-\gamma_w)/\gamma_w = 1.13\tan(\Phi-\Psi_p)$$ (eq. 2.4)

(Cruden, 1999),

and $\qquad \tan\Psi_{fp} = \tan\Phi(\gamma_r-\gamma_w)/\gamma_r = 0.53\tan\Phi$ (eq.2.5)

(D.M. Cruden, personal communication, February 2000).

The values of the different variables are as follows: Ψ_p of between 0 and 7° (the rupture surface would intersect the surface if Ψ_p exceeds 7°), Ψ_f of 9.0°, and γ_r of 20.9 kN/m³ (average γ_r from the Montagneuse (Cruden et al., 1993) and Saddle River (Cruden et al., 1997) landslides). The calculated Φ_r values form table 2.5.

Table 2.5: Estimated friction angles versus rupture surface slopes.

Equation 2.4

Ψ_p	0	1	2	3	4	5	6	7	8
Φ_r	7.9	8.9	9.9	10.9	11.9	12.9	13.9	14.9	15.9

Equation 2.5

Ψ_{fp}	7	8
Φ_r	13.0	14.9

Equation 2.4 produces results consistent with the empirically derived results from the Hines Creek (Lu et al., 1998) and Saddle River (Cruden et al., 1993) landslides (Table2.4), with Ψ_p

values of between 2.0 and 4.2°. Equation 2.4 is also consistent with Skempton (1985) with Ψ_p values greater than 4.5°. Equation 2.5 produces results consistent with Skempton (1985), and the lower bound of values from equation 2.5 (Table2.5) is similar to the high Φ_r value from the Hines Creek (Lu et al., 1998) landslide. Equation 2.5 produces results inconsistent with Φ_r from the Saddle River (Cruden et al., 1998) landslide.

The true Φ_r for the Spirit River landslide is likely similar to the Φ_r of the till at the Saddle River landslide (10.9°) (Cruden et al., 1993), as the two soils have similar material properties (Tables 2.2 and 2.3). A Φ_r of 10.9° for the Spirit River landslide will have a Ψ_p of 3° (Figure 2.11).

To better define the Φ_r value, Ψ_p might be determined by drilling and the till might be shear tested.

2.6.4 Landslide Volume

The volume, VOL, in m³, of this landslide was calculated as follows:

$$VOL = 1/6 \ (\pi \ D_r \ W_r \ L_r)$$

(eq. 2.6)

(Cruden and Varnes, 1996, p. 42).

With the depth of rupture surface values (D_r) being between 20 m to 60 m (for Ψ_p of 7° and 0° respectively), the width of the rupture surface (W_r) being 1800 m (from Figure 2.11), and the length of the rupture surface (L_r) being 550 m (from Figure 2.11), the volume is calculated to be between 10.4 and 31.1 Mm³.

The use of equation 2.6 implies that the landslide can be characterized by a half ellipsoid. The manner in which the rupture surface daylights at the margins of the landslide, suggests that the half ellipsoid is a reasonable characterization for the Spirit River landslide. Nonetheless, the possibility remains that a triangular prism (i.e. eq. 3.6, section 3.6.4) would better approximate the landslide's volume. For comparison, equation 3.6 produces a volume of between 11.7 and 45.2 Mm³ (for Ψ_p of 7° and 0° respectively, with the depth of the rupture surface beneath the bottom of the valley of 3 m, and with the distance of the main scarp behind the former crest of the slope of 80 m).

2.6.5 Landslide Description and Kinematics

The 1995 landslide consists of two main blocks (Figures 2.10 and 2.11, and Figure 2.12). The lower block is 300 m long and 1800 m wide, and was translated in a south-southwesterly direction, for less than 15 m, during the 1995 landslide event. No tilting of the forest cover occurred, due to the displacement of the lower block, therefore the rupture surface beneath the block is assumed to be planar and deep. The margins of this block are coincidental with the margins of the previous (pre-1945) landslide; therefore, the movement of this block likely represents a reactivation of the earlier landslide. The upper block is 150 m long and 730 m wide, and was translated in a south south-westerly direction and rotated backward by about 1° to 2° (based on the depth of a pond, located near the start of the surveyed transect – the area had previously been kept drained by a ditch), during the 1995 landslide. The backward rotation is indicative of a curved rupture surface beneath this block. The backward rotation caused the height of the main scarp (average 6.8 m) to be greater than the uphill facing scarp (1.2 m at the surveyed transect), and ponding to occur against to both scarps. As this block had not previously moved, its movement would represent retrogression.

Between the upper and lower blocks, several smaller blocks were seen (block "C" in Figure 2.12). These small blocks exhibit backwards rotation greater than that of the upper block. The conditions for the formation of these smaller blocks were likely created by the backwards rotation of the upper block; whereby, the rotation of the upper block would have caused constriction near the rupture surface and tension near the surface. The smaller blocks would have then rotated backwards, possibly along a pre-existing rupture surface, filling the gap between upper and lower blocks.

The location of the rupture surface, at the toe of the landslide, was indicated by either a pressure ridge or a thrust block. Each pressure ridge appears as a discontinuous, elongated, almost symmetrical ridge, up to 10 m high, and composed of loose material at the angle of repose. In areas where the Spirit River has eroded into the pressure ridges, the rupture surface could be directly observed (i.e. at kms 8.8, 9.5, and 9.9 (Figure 2.13)). The sole thrust block, at km 10.4, is an asymmetric ridge, with forest vegetation draping the landslide side of the ridge and tilting towards the crown of the landslide (Figures 2.14, and 2.15). The slope on the landslide side (north) of the thrust block's ridge is about 20°; the opposite slope is close to vertical.
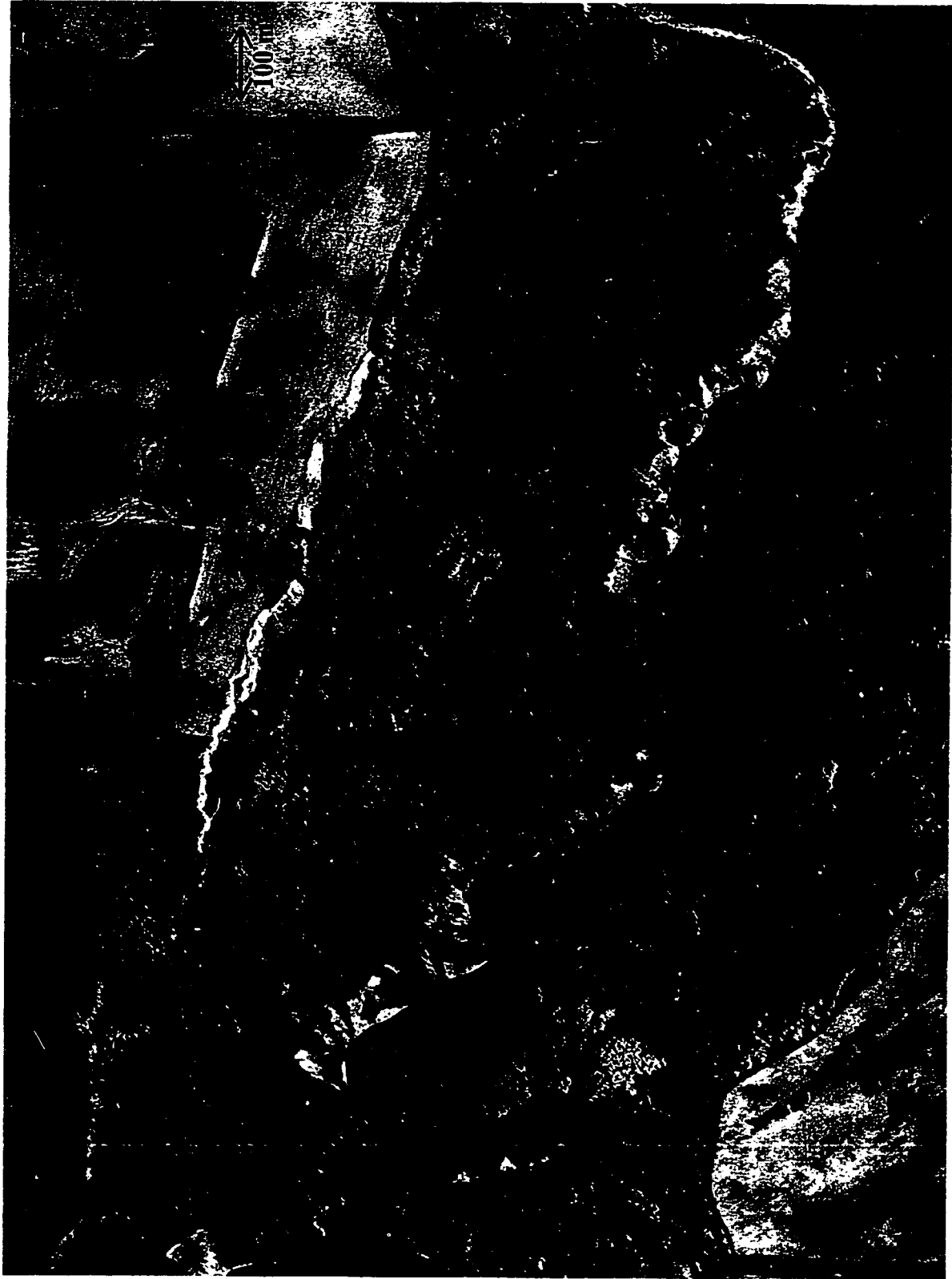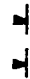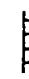
Figure 2.10: 1995 Aerial photograph of the Spirit River landslide (Alberta, AS4680#32; scale 1:6,400).

27

List of Symbols

Breaks in Slope:

- ▼▼▼   -   Concave Sharp
- ⊥ ⊥   -   Concave Rounded
- ▼▼▼   -   Convex Sharp
- ▼ ▼   -   Convex Rounded
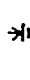
Scarps (length of line gives an indication of length of slope):

- ⊤ ⊤   -   Rounded
- ⊤⊤⊤   -   Sharp
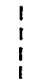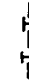
Small Mass Movements:

-   -   Flow
-   -   Translational Slide
-   -   Unclassified Landslide

Streams and Lakes:

- ————   -   Channel
-   -   Abandoned Channel
- ⟶   -   Small Stream
-   -   Lake
-   -   Marsh

Other Symbols:

- – – – –   -   Landslide Boundary (approximate)
- ≫≫   -   Pressure Ridge
- ↦   -   Thrust Block
- ⊤–⊤–   -   Tension Crack
- A⌐ ⌐A'   -   Cross-Section
- ◀   -   Distance Marker (km)
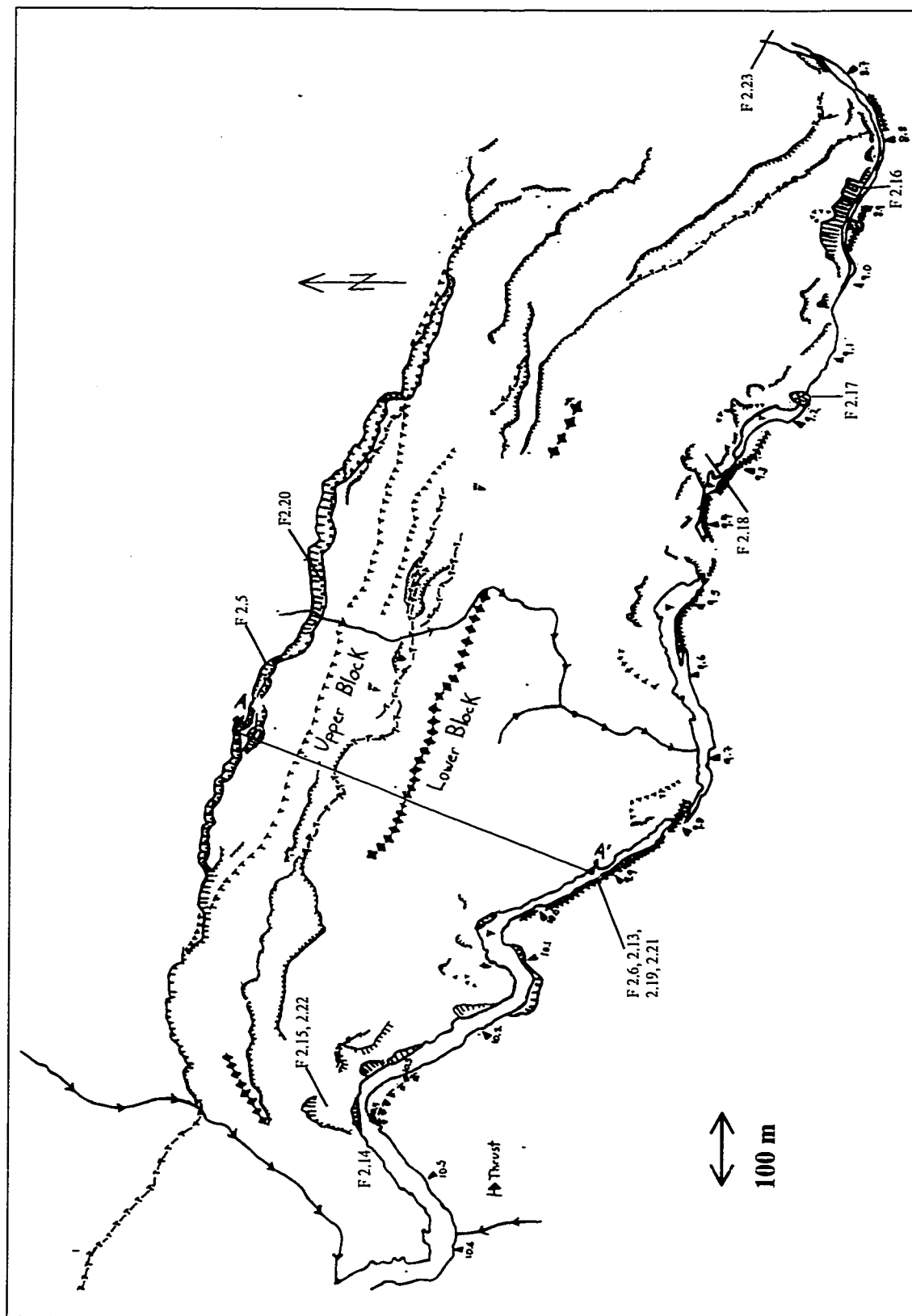
Figure 2.11: Interpretation of aerial photograph Alberta, AS4680#32, with the location of figures (F) indicated (scale 1:6,400; symbols after Cruden and Thomson, 1987).
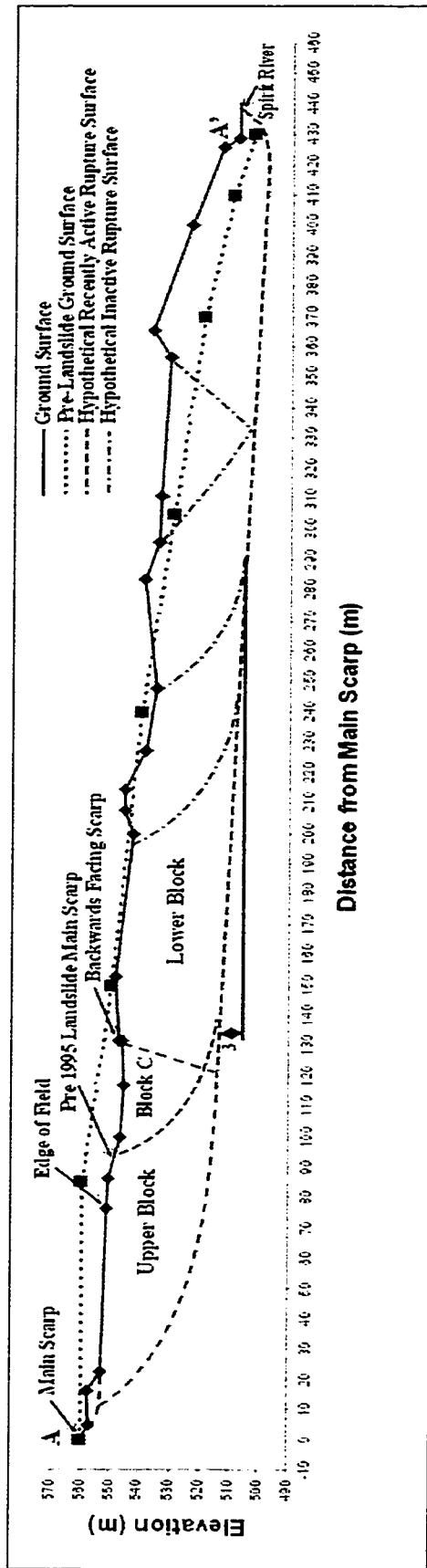
Figure 2.12: Cross-section of the Spirit River landslide (scale 1:1700; pre-landslide topography from Alberta base map 83M/16SW).
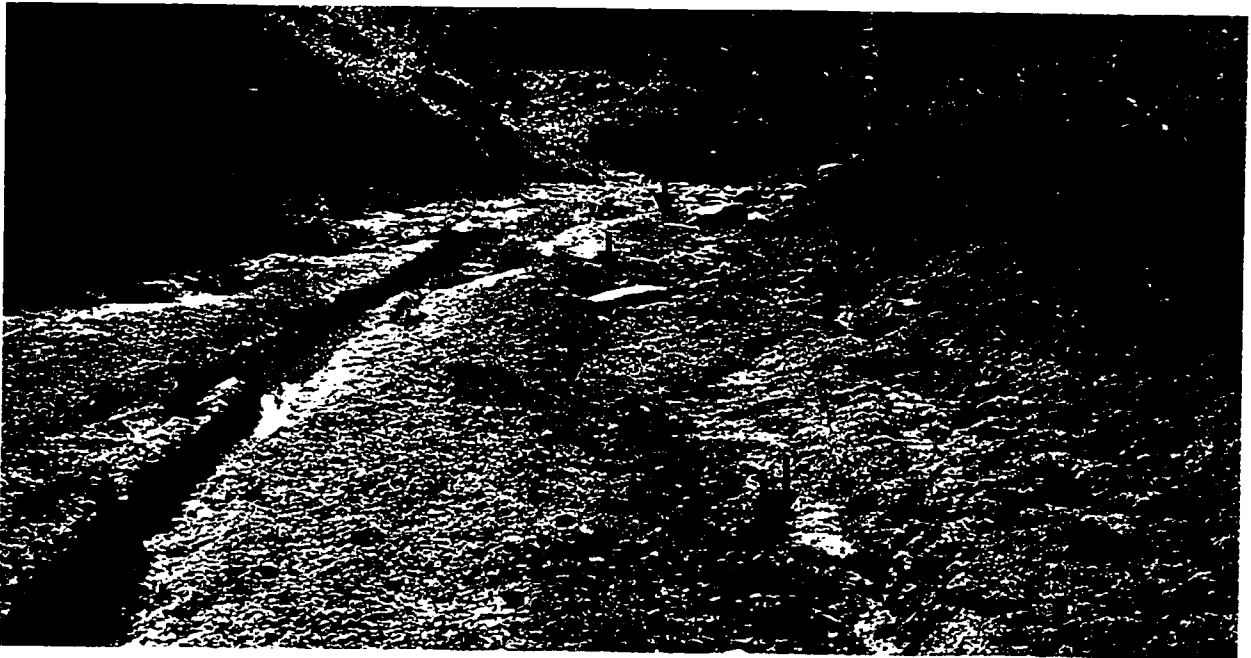
Figure 2.13: Pressure ridge (right and background) eroded by the Spirit River, exposing the rupture surface (arrows) (at km 9.9, looking east).

Figure 2.14: Thrust block (movement towards right; arrow marks ridge) riding over forest (right of arrow) (at km 10.4, looking east).
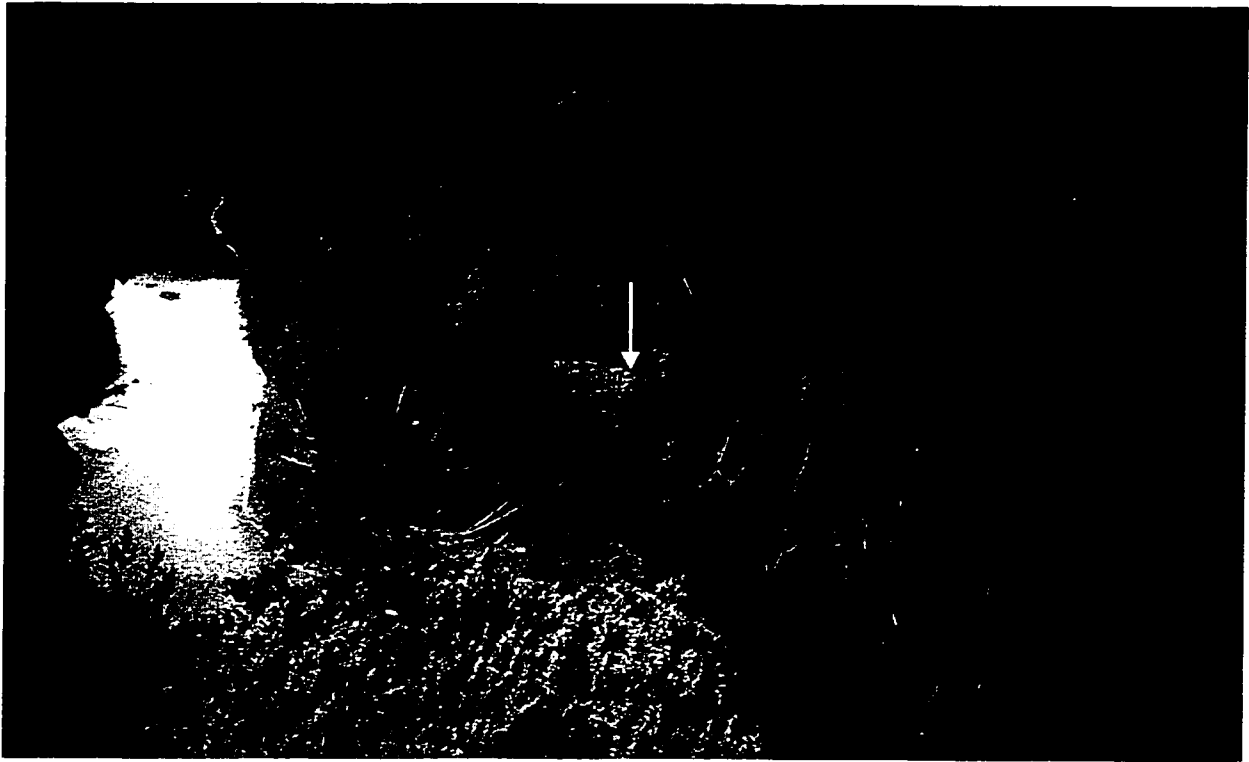
Figure 2.15: Thrust block at km 10.4 (arrow marks ridge; photo from left bank looking downstream).

2.6.6 Landslide Classification

Aerial photographs (Appendix 1) were used to assess the rate of movement of the landslide prior to 1995. The landslide shows no signs of movement between 1945 and 1974, suggesting that the landslide was likely dormant. The first indication of activity of the landslide is from a July 1979 aerial photograph (Alberta, AS1996#223) - the trace of the main scarp was apparent. From July 1979 to July 1995 movement of the landslide was sporadic, with activity during particularly wet springs (P. Nedohin, personal communication, July 2000). While active, the rate of movement would likely have been very slow or slower (less than $5.0*10^{-8}$ m/s or 1.6 m/month). For July 1995, the rate of movement of the landslide is also unknown, but it was likely moderate ($5.0*10^{-6}$ m/s (13 m/month)) or faster. A rate of movement lower than moderate would have been noticed by P. Nedohin while tending his crop; he visited the area at least once a fortnight (personal communication, July 2000). A rate of movement lower than extremely rapid (5 m/s) can also be presumed, as there was very little disturbance to the forest vegetation in front of, or behind the main scarp, after the landslide (Figure 2.1). Extremely rapid movement would have likely caused trees to snap. The current state of activity of the main body of the landslide is unknown.

32

The landslide exhibited little rotation of the upper block, and no rotation of the lower block; therefore, the landslide is a translational block slide. The lower block may have moved along the same rupture surface in 1995, as had the previous (pre-1945) landslide; if so, the slide can be described as reactivated. As the upper block had not moved prior to 1979, the movement of this block would constitute retrogression. If the upper block remained in contact with the lower block, and the two blocks shared a rupture surface, the style of activity can be described as multiple.

The 1995 landslide might also be described as enlarged rather than reactivated and retrogressive. The enlarged descriptor is applicable if the 1995 landslide's rupture surface is beneath the rupture surface of the previous landslide. Evidence for this scenario is the observation of two recently active rupture surfaces at km 8.8. The upper of the two rupture surfaces was traced up the slope to near the contact of the upper and lower blocks.

The material comprising the slide can be described as earth, as greater than 80% of the material is finer than coarse sand (Figure 2.9).

It is likely that the water table was at, or near, the surface prior to the 1995 slide. Evidence for this included ponds within 50 m of the 1995 main scarp in Figure 2.1, and a verbal account of a wet spring and early summer from P. Nedohin (personal communication, July 2000). As such, the landslide is described as wet.

The 1995 Spirit River landslide was a reactivated and retrogressive, or enlarged, multiple, wet, earth slide.

2.6.7 Successive Landslides

At the toe of the 1995 landslide, soil falls, due to the stream over-steepening the banks, are common (Figure 2.16). In addition to the soil falls, a slide-flow was observed at km 9.2 (Figure 2.17), which dammed the stream (Figure 2.11), and a reactivated rotational slide was observed at km 9.3 (Figure 2.18). The pressure ridges, in the valley bottom, are susceptible to instability, as they are composed of loose, broken-up soil, and have been over-steepened by stream erosion (Figure 2.19).

Figure 2.16: Soil fall at km 8.8 (looking east).
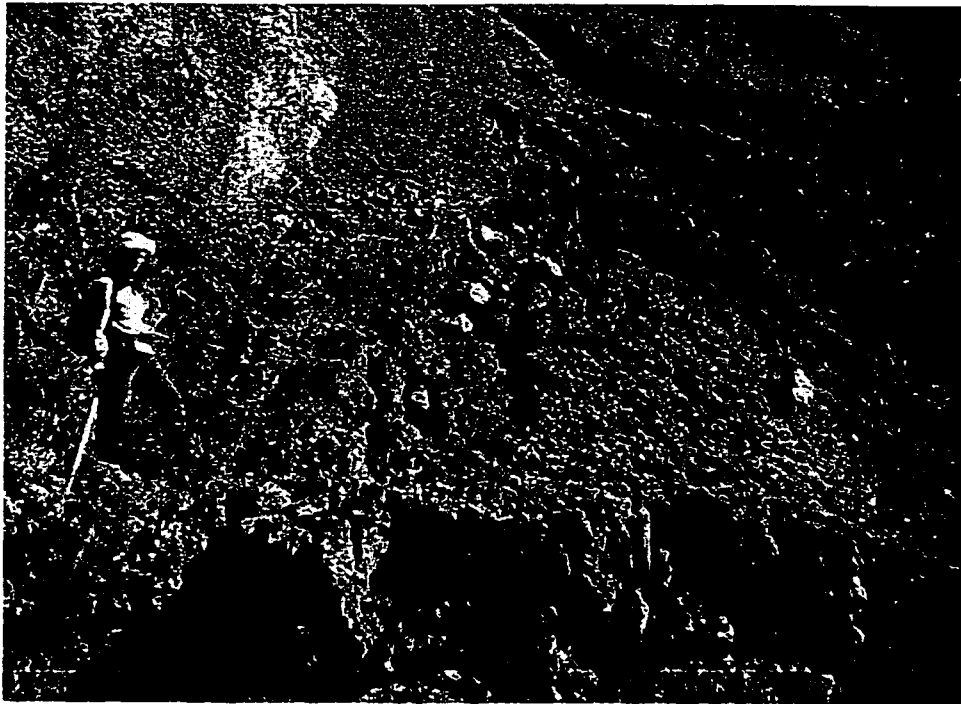
Figure 2.17: Slide-flow at km 9.2 (looking east).

Figure 2.18: Reactivated rotational slide at km 9.3 (looking west).

Figure 2.19: Instability in pressure ridge at km 9.9 (looking south).

At the crown of the landslide, instability, in the form of slide or fall, is common. Where the main scarp transects the field, rotational slides are most prevalent. Substantial main scarp regression has occurred since July 1995, in fielded areas along the main scarp, and is continuing (tension

cracks were evident in several locations). Instability in forested areas along the main scarp is predominantly in the form of soil topple-fall or fall (Figure 2.20). Main scarp regression is less pronounced in the forested areas.

Figure 2.20: Soil topple-fall in wooded area along the main scarp (near the centre of the main scarp, looking west).

2.7 Landslide Dams

2.7.1 Introduction

The 1995 landslide dammed the Spirit River at four locations, km 8.8, 9.3, 9.5, 9.8. A fifth landslide dam (Figure 2.17), evident at km 9.2 (Figure 2.11), was not directly related to the July 1995 landslide. The following section discusses the status of the landslide dams (2.7.2), the types of landslide dams (2.7.3), and the effects of the landslide and dam on river processes, upstream (2.7.4), downstream (2.7.5), and at the landslide (2.7.6).

2.7.2 Status of the Landslide Dams

Four of the five landslide dams (including the dams at km 9.2, 9.3, 9.4, 9.8) are visible on the Alberta aerial photograph AS4680 #32 (September 19, 1995), which was taken approximately 75 days after the landslide event. The dam at km 8.8 was not visible, as this area was shaded when the aerial photograph was taken (Figure 2.10).

The dam at km 8.8 was reported washed out in the spring of 1996 (personal communication to D.M Cruden, from J. Gulick, Transportation Supervisor, Municipal District 19, on 16 July 1997, in Cruden, 1997). Therefore, the longevity of this dam was less than one year.

At the time of my field survey, in July 1999, the dams at km 9.2, 9.3, and 9.4 had already been breached or eroded; thus, the longevity of these dams was less than four years. The dam at km 9.8 was still in existence in July 1999, though the extent of flooding, associated with the dam, had decreased significantly since the 1995 aerial survey.

The reservoir length behind the dam at km 9.8, in 1995, was 2100 m (from Alberta aerial photograph AS 4680 #32), which corresponds to a depth of approximately 9 m. No indications of further upstream flooding (i.e. lacustrine deposits, or debris in the bark and branches of trees) could be found during July 1999 field survey, thus it is assumed that the upstream extent of the reservoir, depicted in the September 1995 photograph, was the maximum reservoir length. By July 1999, the length of the reservoir was 700 m (100 m of the length reduction was from the downstream end of the reservoir). This corresponds to a dam height of about 3 m, of which 0.5 m to 1 m is a beaver dam (Figures 2.13 and 2.21). The greater resistance to erosion of this dam, as opposed to the dams at km 8.8, 9.2, 9.3, and 9.4, may be due to the combined effect of the beaver dam and a remnant patch of alluvium at km 9.8 (Figure 2.13, far ground).

2.7.3 Landslide Dam Types

The landslide dam at km 8.8 was estimated to be 8 to 10 m (Cruden, 1997). Two rupture surfaces were identified in the vicinity of this dam. One rupture surface daylighted above the stream, while the other rupture surface extended under the stream and daylighted on the opposite side to the landslide, forming a pressure ridge. The upper rupture surface was traced upslope to near the margin of the lower and upper blocks. A landslide dam resulting exclusively from the lower rupture surface would be a type 6 landslide dam (one or more rupture surfaces that extend under

the stream and emerge on the opposite valley wall) (Costa and Schuster, 1988). A landslide dam resulting from exclusively the upper rupture surface would be a type 1 (colluvium that does not span the valley floor) or a type 2 (colluvium that spans the entire valley floor) landslide dam (Costa and Schuster, 1988). The dam at km 8.8 would therefore, have been a combination of types 1 and 6, or types 2 and 6.

The landslide dam at km 9.2 was due to a small flow slide within the colluvium of the 1995 landslide, at the toe of the 1995 landslide (Figure 2.17). This event formed a type 2 dam, about 2 to 3 m in height.

The landslide dams at kms 9.3 and 9.4 and 9.8 are due to pressure ridges that cross the stream. These dams are of type 6. Their heights are between 8 and 12 m. The pressure ridge forming the landside dam at km 9.8, follows the valley bottom for 250 m (Figures 2.13 and 2.21). The stream has cut a new channel to the north of the pressure ridge. There is little coarse alluvium within the new channel, along this section of the stream, except where the new stream has eroded through the pressure ridge (Figure 2.13 far ground). The bulk of the alluvium likely remains buried beneath the pressure ridge.

Figure 2.21: Remnants of pressure ridge dam at km 9.8 (arrow points at a beaver dam; at km 9.9, looking upstream).

38

2.7.4 Upstream Fluvial Geomorphic Effects of the Landslide and Dams

With the exception of the areas that were inundated with reservoir floodwaters, in which lacustrine mud (Figure 2.22) and deltaic sand were deposited, there were no apparent upstream effects of the landslide or landslide dam. Deltaic sands extended about 75 m beyond the head of the reservoir.
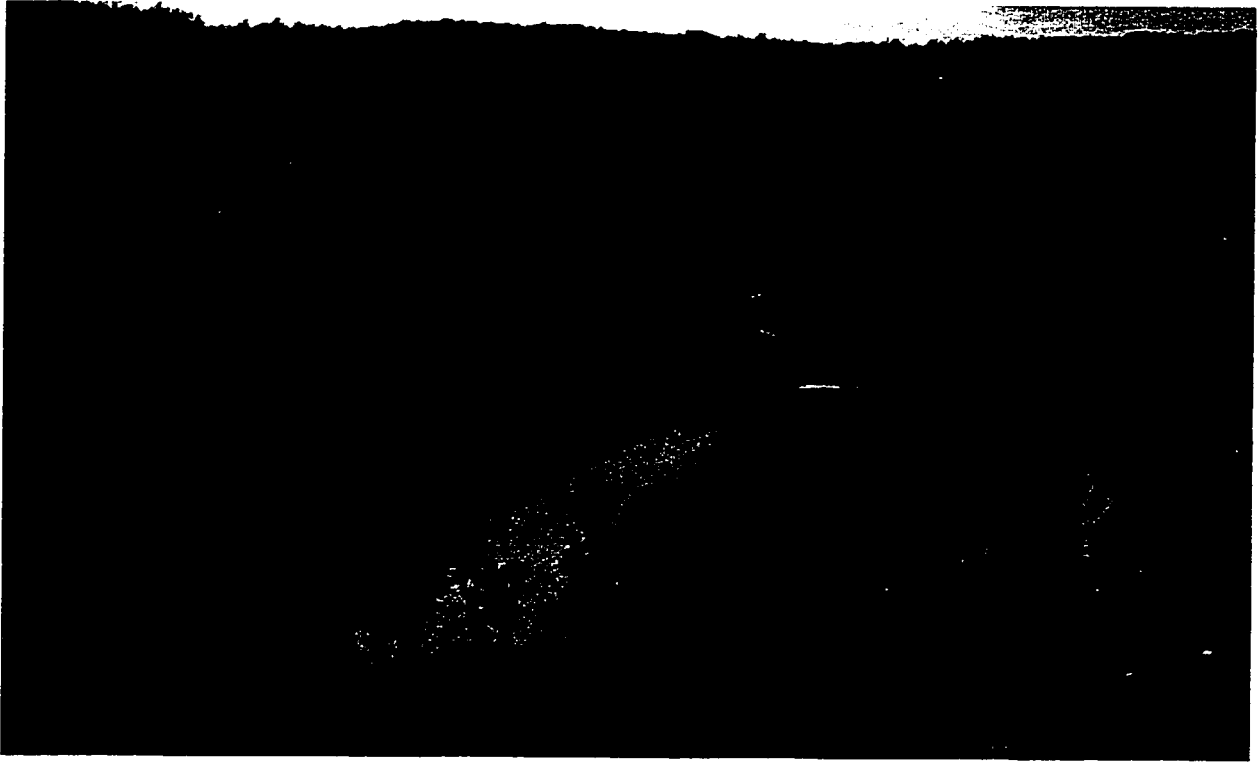
Figure 2.22: Lacustrine mud in reservoir behind km 9.8 dam (at km 10.4, north of the river, looking upstream).

2.7.5 Downstream Fluvial Geomorphic Effects of the Landslide and Dams

When the 1989 pre-slide aerial photographs (Alberta, AS 3895) are compared to the 1995 post-slide aerial photographs (Alberta, AS4680), streambed aggradation downstream of the landslide is evident (including a widening of the channel, and a mantling of the point bars with sediment). A field traverse downstream of the landslide, in July 1999, found that the river had removed most of the in-channel detritus, and mostly coarse alluvium remained. The point bars bore witness to the post-landslide streambed aggradation, as up to 1-m deposits of mostly gravel-sized mud balls interspersed with rock alluvium, were maintained (Figure 2.23). Mud ball alluvium was seen

downstream of other landslides in the vicinity, including the Eureka River landslide (Figure 3.20). Vegetation was recolonizing the point bars. A further pulse of sediment is expected, following the breach of the dam at km 9.8.
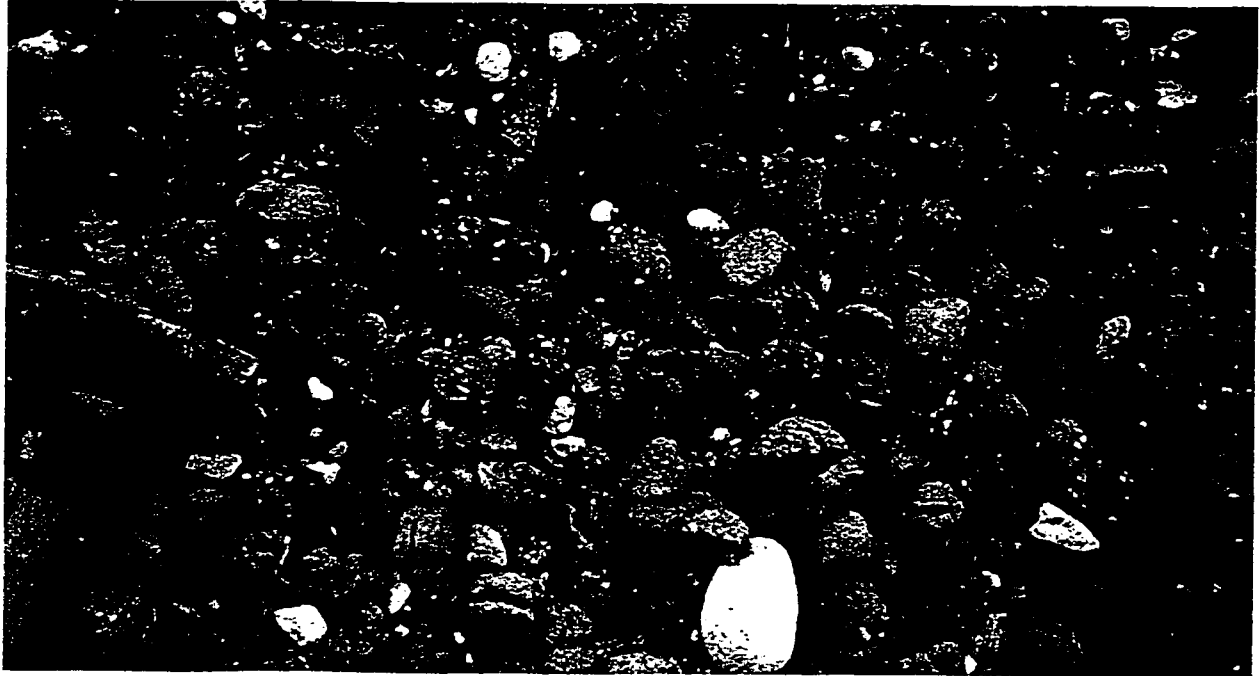
Figure 2.23: Landslide generated mud ball and stone alluvium (photo from the front of a stream eroded point bar at km 8.5).

2.7.6 Fluvial Geomorphic Effects of the Landslide and Dam at the Landslide

Between km 8.8 and 9.9, coarse alluvium was virtually absent. Isolated pockets of coarse alluvium were seen (i.e. at kms 9.5, 9.7, and 9.8); though these, with the exception of the coarse alluvium at km 9.8 (Figure 2.13 far ground), are no longer within the contemporary stream channel, therefore, they provide no resistance to erosion. The pre-landslide armour, assuming it existed, could have been displaced (as occurred at kms 9.5 and 9.7), destabilized and entrained, or buried (as likely occurred between km 9.8 and 9.10). Until armour is re-established, the streambed is susceptible to erosion.

2.8 Discussion on Possible Triggers for the Landslide

3.7.1 Introduction

The conditions for the Spirit River landslide were created by streambed incision in response to a lowering of the base level, the Peace River. Accompanying the streambed incision was the softening of the slope due to the lateral and vertical unloading (Imrie, 1991; Matheson and Thomson, 1973). Movement in the landslide was evident since 1979 (Alberta aerial photograph AS1996#223). Nonetheless, the greatest landslide displacement occurred in July 1995. Within this section I explore possible triggers for the July 1995 event, including seismic triggers (2.8.2), and hydrologic triggers (2.8.3). This is not an exhaustive list but, rather, includes the most likely candidates.

2.8.2 Seismic Triggers

Information from the Canadian National Seismological Database, via their interactive web site, revealed that there were no earthquakes, which could be invoked as the trigger for the 1995 Spirit River landslide. The inputs for this query, were as follows: date: 12 July 1989 to 19 September 1995 (pre and post-landslide aerial photographic survey dates); latitude: 54° to 57°; longitude: -120 to -116°. Another query using an expanded geographical area (latitude: 52.80° to 58.80°; longitude: -121.50 to -115.50) was also performed; the results were also negative.

2.8.2 Hydrologic Triggers

The hydrologic triggers discussed are a decrease in slope toe support due to streambed incision, and an increase in the slope pore water pressure due to an elevation of the water table.

Keegan (1992) and Lu et al., (1998) attribute the triggers for Saddle River and Hines Creek landslides, respectively, to stream incision during a major storm, which occurred in mid June 1990. A storm trigger causing the Spirit River landslide is not obvious. When the maximum daily discharge of the Saddle River (the neighboring watershed) for 1995, is compared to records from 1967 to 1998, the 1995 datum is near the median (Environment Canada, Water Survey of Canada, Saddle River near Woking, 1998) - Saddle River data were used, as the Spirit River is not hydrologically monitored. Although, the maximum daily (24.2 m^3/s) and instantaneous (37.4 m^3/s) discharge for 1995 occurred on July 5, approximately when the landslide occurred.

41

Precipitation data from Grande Prairie Alberta (Environment Canada, Climate Service, Grande Prairie Airport, 1998) show above average precipitation for July 1995 (total 114.6 mm, mean 67.2 mm, rank 4/32 (1967-1992), median 58.5 mm). The effect of the above average precipitation on the water table was likely minimal as perennial wetlands exist within 100 m of the landslide main scarp, though some water table elevation is indicated (Figure 2.1). Pre-1995 movement of the landslide was observed to coincide with wet weather (P. Nedohin, personal communication, July 2000); thus, as the July 1995 landslide event is concurrent with the above average precipitation, elevated pore pressure is likely an important factor in the landslide occurrence.

An examination of long-term hydrologic trends was performed to see if land cover changes, due to human activities, have affected stream discharge, following the work of Laycock (1990). He suggested that agricultural practices, in the Peace River Lowlands, have increased the flow, and hence the erosive potential, of streams. Laycock attributed the flow increases to decreases in transpiration, due to the replacement of the natural forest with grain crops, coupled with agricultural land drainage. He calculated that there was a five-to ten-fold increase in water surplus, between 1971 and 1987, in agricultural areas near Grande Prairie, due to agriculture. Confirming these results in the Spirit River watershed is not possible, as the Spirit River is not gauged. The neighboring watershed, the Saddle River, is gauged and my attempt to confirm Laycock's (1990) thesis through a comparison of land cover (Canada, Energy Mines and Resources. 1994; Canada, Mines and Technical Survey, 1963), stream flow (Environment Canada, Water Survey of Canada, 1998) and precipitation data (Environment Canada, Climate Services, 1998) concluded that the empirical data do not support that hypothesis for the Saddle River (Section 4.0). There was no evidence of an anthropogenic increase in streamflow.

2.9 Conclusions

1. Two surficial units were recognized in the field at the Spirit River landslide, a glacial lacustrine unit, and a diamicton (assumed to be till). The rupture surface of the 1995 landslide was within the till, 60 m below the upland plain. The Spirit River, at the site of the landslide, is likely excavating into a preglacial channel.

2. Aerial photographs show evidence of large prehistoric landslides in the lower Spirit River watershed, to km 12.8 on the north (left) bank, and 14.1 on the south (right) bank. A relatively

steep longitudinal slope, relatively gentle valley slopes, and a straight channel characterize this lower reach. Upstream of the lower reach, the longitudinal slope lessens, the valley slopes steepen, and the river meanders. The Spirit River landslide is near the upstream extent of the lower reach.

3. The interval between the large landslides in the watershed is at least 55 years, and likely substantially longer.

4. The July 1995 Spirit River landslide was a reactivated and retrogressive, or enlarged, multiple, wet, earth slide, which traveled in a south-southwesterly direction for less than 15 m. The estimated volume of the landside is between 10.4 and 31.1 Mm^3, based on rupture surfaces sloping of 7° and 0° respectively. The friction angle for the landslide was estimated to be between 7.9° and 17.8°. The true friction angle is likely similar to that from the till at the Saddle River landslide, 10.9°, as the two landslides are have similar till material properties (texture and Atterberg limits), and are located within 4.2 km of each other. The present state of activity of the main body of the landslide is unknown; however, instability at the crown and at the toe is common.

5. The July 1995 Spirit River landslide dammed the Spirit River at km 8.8, 9.3, 9.5, and 9.8. All of these dams were type 6 dams, with the exception of the dam at km 8.8, which was a combination of type 1 and 6, or 2 and 6. Another dam, at km 9.2, was due to a slide-flow within the colluvium of the 1995 landslide, and is a type 2 dam. The dam at km 8.8 was breached within one year. The dams at kms 9.2, 9.3, and 9.5 were breached within 4 years of the landslide. The dam at km 9.8 is still in existence, though the associated reservoir has shrunk from approximately 2,100 m to approximately 700 m length. The height of the dam has decreased from approximately 9 m to approximately 3 m.

6. Fluvial geomorphic effects of the landslide and dams are varied. Upstream effects, including the deposition of lacustrine and deltaic sediments, are limited to those areas inundated with the reservoir floodwaters. Downstream effects involve the passage of pulses of detritus from the landslide, and from the remobilization of the lacustrine and deltaic sediments, when dam breach occurs. At the landslide, the greatest effect was the breakage, burial or removal of the streambed armour, leaving the stream susceptible to erosion.

7. Attempts to find a trigger for the 1995 Spirit River landslide proved inconclusive, but the above average precipitation in July 1995 is the most likely trigger. Triggering by an earthquake or changes in land use appears unlikely.

References:

Alberta, Environment. 1999. Provincial base map 83M/15SE. 1:20,000, Edmonton.

Alberta, Environment. 1999. Provincial base map 83M/16NE. 1:20,000, Edmonton.

Alberta, Environment. 1999. Provincial base map 83M/16SE. 1:20,000, Edmonton.

Alberta, Environment. 1999. Provincial base map 83M/16SW. 1:20,000, Edmonton.

American Society for Testing and Materials. 1998. Standard test methods for liquid limit, plastic limit, and plasticity index for soils (D4318-95a). 04.08: 519-529.

American Society for Testing and Materials. 1998. Standard test methods for particle-size analysis of soils (D422-63). 04.08: 10-19.

Bidwell, A.K. 1999. The Engineering Geology of the Fort St. John Area. Master of Engineering. Report, Department of Civil and Environmental Engineering, University of Alberta, Edmonton.

Bobrowsky, P.T., Catto, N., and Levson, V. 1990. Reconnaissance Quaternary Geological Investigation in Peace River District, British Columbia (93P, 94A). British Columbia Geological Survey, Victoria, British Columbia, Paper 1991-1.

Brooker, E.W. 1959. Dunvegan Landslide. Alberta Research Council, Edmonton, Open file Report 1959-6, Edmonton.

Bruce, I.G., Cruden, D.M., and Eaton, T.M. 1989. Use of tilting table to determine the basic friction angle of hard rock samples. Canadian Geotechnical Journal, 26: 474-479.

Canada, Energy Mines and Resources. 1990. Codesa, Alberta. Map 83M/16, 1:50,000, Ottawa.

Canada, Energy Mines and Resources. 1994. Grande Prairie, Alberta. Map 83M, 1:250,000, Ottawa.

Canada, Energy Mines and Resources. 1990. Rycroft, Alberta. Map 83M/15, 1:50,000, Ottawa.

Canada, Environment Canada, Climate Services. 1998. Canadian Monthly Climate Data, CD. Grande Prairie, Alberta. Ottawa.

Canada, Environment Canada, Water Survey of Canada. 1998. HYDAT, CD. Saddle River Near Woking, Alberta. Ottawa.

Canada, Geological Survey of Canada. 2000. Canadian national seismological database. Website, http://www.seismo.nrcan.gc.ca/.

Canada, Mines and Technical Survey. 1963. Grande Prairie, Alberta. Map 83M, 1:250,000. Ottawa.

Carlson, V.A. and Hackbarth, D.A. 1974. Bedrock topography of the Grande Prairie Area, NTS 83 M, Alberta. Alberta Research Council Map, 1:250,000, Edmonton.

Catto, N.R. 1991. Quaternary geology and landforms of the eastern Peace River region, British Columbia NTS 94A/1,2,7,8. British Columbia Ministry of Energy, Mines and Petroleum Resources, Open File 1991-11, Victoria.

Catto, N.R., Liverman, D.G.E., Bobrowsky, P.T., and Rutter, N. 1996. Laurentide, Cordilleran and montane glaciation in the western Peace River – Grande Prairie Region, Alberta and British Columbia, Canada. Quaternary International, 32: 21-32.

Costa, J.E. and Schuster, R.L. 1988. The formation and failure of natural dams. Geological Society of America, Bulletin 100: 1054-1068.

Cruden, D.M. 1997. Field notes from Spirit River landslide, 15 and 16 July 1997, unpublished.

_____. 1999. Some forms of mountain peaks in the Canadian Rockies controlled by their rock structure. Quaternary International.

Cruden, D.M., Keegan, T.R., and Thomson, S. 1993. The Landslide Dam on the Saddle River near Rycroft, Alberta. Canadian Geotechnical Journal, 30: 1003-1015.

Cruden, D.M., Lu, Z-Y., and Thomson, S. 1997. The 1939 Montagneuse River landslide, Alberta. Canadian Geotechnical Journal, 34: 799-810.

Cruden, D.M. Ruel, M., and Thomson, S. 1990. Landslides along the Peace River, Alberta. Proceedings, 43rd Canadian Geotechnical Conference, 1: 61-67.

Cruden, D.M. and Thomson, S. 1987. Exercises in terrain analysis. University of Alberta.

Cruden, D.M. and Varnes, D.J. 1996. Landslides Types and Processes. In Landslides: Investigation and Mitigation. Transportation Research Board, National Academy of Science, Special Report 247, Washington, D.C.

Evans, S.G. 1986. Landslide Damming in the Cordillera of Western Canada. In Landslide Dams: Processes, Risk and Mitigation. American Society of Civil Engineers, Geotechnical Special Publication No. 3, New York.

Evans, S.G., Hu, X.Q., and Enegren, E.G. 1996. The 1973 Attachie Slide, Peace River Valley, near Fort St. John, British Columbia, Canada: A Landslide with a high-velocity flowslide component in Pleistocene sediments. Proceedings, 7th International Symposium on Landslides, Trondheim, Norway. A.A. Balkema, Rotterdam, 2: 715-720.

Hackbarth, D.A. 1977. Hydrogeology of the Grande Prairie Area. Alberta Research Council, report 76.4, Edmonton.

Hamilton, W.H., Langenberg, M.C., and Price, D.K. 1998. Geological map of Alberta. Alberta Research Council, map 1:1,600,000, Edmonton.

Hardy, R.M., Brooker, E.W., and Curtis, W.E. 1962. Landslides in over-consolidated clays. Engineering Journal, 45.6: 81-89.

Imrie, A.S. 1991. Stress-induced response from both natural and construction-related processes in the deepening of the Peace River valley, B.C. Canadian Geotechnical Journal, 28: 719-728.

Jones, J.F. 1966. Bedrock Geology of the Peace River district. Research Council of Alberta, Bulletin 16, Edmonton.

Keegan, T.R. 1992. The Rycroft landslide dam on the Saddle River, Alberta. Master of Science thesis, Department of Civil Engineering, University of Alberta, Edmonton.

Knighton, D. 1998. Fluvial Forms and Processes. John Wiley, New York: 205-207.

Laycock, A.H. 1990. Integrated Land Use and Water Management to Limit Erosion in the Peace River Region. In, Smith, P.J., and Jackson, E.L. (editors), A World of Real Places, Studies in Geography, University of Alberta, Edmonton: 115-132.

Liverman, D.G.E. 1991. Sedimentology and history of a Late Wisconsinan glacial lake, Grande Prairie, Alberta, Canada. Boreas, 20: 241-257.

Lu, Z.Y, Cruden, D.M., and Thomson, S. 1998. Landslides and Preglacial Channels in the Western Peace River Lowland. Proceedings, 51st Canadian Geotechnical Conference, Edmonton, Alberta, 4-7 October, 1: 267-274.

Matheson, D.S. and Thomson, S. 1973. Geological implications of valley rebound. Canadian Journal of Earth Sciences. 10: 961-978.

Mollard, J.D. 2000. Ice-shaped ring forms in western Canada: their airphoto expressions and manifold polygenetic origins. Quaternary International. In press.

Nasmith, H. 1964. Landslides and Pleistocene Deposits in the Meikle River Valley of Northern Alberta. Canadian Geotechnical Journal, 1: 155-166.

Norrish, N.I. and Wyllie, D.C. 1996. Rock Slope Stability Analysis. In Landslides: Investigation and Mitigation. Transportation Research Board, National Academy of Science, Special Report 247, Washington, D.C.

Ozoray, G. 1982. Hydrogeology of the Clear Hills-Chinchaga River area, Alberta. Alberta Research Council, Edmonton, Earth Sciences Report 82-4.

Pawlowicz, J.G. and Fenton, M.M. 1995. Bedrock topography of Alberta. Alberta Geological Survey, Map 226, Edmonton.

Rains, R.B., and Welsh, J. 1988. Out-of-phase Holocene terraces in part of the North Saskatchewan River basin, Alberta. Canadian Journal of Earth Sciences, 25: 454-464.

Rains, R.B., Burns, J.A., and Young, R.R. 1994. Postglacial alluvial terraces and an incorporated bison skeleton, Ghostpine Creek, southern Alberta. Canadian Journal of Earth Sciences, 31: 1501-1509.

Rutherford, R.L. 1930. Geology and water resources in part of Peace River and Grande Prairie districts, Alberta. Scientific and Industrial Research Council of Alberta. Report 21. Edmonton.

Schuster, R.L. and Costa, J.E. 1986. A Perspective on Landslide Dams. In Landslide Dams: Processes, Risk and Mitigation. American Society of Civil Engineers, Geotechnical Special Publication No. 3, New York.

Selby, M.J. 1993. Hillslope materials and processes. 2nd ed. Oxford, New York: 270.

Signal. 1995. Ten acres of canola slides. Newspaper. Ed. D. Zahara. Rycroft, 16, 31: 1.

Skempton, A.W. 1985. Residual strength of clays in landslides, folded strata and the laboratory. Geotechnique, 35,1: 3-18.

Skempton, A.W. and De Lory, F.A. 1957. Stability of natural slopes in London clay. Proceedings, 4th International Conference on Soil Mechanics and Foundation Engineering. London, 2: 378-381.

Thomson, S. and Hayley, D.W. 1975. The Little Smoky Landslide. Canadian Geotechnical Journal, 12: 379-392.

Thomson, S. and Morgenstern, N.R. 1977. Factors affecting distribution of landslides along rivers in southern Alberta. Canadian Geotechnical Journal, 14: 508-523.

3.0 Eureka River Landslide

3.1 Introduction

In June 1990 (Lindy Foster, Worsley resident, personal communication, 1999), Eureka River became dammed when its north bank, 11 km upstream of the Clear River confluence, slid southwards (Figure 3.1). The landslide was over 1 km wide, and involved an estimated 18.9 to 54.4 Mm^3 of surficial material. This landslide occurred in an unpopulated region, the nearest residence being several kilometres away, and there are no known witnesses to the event.

The first post-landslide aerial photography survey (Alberta, AS4333 #180), conducted on October 6, 1992 depicts a flooded region 6,300 m in length upstream of the landslide dam. At its peak, the dam was 20 m in height, causing flooding for 8,300 m upstream. The pre-landslide Eureka River channel had been thrust upwards by 20 to 25 m, indicative of a rupture surface extending beneath the valley bottom, making this a class 6 landslide dam (Costa and Schuster, 1988). The river has subsequently cut a new channel around the toe of the landslide, incising 20 m as of August 18, 1999. The reservoir was still in existence, as of August 1999, though its length had decreased to 1,800 m.

Within this chapter, I give background information (3.2), describe my methods (3.3), describe the stratigraphy observed at the landslide site (3.4), discuss slope instability within the watershed (3.5), describe the 1990 landslides (3.6), describe the landslide dam and its effects (3.7), and speculate on possible triggers for the landslide (3.8).
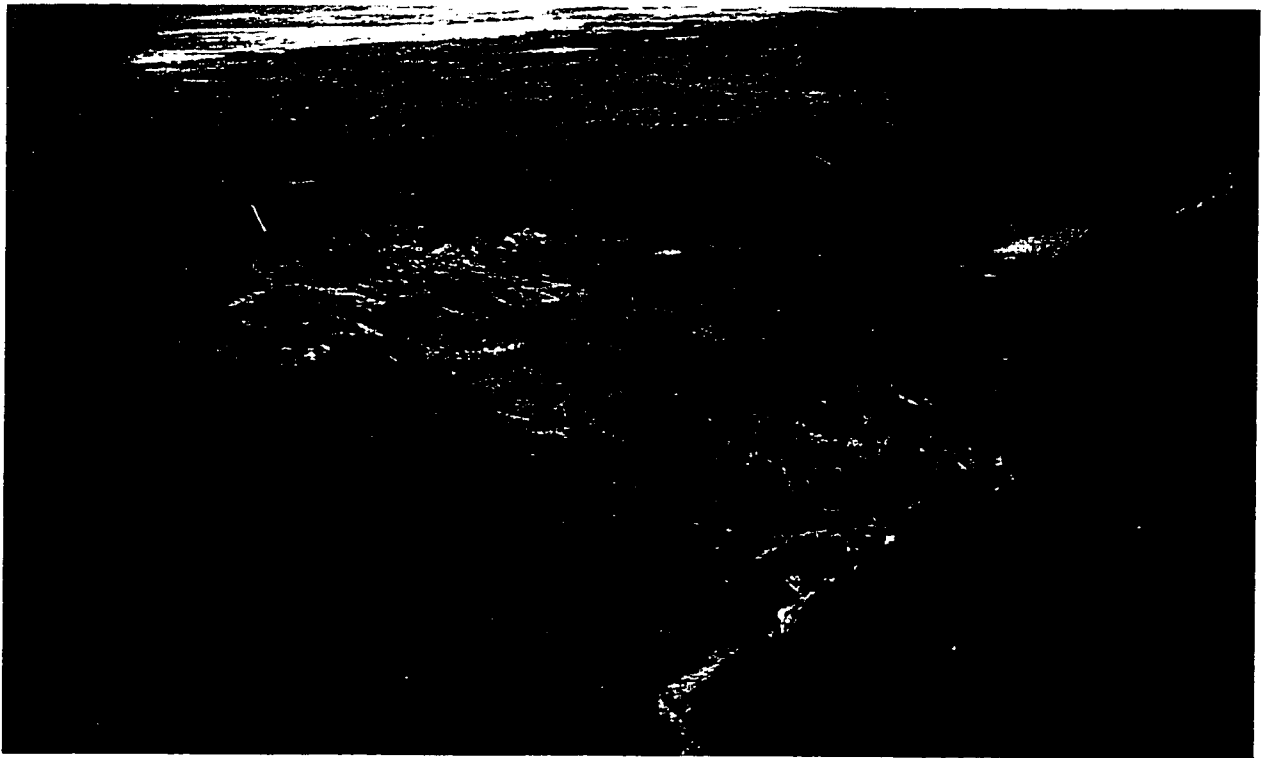
Figure 3.1: 1990 Eureka River landslide.

3.2 Background

3.2.1 Introduction

The background information discussed includes the following: landslide location (3.2.2), watershed physiography (3.2.3), channel form (3.2.4), surficial geology (3.2.5), and bedrock geology (3.2.6).

3.2.2 Landslide Location

The Eureka River landslide is located in 6 − 86 − 9 − 6W, on the north bank of the Eureka River, approximately 11 km from the confluence of the Eureka and Clear Rivers (Figure 3.2). The crown of the landslide is located at 56° 26' 00"N, 119° 24' 15"W, and 620 m.a.s.l. The toe of the landslide is at river level at 520 m.a.s.l., 100 m below the crown of the landslide. The National Topographic System (NTS) maps for the area include 1:50,000, Many Islands, Alberta (84D/6) and 1:250,000, Clear Hills, Alberta (84D). A more detailed map, of the site, is Alberta provincial base map, 84D/6NW (1:20,000).
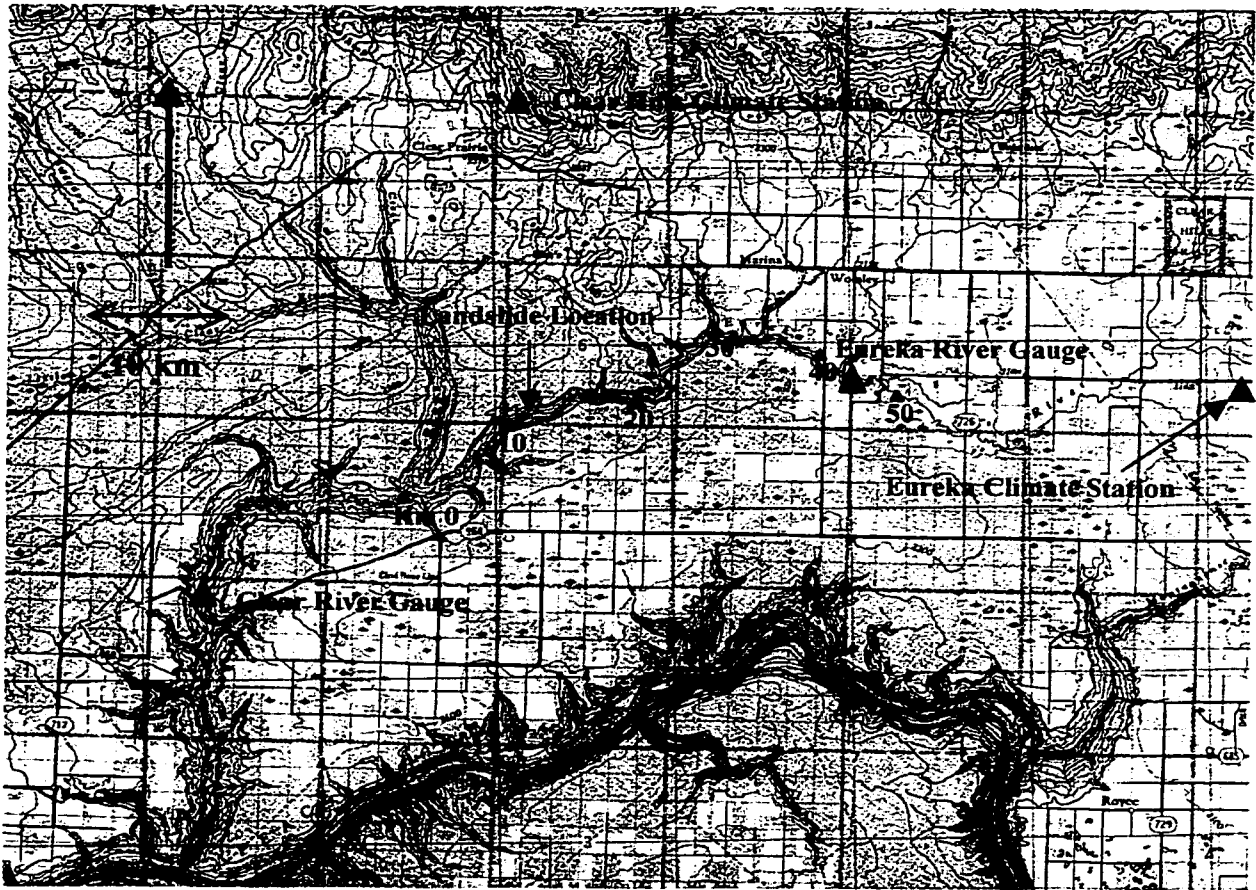
Figure 3.2: Eureka River Watershed (scale 1:460,000, NTS map 84D, 1977).

3.2.3 Watershed Physiography

The Eureka River watershed lies mainly within the Peace River Lowlands; a broad, gently undulating plain, dissected by steep gorges (Figure 3.2). The Eureka River flows within one of these gorges. The river's headwater is the Clear Hills (1035 m.a.s.l.) - "an undulating tableland dissected by deep and wide river valleys" (Ozoray, 1982 p.2). The Eureka River flows into the Clear River at 490 m.a.s.l., with the Clear River in turn, flowing into the Peace River at 375 m.a.s.l. The vertical drop of the Eureka River, from the headwaters to the mouth is 545 m. From the confluence of the Eureka and Clear Rivers (km 0) to km 99.2, the longitudinal slope of the river is $0.14°$; flattening to $0.04°$ at km 107 (distances measured along stream) (Figure 3.3).

3.3.4 Channel Form

From near the confluence of the Eureka and Clear Rivers to km 4.2 (497 m.a.s.l.) the Eureka River is meandering (nomenclature follows Selby, 1985). From km 4.2 to km 18.6 (538 m.a.s.l.), the channel form is straight by definition, as the sinuosity is less than 1.5 (Selby, 1985, p.268). Within this reach, the valley slopes come to the river's edge. From km 18.6 to 32.9 (570 m.a.s.l.) the channel is confined meandering in form. From km 32.9 to km 42.8 the channel is for the most part straight, with the exception of between 39.7 and 41.0, where the channel meanders. From km 42.8 to 60.6 (630 m.a.s.l.) the channel is meandering. Beyond km 60.6 the channel form was not classified. The river's headwaters are another 30 km upstream, at 890 m.a.s.l.

Changes in channel form are largely due to landslides. Reaches where large landslides are evident, are generally straight, and have low average valley slope angles (average of the right and left bank, taken from Alberta provincial base maps, where a contour crosses the stream) (Figure 3.3). Exceptions to this are stretches between km 0 and 4.2, and km 39.7 and 40.1, where the river's form is meandering. Between km 0 and 4.2, the channel form is likely due to the combination of stratigraphy and the geomorphology of the Clear River. The meandering reach between km 39.7 and 40.1 is mostly upriver of a region in which a landslide has occurred; thus, it is conceivable that the river is meandering atop lacustrine sediments deposited behind a landslide dam.
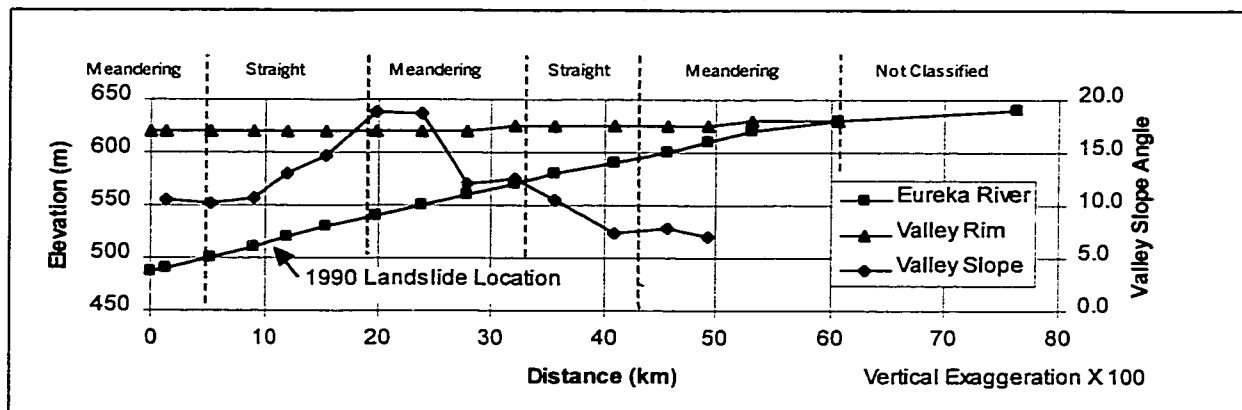
Figure 3.3: Eureka River channel form, longitudinal slope and average valley slope

3.2.5 Surficial Geology

Within the Peace River Lowlands region of the Eureka River watershed, surficial sediment thickness is between 40 and 75 m, except where preglacial valleys exist (i.e. the Shaftesbury channel (Pawlowicz and Fenton, 1995)), where sediment thickness can exceed 200 m (Kerr, 1971). At the site of the 1990 landslide, the depth to bedrock is at least 110 m from the upland plain, indicating that this site is within a preglacial valley. In the Eureka River headwaters, on the upland plains, sediment thickness ranges from 5 to 50 m (Ozoray, 1982).

The sediments filling the preglacial valleys were deposited during the up-drainage advance of the Laurentide ice sheet, and the subsequent down-drainage ice front retreat. These events deposited (from bottom up) preglacial lacustrine sediments, till, and postglacial lacustrine sediments atop, the preexisting fluvial sediments. Out of preglacial valleys, but within the Peace River Lowlands, sediment consists mainly of till with glaciolacustrine sediments atop (Ozoray, 1982; Jones, 1966). The till is described as "ground or hummocky dead-ice moraine" (Ozoray, 1982, p. 5). The postglacial lacustrine sediment is described as "mainly clay and silt with rafted debris" (Ozoray, 1982, p.5). Kerr (1971) also found approximately 15 m of gravel immediately atop the bedrock in the Worsley area. The uplands are mainly covered by till (Reader and Odynsky, 1965).

3.2.6 Bedrock Geology

Underlying the surficial deposits at the site of the 1990 Eureka River landslide are Cretaceous age rocks of the deltaic to marine Dunvegan Formation (Ozoray, 1982; Jones, 1966). This formation is characterized by "gray, fine grained feldspathic sandstone with hard calcareous beds, laminated siltstone and gray silty shale" (Ozoray, 1982, p.4). Above the Dunvegan Formation, outcropping at the Clear Hills (north of the landslide), are the Kaskapau, Bad Heart, Puskwasau, and Wapiti Formations (from bottom up). The Kaskapau Formation is composed of "dark gray silty shale, ... interbedded with fine-grained quartzose sandstone and thin beds of ferruginous oolitic mudstone" (Ozoray, 1982, p.5). The Bad Heart Formation is composed of "fine grained quartzose sandstone, ferruginous oolitic sandstone and mudstone" (Ozoray, 1982, p.5). The Puskwasau Formation is a "dark gray fossiliferous shale" (Ozoray, 1982, p.5). The Wapiti Formation is a non-marine "gray feldspathic clayey sandstone, gray bentonitic mudstone, [and] bentonite [unit with] scattered coal" (Hackbarth, 1977, p.3). The regional bedrock dip of these formations is towards the south at greater than 15 m/km (0.9°) (Hackbarth, 1977). Below the Dunvegan formation is the upper

member of the Shaftsbury Formation – a Cretaceous, marine, dark gray silty shale (Ozoray, 1982, p.4).

3.3 Methods

3.3.1 Introduction

The methods employed in this study, ordered chronologically, are detailed in the following sections: Preliminary Investigation (3.3.2), Field Investigation (3.3.3), and Post-Field Investigation (3.3.4).

3.3.2 Preliminary Investigation

My preliminary study, conducted mostly between September 8, 1998 and June 30, 1999, reviewed topographic maps (3.4.2.1), aerial photographs (3.4.2.2), geotechnical reports (3.4.2.3), and regional physiographic information (3.4.2.4). A search for available satellite imagery was also conducted (3.4.2.5).

3.3.2.1 Topographic Maps

Alberta provincial base maps 84D/4NE, 84D/5SE, 84D/5NE, 84D/6NW, and 84D/6NE (1:20,000) were used to determine the stream's longitudinal profile and valley gradients (Figures 3.3, 5.4, and 5.5). Information extraction, from the topographic maps, was done using an Ushikata Computer Co-ordinating Area–Curvimeter X-PLAN 360d. Distances used for referencing physiographic features, are measured along the length of the stream from the confluence of the Clear and Eureka Rivers (0 km). Valley length is approximately equal to stream length between km 4.2 and km 18.6. Before km 4.2 and after km 18.6, valley length is less than stream length due to river meandering. The difference between valley and stream lengths from km 0 to km 4.2 is 1300 m.

Valley slope measurements were taken where the topographic contour lines cross the stream on the 1:20,000 map. To avoid erroneous slope values due to the flood plain or the topographic contour line being above the top of the slope, I measured from one contour interval (10 m) above the stream to the contour just below the edge of the Peace River Lowland plain.

54

3.3.2.2 Aerial Photographs

Aerial photographs were used to produce a preliminary map of the landslide. The mapping of the landslide used the most recent (1998) publicly available aerial photographs (Alberta, AS4917 #44, 45), which I had enlarged to a scale of 1:5000 from the original scale of 1:20,000. The most recent (1989) pre-landslide aerial photograph (Alberta, AS3867 #94), also enlarged to a scale of 1:5000 from a scale of 1:20,000, was used to distinguish preslide features from features associated with the 1990 landslide.

The most recent, publicly available, post-landslide aerial photographs (Alberta, AS4333 #179, 181 (1992)) were also used to map the landslide dam reservoir, at original scale (1:20,000).

All preliminary mapping was done on Mylar overlays using a Wild type 392824 stereoscope, with magnification capabilities of between 3 and 15.5 times.

Aerial photographs were also used to determine the frequency of landslides (of volume greater than 1 Mm^3) within the watershed. This involved examining nineteen different series of aerial photographs, dated between 1945 to 1998 (Appendix 2), for indications of recent landslides (i.e. unvegetated scarps, tilted trees, broken ground).

3.3.2.3 Geotechnical Reports

Geotechnical reports of other landslides (Bidwell, 1999; Cruden et al., 1990, 1993, 1997; Evans et al., 1996; Hardy et al., 1962; Keegan, 1992; Lu et al., 1998; Nasmith, 1964; Thomson and Hayley, 1975) and landslide dams (Bidwell, 1999; Cruden et al., 1993, 1997; Evans et al., 1996; Hardy et al., 1962; Keegan, 1992; Lu et al., 1998) in the Peace River Lowlands, and further afield (Costa and Schuster, 1988; Evans, 1986; Schuster and Costa, 1988) were reviewed for possible models for the Eureka River landslide and landslide dam, and for regional physiographic information.

3.3.2.4 Regional Physiographic Information

Regional physiographic information was used to provide pre-field background information, and included the following: topographic and land cover information (Canada, Energy Mines and Resources, 1977, 84D, 1977), geological information (Hackbarth, 1977; Jones, 1966 (1:510,000);

55

Ozoray, 1982); surficial geology information (Kerr, 1971; Bobrowsky et al., 1990; Catto, 1991; Catto et al., 1996; Jones, 1966; Liverman, 1991; Liverman et al., 1988; Reeder and Odynsky, 1965; Thurber Engineering, 1997 and 1998), hydrographic information (Canada, Environment Canada, Water Survey of Canada, Clear River near Bear Canyon, 1998; Canada, Environment Canada, Water Survey of Canada, Eureka River near Worsley, 1998), climatic information (Canada, Environment Canada, Climate Services, 1993, 1998), seismic information (Canada, Geological Survey, 2000).

3.3.2.4 Satellite Imagery

A search was conducted for the availability of satellite imagery depicting the Eureka River landslide, with the aim of corroborating local accounts of the date of occurrence of the landslide. This search involved utilizing the Canada Centre for Remote Sensing (2000) website. The best available image for this purpose was a 27 August 1990, SPOT 2 image. The SPOT image was selected as the pixel resolution is 10m, the image is centered (56° 25' 50"N; 119° 27' 02"W) less than 2.5 km from the Eureka River landslide, the cloud cover was minimal (less than 10%), and the date of image is timely (less than 3 months after the landslide's alleged occurrence). The images were not procured however, as the cost of the image was prohibitive ($1,700 − Radarsat International, 2000).

3.3.3 Field Investigation

The field investigation was conducted from July 21 to August 12, 1999 by Susan Shirkoff (field assistant) and myself. Tasks performed included ground-truthing the preliminary map (3.3.3.1), surveying the length of the landslide (3.3.3.2), gathering information pertaining to the landslide kinematics (3.3.3.3), classifying the landslide dam (3.3.3.4), assessing the state of activity of the landslide and status of the landslide dam (3.3.3.5), assessing the geomorphic significance of the landslide and landslide dam (3.3.3.6), and determining the site stratigraphy.

3.3.3.1 Ground-Truthing the Preliminary Map

The preliminary map of the Eureka River landslide was ground-truthed. Modifications to the initial aerial photographic interpretation were done in the field, directly on the aerial photograph. After the day's field reconnaissance all modifications were checked and, using a Sokkia MS27 stereoscope with 3-times magnification binoculars.

56

3.3.3.2 Surveying

Surveying was carried out using a 60-m measuring tape, Suunto clinometer, Sylva compass, and Brunton compass. The Sylva compass was used for short distance sighting, as it is reasonably accurate for shorter distances and quick to use. The Brunton compass was used only for the initial sighting, where the target was located at a distance of 242 m. The Sylva and Brunton compasses were compared prior to surveying, and found to produce results within 1°. The Suunto clinometer was used instead of the Brunton clinometer, as the Suunto was easier to operate and the difference in measurement between the two devices was determined to being less than 2° on gentle slopes and less than 1° on steeper slopes.

During the survey, the locations of breaks in slope, scarps, tension cracks, and other important physiographic information were recorded (Figure 3.13). The information derived from the survey was plotted during the evening, and a preliminary cross-section was produced. Surveying error was determined to be less than 5% in the vertical (when compared to 1:20,000 topographical maps) and the horizontal (when compared to the 1998 (Alberta, AS4917 #45) aerial photographic enlargement (1:5,000)).

3.3.3.3 Landslide Kinematics

Besides the information gathered while mapping the landslide, information concerning the kinematics at the toe of the landslide was gathered. Acquiring this information involved measuring the orientation of the bedding in the valley bottom at 24 locations. The Brunton compass/clinometer was used for this task.

3.3.3.4 Landslide Dam Classifications and Maximum Height Determination

The classification of the landslide dam, according to the dam classification system of Costa and Schuster (1988), was accomplished remotely, prior to field study, via aerial photographs inspection, as elevated remnants of the original channel were apparent on aerial photographs.

The maximum dam height was deduced by determining the reservoir high stand. This was accomplished by examining trees for indications of recent submersion (i.e. mud and twigs caught in the branches and bark). This methodology has several problems; for example: if the high stand is maintained for a short period the indicators of flooding might be overlooked, or the dam may

have partially failed prior to being overtopping, or a beaver dam built atop the landside dam will exaggerate the flooding. Nonetheless, the results form this analysis are considered reasonable, given the August 1999 elevation of the former channel above the contemporary channel, and the August, 1999 reservoir length.

3.3.3.5 Landslide Dams Status

The status of the landslide dam was, for the most part, known prior to the field study, as Alberta aerial photographs depicting the site are available for 1992 (Alberta, AS4333 #179, 181), 1997 (Alberta, AS4892 #148), and 1998 (Alberta, AS4917 #45). Field investigation to assess the 1999 status involved traversing the extent of the dam and observing the extent of flooding.

3.3.3.6 Landslide Activity Assessment

The activity of the landslide was determined by searching for signs of recent movement. This was accomplished by comparing post-landslide aerial photographic series (i.e. Alberta, AS4333 #178, AS4892 #148, AS4917 #45) with each other and with field observations.

3.3.3.8 Geomorphic Significance of the Landslide and Landslide Dam

The geomorphic significance of the Eureka River landslide, and landslide dam was accomplished visually while traversing the stream, from head of reservoir (km 17.8) as depicted in the 1992 aerial photographs to km 14.6, and km 12.4 to km 9.8 (the landslide dam extends from km 10.6 to km 11.7). The stream between km 12.4 and 14.6 was not visited due to time constraints, but was viewed from the air on August 9, 1999. The downstream inspection was stopped at km 9.8 due to time constraints.

3.3.4 Post-field Investigation

The post-field investigation involved tilt-table tests (3.3.4.1) and determining the Atterberg limits (3.3.4.2), texture (3.3.4.3), and friction angle (3.6.4) of the unit in which the rupture surface was located, and estimating the landslide's volume (3.6.5) and kinematics (3.6.6).

3.3.4.1 Tilt Table Testing

The tilt table tests were performed by myself, on the day that the sample was collected. The tilt table testing involved slowly increasing the inclination of the table, to which the lower rupture surface (plate) was fastened, until the upper rupture surface (slider) completely detached from the plate (Bruce et al., 1989). The inclination of the table was adjusted by opening a valve and allowing oil to flow from a hydraulics piston to a reservoir. This apparatus enabled the rate of inclination increase of the table to be carefully controlled. The plate was attached to the table, so that the surface of the plate roughly paralleled the table. The orientation of plate and slider, with respect to the table, was positioned so the displacement of the slider, relative to the plate, would be the same as had occurred during the landslide events (determined by striations on the rupture surfaces). The increase in inclination proceeded at a constant rate until the slider began to move; at this point, the inclination increase rate was reduced until the slider detached from the plate, and the experiment was halted. The initial movement of the slider involved the displacement of only a few millimetres. The final movement of the slider was very abrupt. Once the experiment was halted, the inclination of the table was determined using a Brunton clinometer. The tests were repeated six consecutive times and averaged.

3.3.4.2 Atterberg Limits

The Atterberg limits were performed to American Society for Testing and Materials (1998, D4318-95a) standards. Christine Hereygers (Department of Civil and Environmental Engineering, University of Alberta) assisted in providing equipment, instructions, and reviewing the results.

The liquid limit of the samples was determined using a Casagrande cup. This test involved partially filling a brass (Casagrande) cup with soil. A groove was cut into the soil using a standard tool. By mechanically turning a lobed crank, at two revolutions per second, the cup was raised and then dropped a distance of 0.624 mm. The dropping action causes the groove to close. When 12 mm of the groove had closed, the experiment was halted, the soil was extracted from the cup, and the number of blows was recorded. This procedure was repeated thrice. Distilled water was then added to the soil and the procedure was repeated thrice more. The intent was to have groove closure with 35 blows for the first three tests, and closure with 15 blows for the remaining three tests. The soil from each successive test was weighed, oven dried (at 110°C for 24 hours), and weighed again - to determine the moisture content. The number of blows versus

moisture content was plotted on semi-logarithmic graph paper (blows were plotted on the logarithmic horizontal axis), and a best-fit line was drawn between the two clusters. The moisture content at 25 blows is the liquid limit.

Determining the plastic limit involved rolling approximately 0.5 mL of soil, by hand, into a thread 3 mm in diameter. The sample was then formed back into a ball and then rolled into a thread again. The test was repeated until the sample would no longer form a 3mm thread. The sample was then weighed, oven dried (at 110°C for 24 hours), and weighed again – to determine the moisture content. This test was repeated thrice. The plastic limit is the average moisture content from the three tests.

The plasticity index is the liquid limit minus the plastic limit.

3.3.4.3 Textural Analyses

The textural analysis was done using a hydrometer, to American Society for Testing and Materials (1998, D422-63) standards. Christine Hereygers (Department of Engineering, University of Alberta) performed the tests, with my assistance. The methods are as follows:

1. the sample was broken up using a milk shake machine;
2. the sample was transferred to a graduated cylinder then filled with a solution of distilled water (at 20°C) and sodium hexametaphosphate (0.5%), to the 1000 ml mark;
3. the cylinder was then sealed, with a rubber stopper, and shaken in a teeter totter motion, 25 times;
4. a type 152H hydrometer was placed within the cylinder;
5. hydrometer and temperature readings were taken at 0.5, 1, 2, 4, 8, 16, 32, 60, 117, 182, 265, 385, 1410, 1612, 1780, 3368, 4520, and 5732 (95h 32min) minutes;
6. the data were entered into the University of Alberta, hydrometer program, and plotted (Figure 3.9).

3.4 Stratigraphy

3.4.1 Introduction

Three distinct sedimentary units were identified in the field, at the landslide site; namely, till (3.5.3) and a preglacial and postglacial lacustrine deposit (3.5.2 and 3.5.4 respectively). Figure 3.4 shows the stratigraphy at the 1990 Eureka River landslide and that of proximal landslides (Cruden et al., 1997; Evans et al., 1996; Lu et al., 1998).
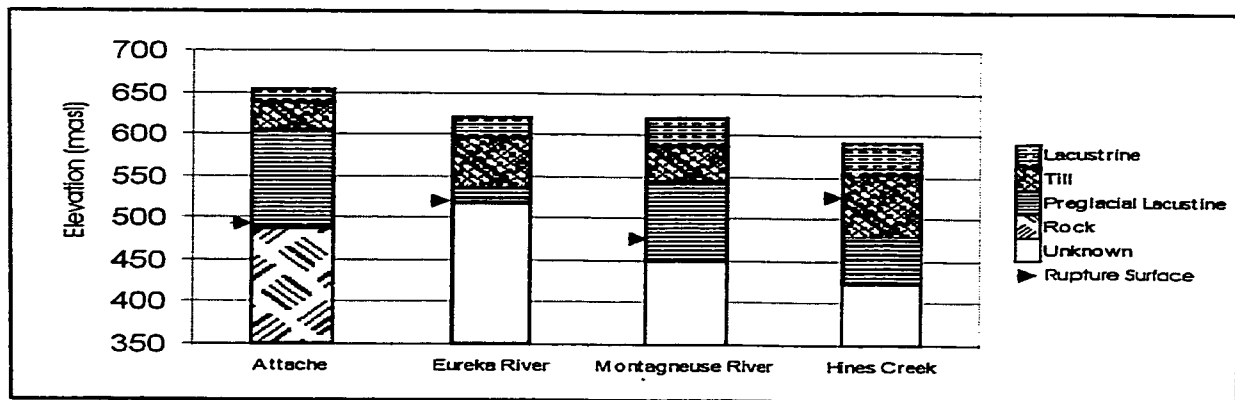
Figure 3.4: Stratigraphy at Attachie (Evans et al., 1996), Eureka River, Montagneuse River (Cruden et al., 1997), and Hines Creek (Lu et al., 1998).

3.4.2 Postglacial Lacustrine Deposit

This unit is 20 m thick (exposure at the main scarp (600 to 620 m.a.s.l.)). The top 2 to 5 m of the unit is mottled grey to tan, clay and silt, with no apparent structure, likely a result of pedogenesis and frost action (Catto, 1991). The mottled weathered zone was observed to extend as deep as 15 m depth in the Winagami Region, Alberta (S.A. Balzer, personal communication, April 6, 2000).

Below the weathered zone, lies 15 m of rhythmite couplets (Figure 3.5), each millimetres to tens of millimetres thick. The couplets are characterised by a high sedimentation, tan, clayey silt layer, underlying a low sedimentation, black, clay layer. At least one turbidite, containing rip-up clasts, punctuates the rhythmite couplets. The deposit also contains larger clasts, up to cobble size, presumed to be dropstones. (Catto, 1991; Liverman, 1991).
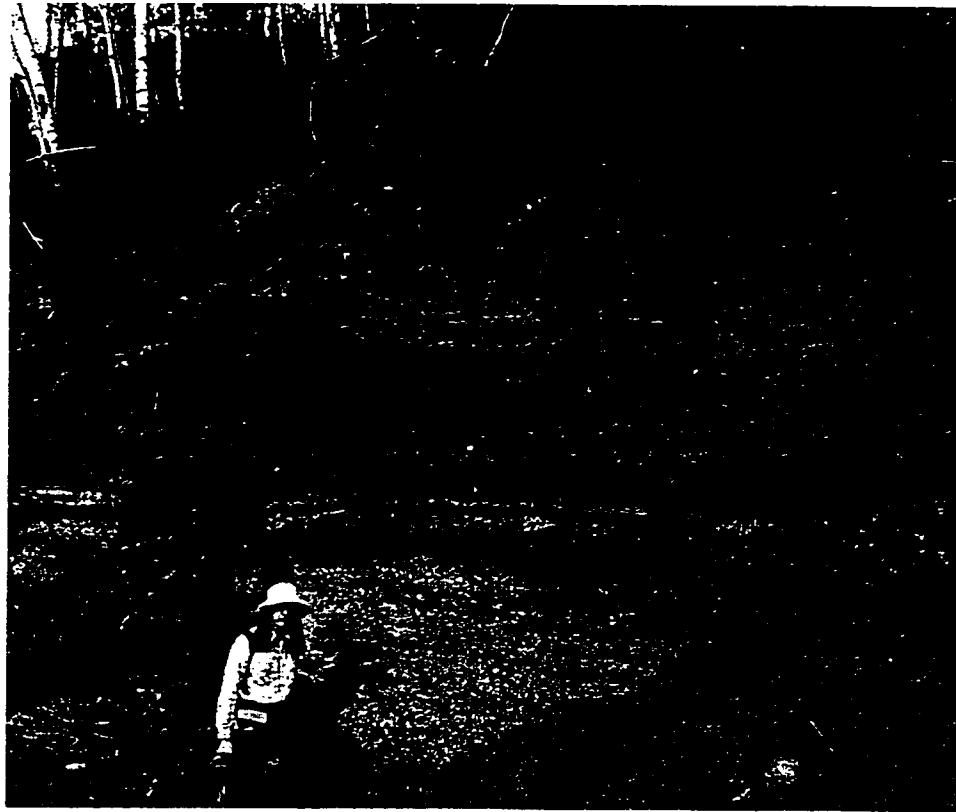
Figure 3.5: Postglacial lacustrine rhythmites with diamicton below (at main scarp, 350 m southwest of surveyed transect (Figure 3.12)).

3.4.3 Till

The till is a maximum thickness of 75 m, and contains clasts of shield material, thus can be correlated to being of Laurentide provenance. Catto et al., (1996) set the western limit of the Laurentide glacier to the southwest of Dawson Creek, British Columbia.

The contact of the till with the overlying glaciolacustrine deposit is gradational. Catto (1991, p. 6) comments that the, "contact between these materials is commonly gradational and, thin, discontinuous beds and lenses of diamicton are frequently present in the basal 1 metre of the thicker glaciolacustrine assemblages". I am placing the top of the till at about 600 m.a.s.l., making the top 1 to 2 m of the till exposed at the main scarp. Thurber Engineering (1997, 1998) has the top of the till at 589 m.a.s.l. at the Highway 726 crossing of the Eureka River.

The top of the till is characterized by cemented silt layers, up to 20 cm thick, punctuated by very thin coarser layers. Continuation of the till was seen in a colluvial block exposure of about 2.5 m, located about 100 m south of the main scarp and 200 m west of the surveyed transect. Here, the till is a matrix-supported diamicton, grading downwards into a banded till. The banded till is similar to that seen at the main scarp, but with layers of about 10 cm thickness, containing 5% to 10% Laurentide provenance pebbles. Catto (1991) suggested that the till was deposited via three processes: direct from the ice, directly from the ice and subsequently modified by mass movement prior to the deposition of the overlying glacial lacustrine sediment, and directly from the ice and subsequently modified by mass movement within a lacustrine environment. Catto (1991) recognized that the latter two depositional modes would preclude the deposit from being morainic, but for the sake of practicality, maintained this classification, for all diamicton containing at least 5% coarse clast content. The same approach is followed here for the diamicton at Eureka River landslide.

At the bottom of the colluvial exposure (100 m south of the main scarp and 200 m west of the surveyed transect) is a clean, pebbly sand. The pebbles within the deposit are well rounded and predominantly metamorphic and igneous clasts of Laurentide provenance. The deposit was traced laterally for about 150 m. It is possible that this layer represents an esker. Below this deposit, exposures are rare and highly weathered, until near the toe of the landslide.

At the toe of the landslide, the bottom of the till was located at about 525 m.a.s.l. Material at this level is similar in composition to the underlying lacustrine deposit, though lacking structure. The till is massive, dark grey, clay and silt, containing occasional angular isolated sand blocks.

3.4.4 Preglacial Lacustrine Deposit

The preglacial lacustrine unit extends from about 525 m.a.s.l. to below the bottom of the valley floor (511 m.a.s.l.). The top of the unit is classed as a glaciotectonite, as original structure is apparent and discernable (Benn and Evans, 1998), though contorted (Figure 3.6). Bedding contortion at the toe is also due to the landslide. Folds with axes perpendicular to the valley are likely glaciogenetic features (i.e., Figure 3.6). Folds with axes parallel to the valley are likely due to the landslide (see Figure3.14).

The unit is characterised by silt and clay rhythmites of about 1 cm thickness. The rupture surface of the landslide was seen within this deposit. The liquid limit (Section 3.7.3.2) and texture (Section 3.7.3.3) of this unit differs considerably from the preglacial lacustrine deposits at Saddle River (Cruden et al., 1993), and Montagneuse River (Cruden et al., 1997). Conversely, the Atterberg Limits of the preglacial lacustrine at the Attachie landslide (Evans et al., 1996) are consistent with those at Eureka River. The unit texture at Attachie showed too much variability to be useful for comparative purposes.
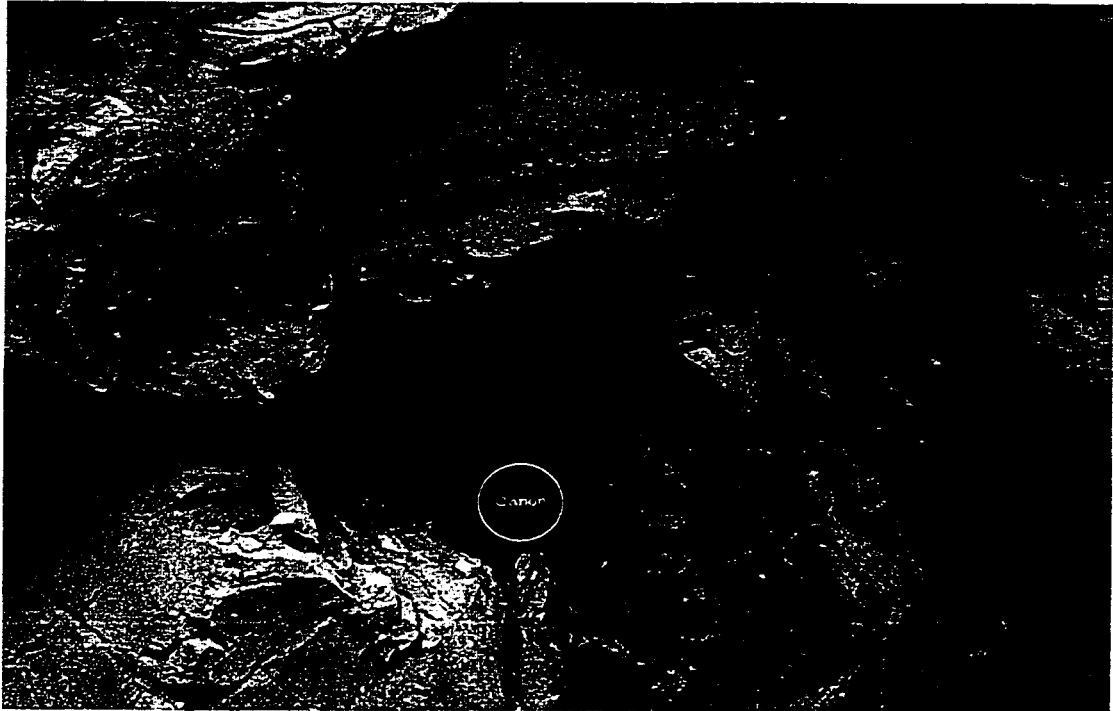
Figure 3.6: Preglacial lacustrine glaciotectonite (near bottom of surveyed transect (Figure 3.12)) (lens cap is 5.5 cm).

3.5 Landslides in the Eureka River Watershed

3.5.1 Introduction

An analysis of aerial photographs was conducted to determine the frequency and the distribution of landslides within the Eureka River watershed (Section 3.5.2 and 3.5.3 respectively). The objective of this procedure was to situate the 1990 landslide within temporal and spatial contexts.

3.5.2 Landslide Frequency

An analysis of eighteen series of aerial photographs, taken from 1945 to 1998 (Appendix 2), reveals that the only large landslide (greater than 1 Mm^3) within the Eureka River watershed during this interval was the 1990 landslide. Further, the lack of large unvegetated scarps (of length greater than 500 m), the state of advanced floral recolonization of sag ponds, and the maturity of the forest in the 1945 aerial photographs (Canada A8142 #68-80, A8143 #56-60 and 65-74, A8303 #53-63, A8304 #52-55, A8348 #79-81) lead to the conclusion that there had been no large landslides (greater than 1 Mm^3) for several years prior to 1945.

3.5.3 Distribution of Large Landslides

Aerial photographs show inactive large slides ($\geq$ 1 Mm^3) from the confluence of the Eureka and Clear Rivers to km 18.2 on the north bank of the Eureka River, and to km 15.2 on the south bank. As these slides appear to involve the entire slope, their volumes likely decrease upstream with decreasing valley depth. The mode of instability appears to be translational slides. The evidence for these slides includes scarp surfaces (often highly modified), sag ponds, irregular (broken) topography, and uphill facing slopes.

The 1990 landslide is located between km 10.2 and km 12.0 on the north (left) bank of the Eureka River. The landslide incorporates three earlier landslides, with retrogression at the eastern extent. These earlier slides, evident on the 1945 series aerial photographs (Canada A8303 #54-56), likely occurred several years before 1945, as the main scarps had been extensively modified by this time.

Upstream of the zone of instability (north bank, km 18.2 and south bank, 15.2), soil falls predominate, usually a result of the Eureka River undercutting its banks. Exceptions to this are between km 33.1 and 33.6, km 35.0 and 35.6, km 36.8 and 40.9, and km 42.0 and 42.6, on the north bank, where large translational landslides have occurred. The evidence for these slides includes, irregular topography, sag ponds, and backward facing slopes.

The results from an assessment of the valley slope gradients (Figure 3.7), for the purpose of identifying areas of instability, are generally consistent with the results from the aerial photographic analyses, for the lower reaches. That is, where there is evidence of large landslides valley slope gradients are less than where there is no indication of instability. Channel form also

reflects the occurrence of landslides (Figure 3.3); in that, where landslides are common the channel is straight. The channel gradients however, are not obviously affected by the landslides (Figure 3.3). This lack of an obvious reflection of areas of instability in the longitudinal slope is contrary to what was observed in the Montagneuse River (Cruden et al., 1997), Spirit River (Section 2.2.3), and Saddle River (Cruden et al., 1993).
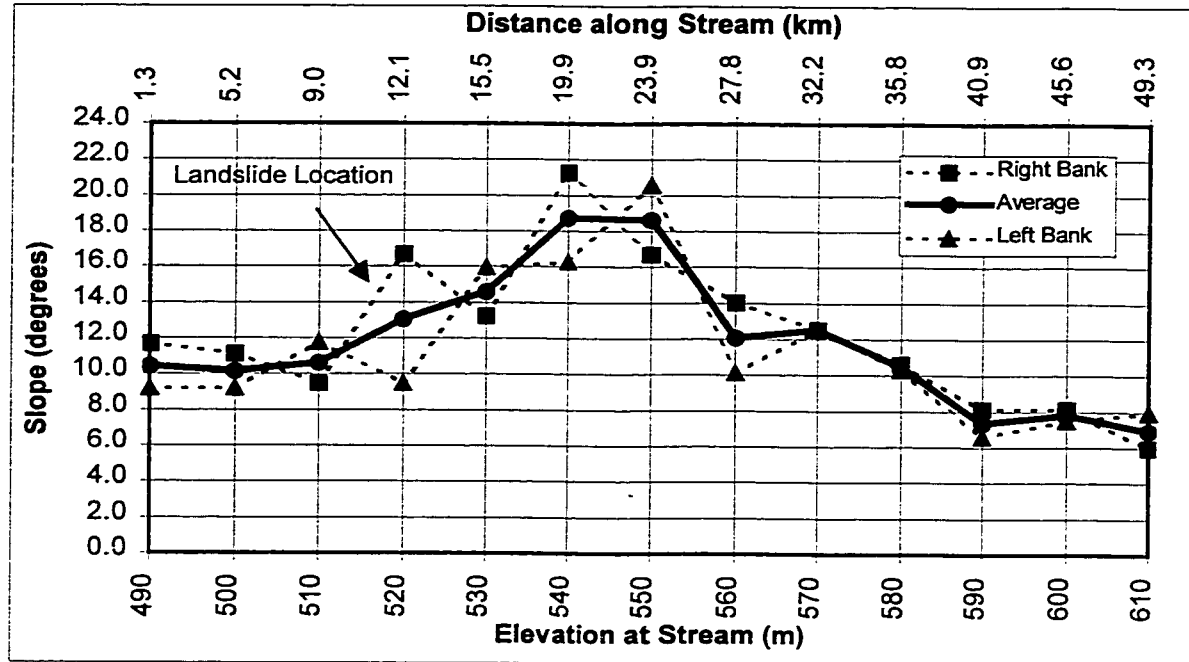
Figure 3.7: Valley slopes of the Eureka River

3.6 Description of the 1990 Eureka River Landslide

3.6.1 Introduction

The following includes the empirically derived landslide properties (3.6.2), an estimation of the landslide friction angle (3.6.3) and volume (3.6.4), a description of the landslide and landslide kinematics (3.6.5), the classification of the landslide (3.6.6), and an analysis of instability associated with the 1995 landslide (3.6.7). The nomenclature used in this section follows Cruden and Varnes (1996).

3.6.2 Empirically Derived Properties

This section includes the results from the tilt table tests (3.6.2.1), and the determined texture (3.6.2.2) and Atterberg limits (3.6.2.3) of the preglacial lacustrine soil bounding the rupture surface. These procedures were performed on only one sample of the rupture surface (Figure 3.8), collected at the river level, at the end of the surveyed transect (Figures 3.12 and 3.13).
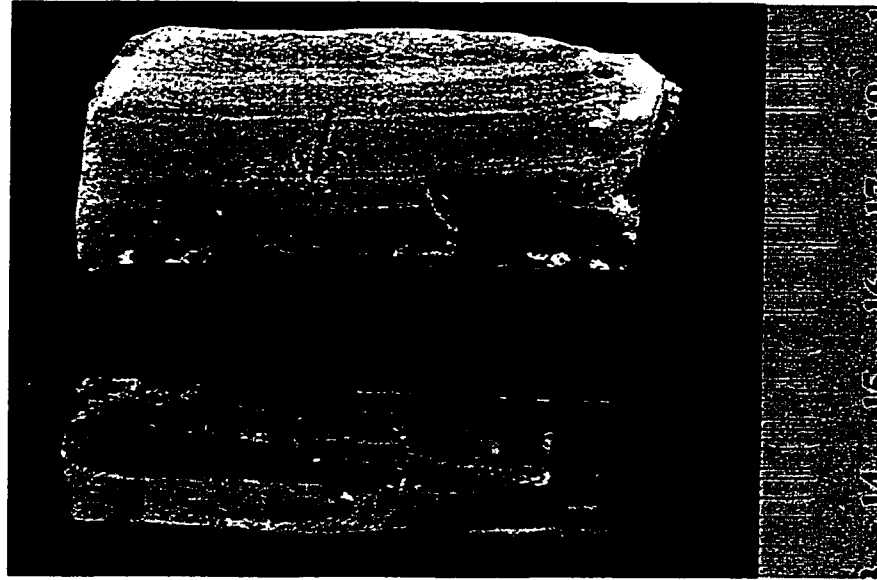
Figure 3.8: Sample used for testing (arrow points towards rupture surface; scale in cm)

3.6.2.1 Tilt Table Test Results

The results of the tilt table tests are Table 3.1.

Table 3.1: Tilt table test results.

Test	Plate Angle at Detachment	Comments
1	47.2	Equivalent to slider moving southward
2	44.5	Equivalent to slider moving southward
3	40.7	Equivalent to slider moving southward
4	46.0	Equivalent to slider moving northward
5	46.0	Equivalent to slider moving northward
6	44.5	Equivalent to slider moving northward
Average	44.8	

An inferred friction angle, based on these results would clearly be a maximum (Section 3.6.3). The high values generated from this experiment might be due to the samples being drier and under a lower normal load than during the landslide.

3.6.2.2 Texture of the Preglacial Lacustrine Units

Texture analysis was performed on one sample of preglacial lacustrine soil, collected adjacent to the rupture surface (Figure 3.9). Another sample, collected at the same location, was washed with hydrochloric acid, to remove calcium carbonate, and then texturally analyzed (Figure 3.9). Despite a 6.9% reduction in mass, following decalcification, no substantive change in texture occurred (a portion of the mass reduction is due to sample loss during the experiment).
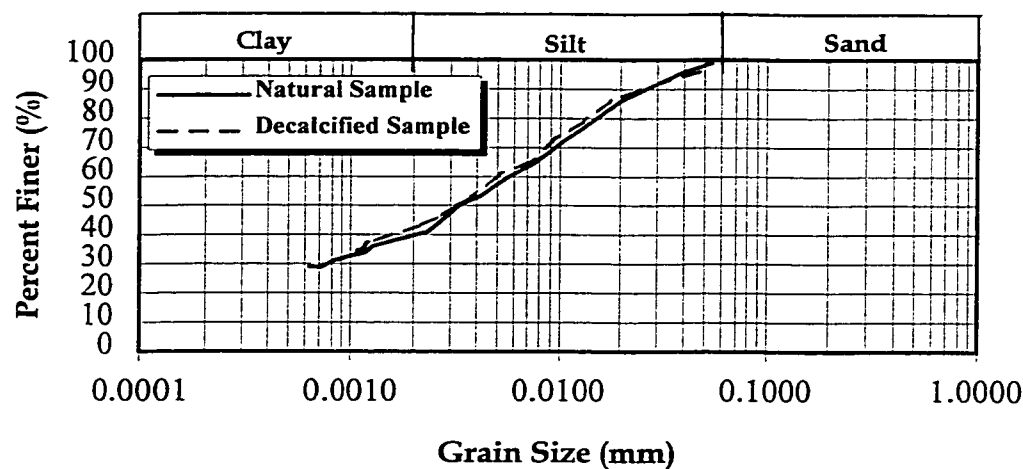
Figure 3.9: Grain size distributions of sample of Eureka River preglacial lacustrine deposit.

The textures of preglacial lacustrine soil from the landslides at Eureka River (natural sample), Montagneuse River (Cruden et al., 1997), Saddle River (Cruden et al., 1993), and Attachie (Evans et al., 1996) form Table 3.2. Considerable textural variability exists at each landslide site. Evans et al., (1996), found no apparent relationship between sample texture and location at the Attachie landslide. The texture of the preglacial lacustrine soil at the Eureka River landslide is similar to the texture at the Attachie landslide, and dissimilar to the texture at the Montagneuse and Saddle River landslides.

The textures of the preglacial lacustrine soil from the Montagneuse and Saddle River landslides are similar to one another. The Saddle River landslide occurred within the preglacial Saddle River valley (Keegan, 1992), thus the source of the preglacial lacustrine sediments is likely local. The similarity between the material textures at the Montagneuse and Saddle Rivers, suggest that the source of the preglacial lacustrine sediments at the Montagneuse River landslide is also local.

Table 3.2: Textures of preglacial lacustrine soils at Eureka River, Attachie landslide (Evans et al., 1996), and Montagneuse (Cruden et al., 1997) and Saddle River (Cruden et al., 1993) (minimum and maximum values in brackets).

Landslide	Eureka River	Attachie	Montagneuse River	Saddle River
Clay %	40	39 (15-64)	62 (51-73)	68 (59-74)
Silt %	60	61 (36-85)	37 (27-49)	32 (26-40)
Sand %	0	0	1	1

3.6.2.3 Atterberg Limits

The Atterberg limits and activity of preglacial lacustrine soils at the Eureka River landslide, the Attachie landslide (Evans et al., 1996), and the Montagneuse (Cruden et al., 1997) and Saddle (Cruden et al., 1993) River landslides form Table 3.3. The Atterberg limits for the decalcified preglacial lacustrine soil from the Eureka River landslide are similar to the non-decalcified soil and therefore are not indicated in Table 3.3. As with textures (Table3.2), the Atterberg limits and activity of the preglacial lacustrine soil from the Eureka River landslide are similar to those of the Attachie landslides, and dissimilar to those of the Saddle and Montagneuse River landslides. Variations in the activity and Atterberg limits suggest differences in clay mineralogy, possibly due to different sediment sources. The plasticity is also influenced by the clay fraction (Selby, 1993).

Table 3.3: Atterberg Limits of preglacial lacustrine soil at the Eureka River, Attachie (Evans et al., 1996), and Montagneuse (Cruden et al., 1997), and Saddle River (Cruden et al., 1993) landslides (minimum and maximum values in brackets).

Landslide	Eureka River	Attachie	Montagneuse River	Saddle River
Liquid Limit	43.5	42.5	65 (52-74)	73 (69-73)
Plastic Limit	22.5	22.9	21 (18-24)	25 (22-29)
Plasticity Index	21	19.6	44	48
Activity	0.53	0.49	0.71	0.72
Unit Weight (kN/m3)			19.77	19.06

The type of clay present affects the residual friction angle (Φr). Selby (1993, p.111) reported a Φr of $10°$ for illite, and higher values for inactive clays (activity values of less than 0.75). The activity and liquid limit values of the soils from the Montagneuse and Saddle Rivers suggest the presence of illite (Selby, 1993, Table 7.2, p.111). The volume fraction of clay is also an important parameter, with residual strength values for soils containing less than 20% clay being controlled by the sand and silt fraction, and with greater than 50% clay being dependent upon the clays present (Skempton, 1985).

3.6.3 Estimated Friction Angle

The residual friction angle (Φ_r) at the Eureka River landslide was estimated in three ways: using Φ_r from the Montagneuse River (Cruden et al., 1997), Saddle River (Cruden et al., 1993) and Attachie (Evans et al., 1996) landslides, using an empirical relationship between clay fraction and friction angle from Skempton (1985), and using models in Norrish and Wyllie (1996, eq. 15.3, p. 399) and Skempton and De Lory (1957) (in Selby, 1993).

Values of Φ_r, peak friction angle (Φ_p), and cohesion (c), from the Montagneuse and Saddle River landslides (Cruden et al., 1997, and 1993 respectively) and Attachie landslide (Evans et al., 1996) form Table 3.4. Table 3.4 shows reasonable consistency between the Saddle and Montagneuse River landslides. The Φ_r from the Attachie landslide is however, inconsistent with the friction angles from the Saddle and Montagneuse River landslides (Table3.4). The Φ_r at Eureka River is assumed to be between the low value at Montagneuse River ($6°$) and the value at Attachie ($22.2°$). With respect to employing Φ_r from the Montagneuse River for the lower bounds, both the Montagneuse and Eureka River landslides have been situated within (or near) the Shaftsbury valley (Cruden et al., 1993; Kerr, 1971), thus the geotechnical properties of the preglacial soils can be expected to be similar; though, the differences in the textures and Atterberg limits of the two landslides suggests possible influences from other sediment sources. Employing Φ_r from Attachie for the upper bounds is justified, due to the similar material properties of the Attachie and Eureka River landslides.

Table 3.4: Friction angles (degrees) from preglacial lacustrine soils at Montagneuse River (Cruden et al., 1997), Saddle River (Cruden et al., 1993), and Attachie (Evans et al., 1996) landslides.

Landslide	Depth (m)	Direction	Φp	c(kPa)	Φr	c(kPa)	Tests
Montagneuse	87-88	along bedding	14	0	8	0	reverse direct shear
		across bedding	21	120	10	0	reverse direct shear
	104	along bedding	14	0	6	0	reverse direct shear
		across bedding	19	110	8	0	reverse direct shear
Saddle	surface	along bedding	14.4	0	6.7	0	reverse direct shear
		across bedding	20	0	9.3	0	reverse direct shear
Attachie	35-160	along bedding and remoulded samples			22.2		reverse direct shear

Skempton's (1985) relationship between clay fraction and Φ_r, for soils with activities between 0.5 and 0.9, produces a non-normalized Φ_r of between $11°$ and $16°$ for the Eureka River landslide. Skempton normalized his data to an effective stress (σ_n') of 100kPa, using the following relationship:

σ'(kPa)	25	50	100	150
$\tan\Phi/\tan\Phi_{100}$	1.12	1.07	1.00	0.96

The pre-landslide σ' values at Eureka River range between 785 kPa and 1800 kPa (for rupture surface slopes (Ψ_p) of $11°$ and $0°$ respectively, with average normal landslide thicknesses (z) of 40 and 90 m respectively) (from Figure 3.13). Using my derived approximate relationship

$$\tan\Phi/\tan\Phi_{(\sigma n=100)}= -0.20\log \sigma'+1.41 \qquad \text{(eq.3.1)},$$

Φ_r values between $8.2°$ and $13.1°$ are produced: These values are consistent with the upper bounds of Φ_r from the Montagneuse and Saddle River landslides (Cruden et al., 1993 and 1997 respectively) (Table 3.4).

In numerically assessing the residual friction angle, equations 3.2 and 3.3 were employed. Equation 3.3 requires valley slope (Ψ_f), Ψ_p, and water table parallelism and as such is not directly

applicable to the Eureka River landslide, but has been included for comparative purposes. Equation 3.2 and 3.3 are as follows:

$$FS = \frac{[cA + (W\cos\Psi_p - U - V\sin\Psi_p)\tan\Phi]}{(W\sin\Psi_p + V\cos\Psi_p)} \qquad \text{(eq. 3.2)}$$

(Norrish and Wyllie, 1996, eq. 15.3, p. 399),

and

$$FS = \frac{c + (\gamma_r - m\gamma_w)z\cos^2\Psi_{fp}\tan\Phi}{\gamma_r z\sin\Psi_{fp}\cos\Psi_{fp}} \qquad \text{(eq. 3.3)}$$

(Skempton and De Lory, 1957, in Selby, 1993, p.270).

In the calculations the following assumptions were made:

1. the factor of safety would be equal to one (FS=1), as the slope had failed;

2. the water table was at surface ($Z=Z_w$; m=1) – a near surface water table was observed in the vicinity of the landslide during the field study (August 1999) despite minimal rainfall; June 1990 had above average rainfall (Canada, Environment Canada, Climate Services, Eureka River, 1998, and Canada, Environment Canada, Climate Services, Clear Hills Lookout, 1993);

3. the main scarp is at the top of the valley – this assumption is made to ease calculations, and is true only for those areas in which there was no retrogression;

4. there was no cohesion (c=0) and Φ was at residual ($\Phi = \Phi_r$).

The assumptions of no cohesion and the friction angle being at residual are justified as the trace of the main scarp is visible in 1989 Alberta aerial photograph 38567 #94, indicating pre-1995 landslide movement.

With the preceding assumptions equations 3.2 and 3.3, can be respectively simplified to

$$\tan\Psi_f = \tan(\Phi-\Psi_p)(\gamma_r-\gamma_w)/\gamma_w = 0.98\tan(\Phi-\Psi_p) \qquad \text{(eq. 3.4)}$$

(Cruden, 2000),

and

$$\tan\Psi_{fp} = \tan\Phi(\gamma_r-\gamma_w)/\gamma_r = 0.49\tan\Phi \qquad \text{(eq.3.5)}$$

(D.M. Cruden, personal communication, February 2000).

With Ψ_p being between $0°$ and $11°$ (the rupture surface would intersect the surface if Ψ_p exceeds $11°$), Ψ_f being $12.8°$, γ_r being 19.4 kN/m^3 (average γ_r from Montagneuse River (Cruden et al.,

1997) and Saddle River (Cruden et al., 1997)), and γ_w being 9.8 kN/m^3, the range of Φ_r is as follows (Table3.5):

Table 3.5: Mathematically determined friction angles versus rupture surface slopes.

Equation 3.4

Ψ_p	0	1	2	3	4	5	6	7	8	9	10	11
Φ_r	13.1	14.1	15.1	16.1	17.1	18.1	19.1	20.1	21.1	22.1	23.1	24.1

Equation 3.5

Ψ_{fp}	10	11
Φ_r	19.8	21.6

Equations 3.4 and 3.5 produce Φ_r ranges higher than the Φ_r values determined for the Saddle River and Montagneuse River (Cruden et al., 1993 and 1997 respectively), though consistent with Skempton (1985) when using equation 3.4 with a Ψ_p of 0°, and with Attachie (Evans et al., 1996) when using equation 3.4 with a Ψ_p of 9°, or equation 3.5 with a Ψ_{fp} of 11°.

From the preceding assessments, it seems that Φ_r is likely between 13.1° (from Skempton, 1985 and equation 3.4) and 22.2° (from Attachie (Evans et al., 1996)). To better define the Φ_r, the Ψ_p might be determined by drilling or the lacustrine soil might be shear tested.

3.6.4 Landslide Volume

The volume (VOL) of this landslide was calculated as follows:

$$VOL = W_r/2 \ (L_r^2{}^*\tan \ \Psi_f - B_s^2{}^*\tan \ \Psi_f - L_r^2{}^*\tan \ \Psi_p + 2L_rZ_b) \qquad \text{(eq. 3.6).}$$

This formula was derived as follows:

$$VOL = W_rA_X(total) = W_r\{A_X(A) - [A_X(B) + A_X(C)] + A_X(D)\} \qquad \text{(eq 3.7) (see Figure3.10).}$$
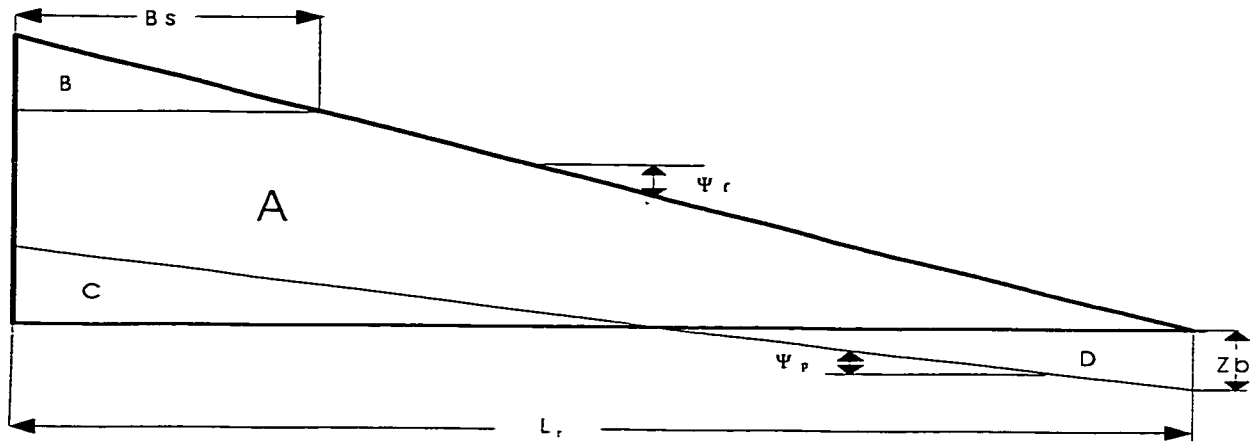
Figure 3.10: Volume estimation geometry.

With the distance of the main scarp behind the crest of the slope (B_s) being 160 m, the depth of rupture surface beneath the bottom of the valley (Z_b) being 20 m, the length of landslide (L_r) being 570 m, the width of landslide (W_r) being 1370 m, Ψ_f being 12.8°, and Ψ_p being between 2° and 11° (with $Z_b = 20$ m and $L_r = 570$ m, Ψ_p must be greater than or equal to 2° for this formula to work), the volume is between 18.9 and 54.4 Mm^3 (for Ψ_p of 11° and 2° respectively). For comparison, volume equation 2.6 (Cruden and Varnes, 1996, section 2.6.4) produces a volume between 11.9 and 42.9 Mm^3, with depths of rupture surface (D_r) of 29 m and 105 m respectively (equivalent to Ψ_p 11° of 2° respectively).

Implicit in the use of equation 3.6 are the assumptions that the landslide can be characterised by a modified triangular prism, and the cross-sectional area is constant along the entire width of the landslide. This necessitates that both lateral margins be vertical. An assumption of main scarp verticality is also implicit in equation 3.6. These assumptions are unlikely to be true, and will lead to an overestimation of the volume.

3.6.5 Landslide Description and Kinematics

The 1990 landslide appears to be composed primarily of four main blocks (Figures 3.11, 3.12, and 3.13). Attempts to reconstruct the kinematics of these blocks are not well constrained, due to the lack of subsurface information.

Block 1 is 1370 m wide (extending from km 10.3 to km 11.9), and 300 to 375 m long. The block was translated southwards by a maximum of 20 to 30 m (obtained from comparing pre and post-landslide aerial photographs (Alberta, AS3867 #94 and AS4917 #45 respectively)) between km 11.3 and 11.9. There was little disturbance to the forest cover across most of this block, indicating a deep and planar rupture surface, and a translational slide. There was downward translation of the upslope margin of this block, suggesting a southward dipping rupture surface.

At the surface, block 1 consists of the colluvial deposits of three neighbouring earlier landslides. The margins of the block follow the main scarps for the eastern and central earlier landslides, and a major fracture of the western earlier landslide, suggesting the reactivation and amalgamation, of the rupture surfaces of the earlier slides. Alternatively, the rupture surface associated with the 1990 landslide may be deeper then those of earlier landslides making the 1990 landslide an enlargement rather than a reactivation. The latter possibility is suggested by a major fracture of the central earlier landslide that shows no signs of recent movement. The displacement of this block was most extensive to the east (beneath the eastern earlier landslide), and decreases westward, with less than 2 m southward translation, between km 10.8 and 9.9 (beneath the western earlier landslide). North-south fractures, approximately coincidental with the lateral margins of the central earlier landslides accommodate the differential displacement.

The toe of block 1, which includes the pre-landslide riverbed, was thrust upwards by 20 to 25 m (obtained from the extent of flooding upstream of the landslide dam) at km 11.4. East and west of km 11.4, the magnitude of lift decreases. Structural measurements made at the toe of the landslide (Figure 3.14) suggest folding of the toe occurred initially, followed by rupturing, likely along the fold's axial surface, and then thrusting of the hanging wall. Subsequent stream incision around the toe of the landslide has left sections of the original channel elevated above the contemporary channel. The rupture surface was located 20 m beneath the pre-landslide stream channel, 1 m above river level, at km 11.4. Further incision is likely.

Block 2, above block 1, was in place prior to the landslide. As such, the movement of block 2 would represent landslide retrogression. The upper surface of the block was the modified landslide scarps of the eastern and central earlier landslides. The block extends from km 11.0 to 11.7, although, only the portion between km 11.3 and 11.7 is intact. Between km 11.0 and 11.3, the block is highly fractured. Between km 11.3 and 11.7, the block is about 350 m wide and between 55 and 110 m long. During the landslide, this block was dropped by 20 to 45 m,

translated southward by 20 to 35 m, and rotated backwards by about 20° (from four tree tilt measurements). The rotation is indicative of a curved rupture surface beneath this block, with an estimated radius of curvature of about 190 m.

Between blocks 1 and 2 are a minor scarp, 3 tension cracks, and 4 uphill facing scarps. These create a graben. The depth to rupture surface beneath the graben (53 m) to graben width (61 m) (in Figure 3.13), is consistent with the width to 1.1 times depth relationship noticed by Cruden et al., (1991). The series of tensional cracks and uphill facing scarps suggest that the graben formed in response to extension, and therefore, likely provided no impetus for block 1.

Block 3 extends from km 11.3 to 11.7. The block is wedge shaped, and almost devoid of vegetation, suggesting that most of this block was not previously exposed at the surface. Vegetation was found in one small area (less than 2 m^2) near the centre of the block (Figure 3.15). The block was translated southward by about 30 to 50 m, and downwards by about 20 m. During the landslide, the upslope end of block 3 likely lost contact with the rupture surface. Fracturing of block 3 resulted, forming blocks 3 east and 3 west (about 0.75 ha each), which rotated backwards to fill the void (Z. Lu, personal communication, 10 April 2000) (Figure 3.15). Block 3 west did not form a graben, as there is no difference in elevation between the down slope margin of the block and the forested patch on block 3 (Figure 3.15). The same is also likely true for block 3 east. The orientation of the surfaces of blocks 3 east and 3 west are (strike, dip) 206°, 13°N and 136°, 10°N respectively. The upper surfaces of these blocks were formerly at Lowland plain level, and have forest vegetation growing on them.

Block 4 is located between km 10.3 and 10.8, 200 m north of the Eureka River. The block is 150 m long and 450 m wide. The block was displaced southward and downward by less then 2 m, in response to a loss of toe support following the movement of block 1. There was no disturbance to the forest on this block as a result of the landslide. As block 4 consists entirely of colluvium of the western landslide, its movement represents a reactivation.
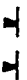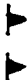
In Figure 3.13, there appears to be a loss of volume when pre-landslide topography is compared to post-landslide topography. Post-landslide loss of volume at the landslide toe has occurred, due to stream erosion. Error in the topographic maps, due to the mature forest at the landslide site, could also be a contributing factor to the apparent loss of volume.

76
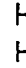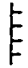
Figure 3.1: Aerial photograph of Eureka River landslide (scale 1:5,900; Alberta A4917 #45, 1 May 1998).

77

List of Symbols

Breaks in Slope:

- Concave Sharp
- Concave Rounded
- Convex Sharp
- Convex Rounded

Scarps (length of line gives an indication of length of slope):

- Rounded
- Sharp

Small Mass Movements:

- Flow
- Translational Slide
- Unclassified Landslide

Streams and Lakes:

- Channel
- Abandoned Channel
- Small Stream
- Lake
- Marsh

Other Symbols:

- Landslide Boundary (approximate)
- Pressure Ridge
- Thrust Block
- Tension Crack
- Cross-Section
- Distance Marker (km)
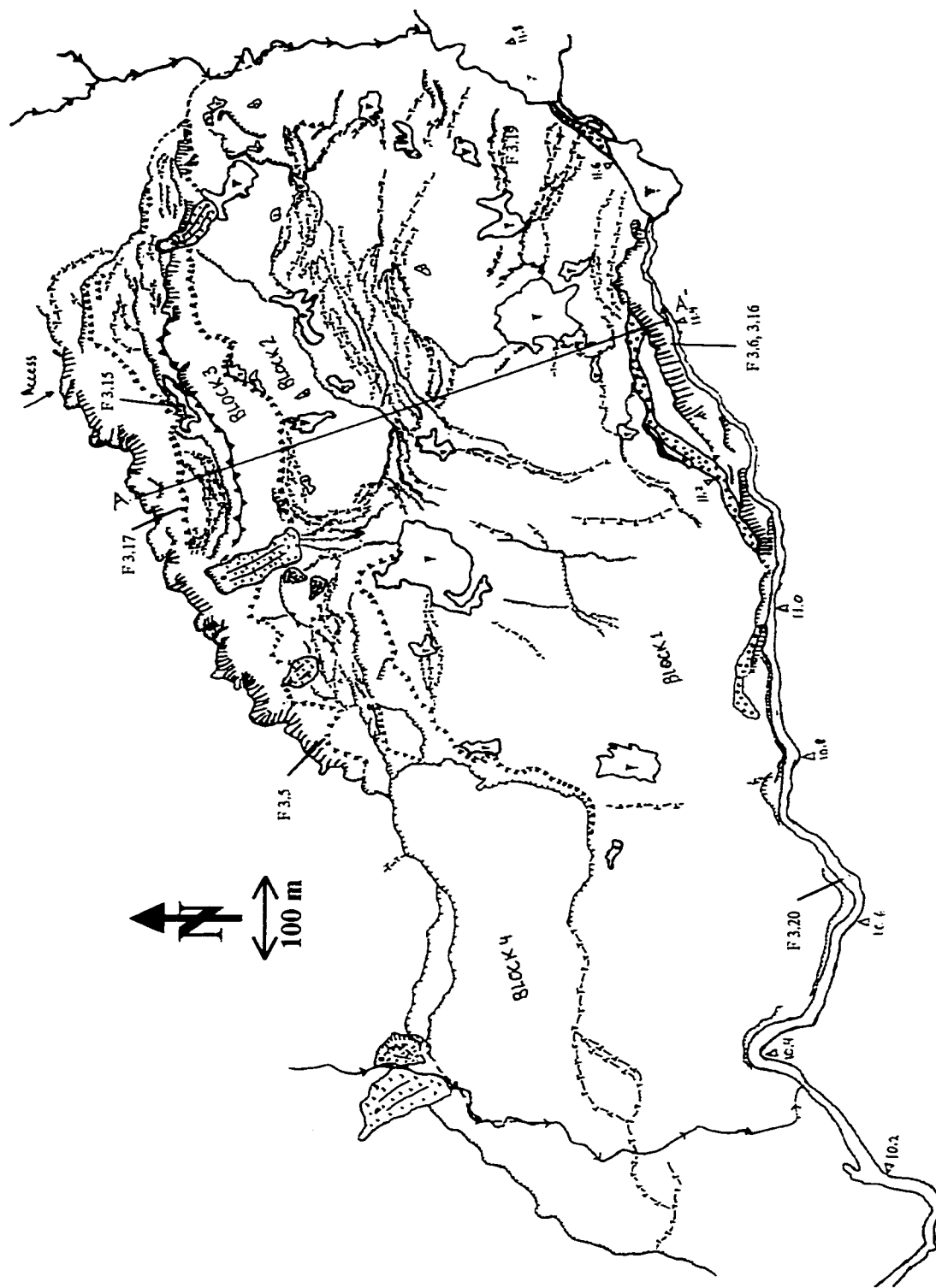
Figure 3.12: Interpretation of photograph A4917#45, with figure (F) locations (scale 1:5,900; symbols from Cruden and Thomson, 1987).

79
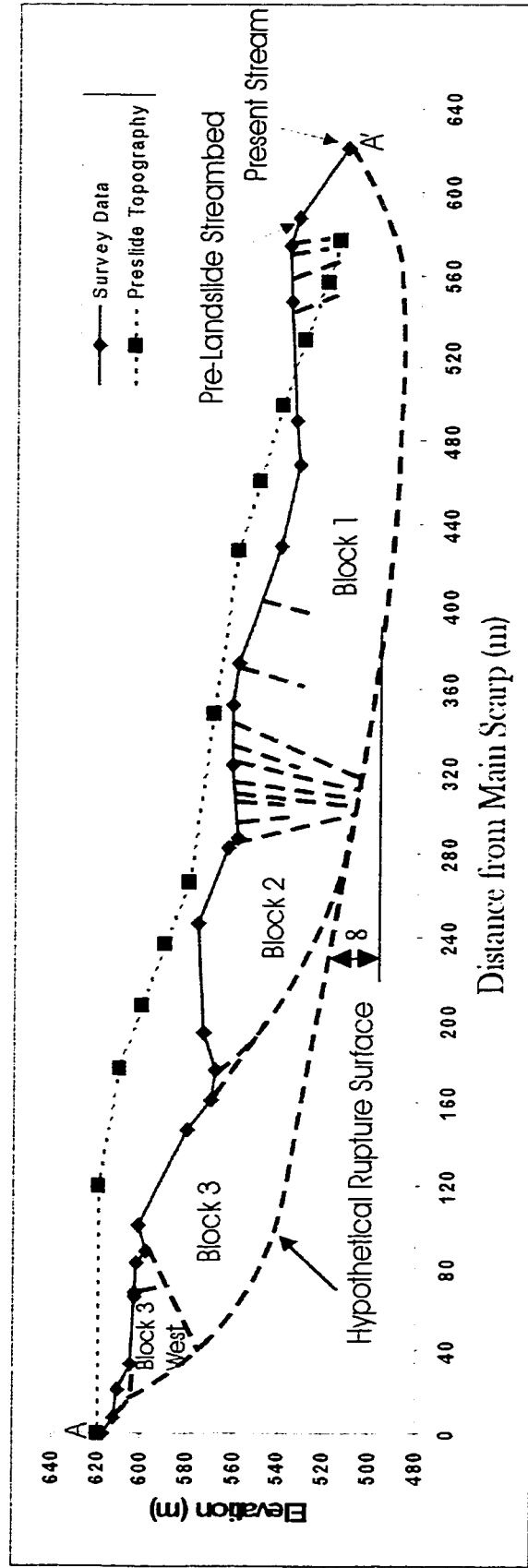
Figure 3.13: Cross-section of Eureka River Landslide (scale 1:2,600; preslide topography from Alberta base map 84D/6nw)

Figure 3.14: Structural orientations in the preglacial lacustrine sediments, at the toe of the landslide (scale 1:3,400).
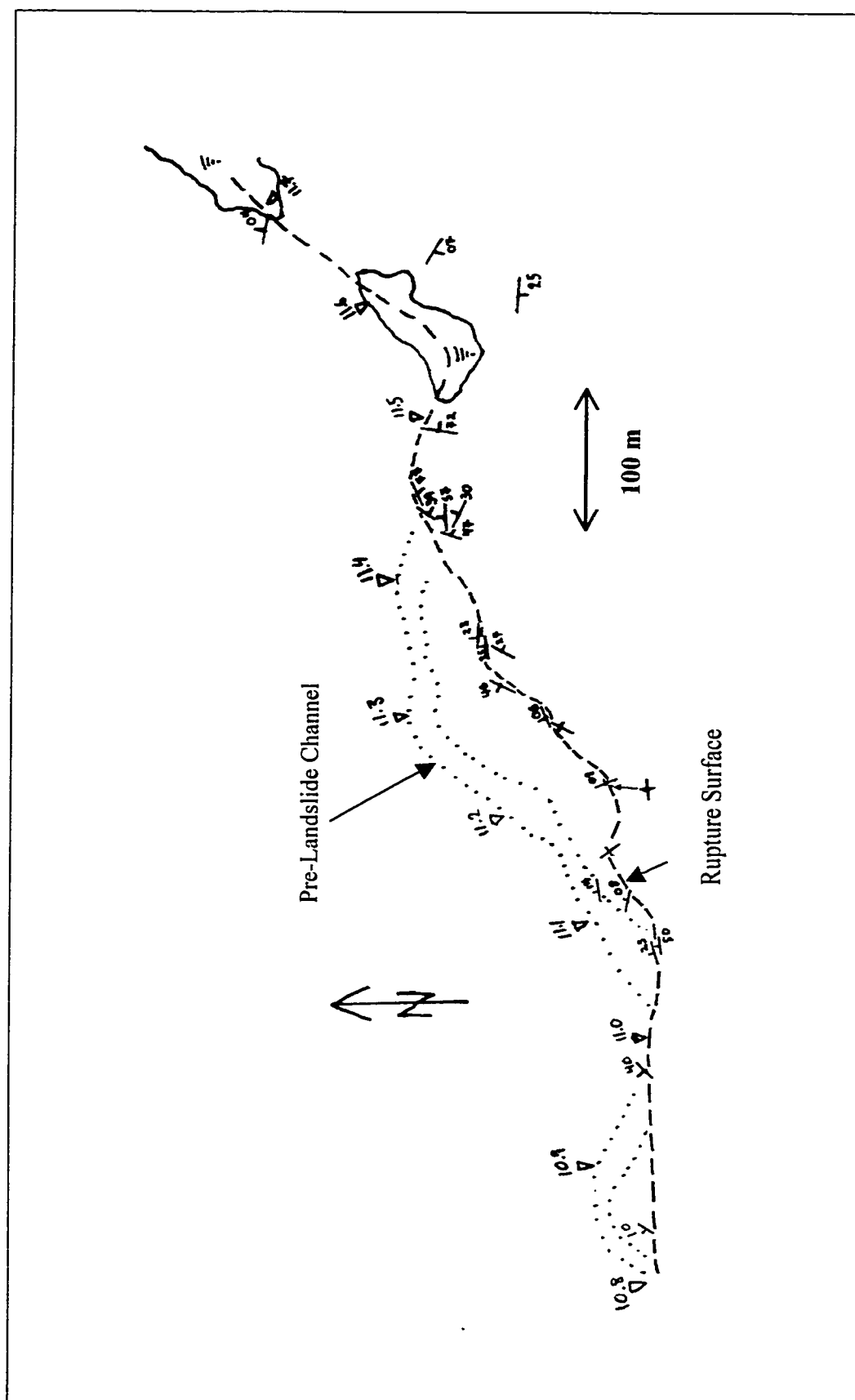
Figure 3.15: Blocks 3 east (left) and 3 (right), seen from surveyed transect, looking east (note remnant forest on block 3 (arrow)).

3.6.7 Landslide Classification

Prior to the 1990 landslide, the Eureka River landslide was active (based on the trace of the main scarp being discernable in the 1989 aerial photograph, Alberta, AS3896 #94), although the initial rate of movement was likely extremely slow (less than 5.0×10^{-10} m/s). The landslide velocity in June 1990 is unknown, however, Lindi Foster (personal communication, August 1990), in the late spring of 1990, observed several trees behind the main scarp had been snapped, possibly indicating very rapid movement or faster (greater than $5.0 * 10^{-3}$ m/s). The broken trees might also be due to wind. A velocity higher than slow ($5.0 * 10^{-3}$ mm/s) is assured (from the 1989 (Alberta, AS3867#93) and 1992 (Alberta, AS43333#175) aerial photographs). Since 6 October 1992 (first post-landslide aerial photograph (Alberta, AS4333#175)) until 1 May 1998 (most recent aerial photograph (Alberta, AS4917#45)), horizontal movement in blocks 2 and 3 was about 29 and 27 m respectively (from comparing aerial photographs). Therefore, between 6 October 1992 and 1 May 1998, the velocity of the landslide would be described as slow. Since 1 May 1998, the velocity of the landslide is unknown.

The landslide is classed as a translational block slide as blocks 1, 3 and 4 exhibit no rotation. As block 1 is the amalgamation of the colluvial deposits of three earlier landslides, the 1990

landslide can be classified as enlarged, irrespective of whether the landslide moved along a pre-existing rupture surface or along a new rupture surface. The retrogression of blocks 2 and 3, are also accommodated by the enlarged descriptor. The style of activity would be multiple, as the blocks are in contact with each other, and likely share a rupture surface.

The material comprising the slide can be described as earth, as greater than 80% of the material is finer than coarse sand.

Groundwater conditions prior to the 1990 landslide are not known. However, it is likely that the water table was near the surface, as a near surface water table was observed in the vicinity of the landslide during the field study (August 1999) despite minimal rainfall, and June 1990 had above average rainfall (Canada, Environment Canada, Climate Services, Eureka River near Worsley, 1998; Canada, Environment Canada, Climate Services, Clear Hills Lookout, 1993). As such, the landslide would most likely be described as wet.

The 1990 Eureka River landslide was an enlarged, multiple, wet, earth slide.

3.6.8 Successive Landslides

Instability is common at the crown and toe of the landslide. At the toe, the stream has cut a new channel to the south of the original channel. About 20 m of incision has taken place in 9 years (2.2 m per year). Due to this rapid incision, slides, falls, and flows, from both banks are common (Figure 3.16). At the crown of the landslide, by the landslide access, about 30 m of scarp retrogression has occurred between 6 October 1992 and 1 May 1998 (from the comparison of Alberta aerial photographs AS4333 #177 (1992) and AS4917 #45 (1998)). The retrogression is due to soil falls and slides (Figure 3.17). Flows, generated from within the talus beneath the scarp, are also common.

Four slide-flows to the west of block 3, and one to the east of block 3 were mapped (Figure 3.12). The largest of these, immediately west of block 3, is 65 m long (length of rupture surface), 35 m wide and up to 2.5m deep, making for a volume of 3000 m^3. Many examples of smaller slides, flows, and falls were observed from the south flank of block 3.

West of block 4, and on the opposite bank of small tributary stream that enters the Eureka River at km 10.35, is a sizeable slide (Figure 3-12). This slide might be a westward extension of the 1990 slide, but was not considered as such in the volume calculation. To the north of this slide are two sizeable flow-slides (Figure 3.12).

Figure 3.16: Complex earth slide-earth flow from the south bank of the Eureka River (near the end of the surveyed transect).

Figure 3.17: Earth slide at the main scarp (near start of surveyed transect).

3.7 Landslide Dam

3.7.1 Introduction

The 1990 Eureka River landslide dammed the Eureka River between km 10.7 and 11.7. The following discusses the status of the landslide dam (3.7.2), the landslide dam type (3.7.3), the effects of the landslide and dam on river processes, upstream (3.7.4), downstream (3.7.5), and at the landslide site (3.8.6).

3.7.2 Status of the Landslide Dam

At its maximum, the dam stood 20 m to 23 m high, creating a reservoir >8 km in length (km 11.5 to 19.8). The reservoir high stand was surmised from observation of flood debris in the branches and on the bark of trees at km 17.1, 6 m above the contemporary stream. By 6 October 1992, the reservoir had shrunk by almost 2 km, extending to km 17.8 (from aerial photograph Alberta, AS4333 #181), and shallowed by about 5 m (Figure 3.18). By 01 September 1997, the reservoir extended to km 14.7, which corresponds to regression of 3.1 km and a depth reduction of 7 m, since 6 October 1992 (from aerial photograph Alberta, AS4892 #148). Alberta aerial photograph AS4892 #148 shows two reservoirs, with a high point at km 11.7, making for a smaller reservoir between km 11.5 and 11.6, and a larger one between km 11.7 and 14.7.
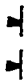
By 09 August 1999 (Figure 3.19) flooding extended to km 13.5. This corresponds to a reservoir regression of 1.2 km and a reduction in depth of about 4 m, in about 23 months. If the Eureka River incises into the landslide dam by another 4 to 5 m, the reservoir will completely drain.

3.7.3 Landslide Dam Type

Post-landslide aerial photographs (Alberta, AS4333 #176 (1992), AS4892 #148 (1997), AS4917 #45 (1998)) show an abandoned pre-landslide Eureka River channel, with a new channel to the south and at a lower elevation than the original channel. By August 1999, the original channel was 20 m above the new channel, at km 11.4. The landslide rupture surface was observed 1 m above river level, at km 11.4. As the rupture surface extended beneath the former riverbed, and emerged at the valley wall opposite to the landslide, the landslide dam would be a type 6 dam, according to Costa and Schuster (1988).

List of Symbols

Breaks in Slope:

- Concave Sharp
- Concave Rounded
- Convex Sharp
- Convex Rounded

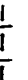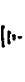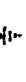## Scarps (length of line gives an indication of length of slope):

- Rounded
- Sharp
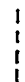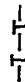
Small Mass Movements:

- Flow
- Translational Slide
- Unclassified Landslide

Streams and Lakes:

- Channel
- Abandoned Channel
- Small Stream
- Lake
- Marsh

Other Symbols:

- Landslide Boundary (approximate)
- Pressure Ridge
- Thrust Block
- Tension Crack
- Cross-Section
- Distance Marker (km)
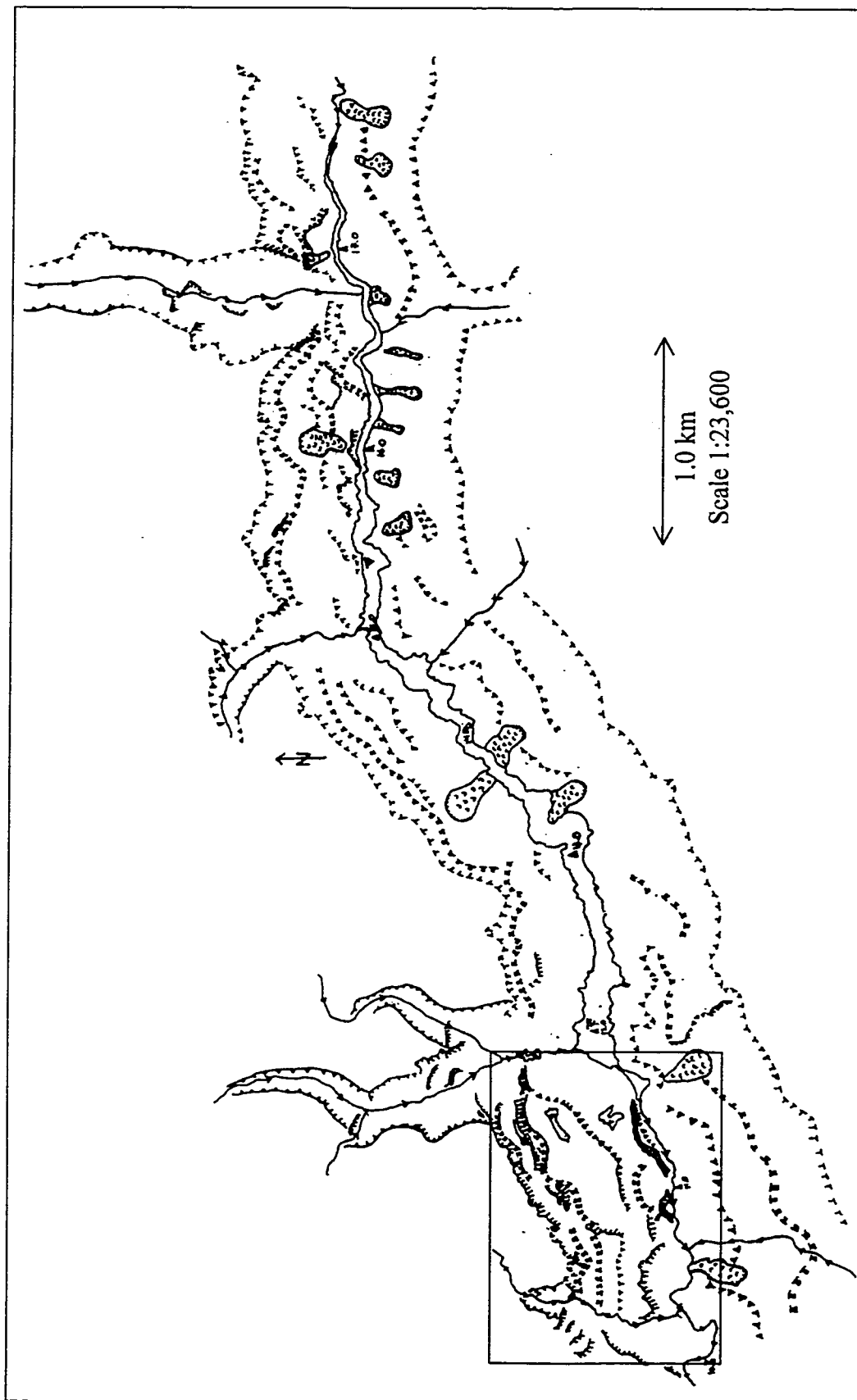
Figure 3.18: Extent of flooding on 6 October 1992 (box delineates Figures 3.11 and 3.12; symbols after Cruden and Thomson, 1987).

1.0 km
Scale 1:23,600

Figure 3.19: Reservoir in August 1999.

3.7.4 Upstream Fluvial Geomorphic Effects of the Landslide and Dam

A field traverse upstream of the landslide dam found minimal amounts of sediments associated with the reservoir. Thick vegetation in formerly flooded areas upstream of the reservoir obscured any lacustrine sediment (silts). Within the Eureka River channel, upstream of the reservoir, only channel sediments (cobbles and boulders) were obvious, except near beaver dams. A 2-m deposit of deltaic sands was seen at the mouth of a small tributary, near km 15.0. Adjacent to the reservoir, near the dam, only minor amounts of lacustrine silts were seen (i.e. a decimetre or less in depressions). Deltaic sediments were seen at the mouth of the tributary, which enters the reservoir at km 11.8, the thickness and extent of which could not be easily assessed. Thicker lacustrine deposits are expected in areas that remain flooded.

Two landslides within previously flooded areas were observed, at km 15.4 and 17.8. The association of the landslides to the reservoir is unknown.

3.7.5 Downstream Fluvial Geomorphic Effects of the Landslide and Dam

For most of the length of the Eureka River, downstream of the landslide dam, the valley walls come to the river's edges, thus making it difficult to assess the effects of the 1990 landslide on the channel.

The effects of the landslide are most apparent just downstream of the landslide dam (km 10.1 to 10.8). At km 10.8, streambed aggradation is over 2 m. Aggradation decreases downstream of km 10.8. This deposit is tantamount to a fluvial fan (Figure 3.20). The fan shape is not apparent due to the lateral restriction of the valley walls.

Figure 3.20: Aggradation of about 1.5 m at km 10.6.

The fluvial geomorphology below km 9.9 could not be assessed in the field, as a beaver dam had flooded the valley to km 9.9, making passage difficult. Comparison of 1998 (Alberta, AS4917 #23 to 26, and #34 to 36) and 1989 (Alberta, AS3867 #67 to 67, 93, 94) aerial photographs show post-landslide sediment accumulations on lower point bars, further down river, though topography restricted deposition to isolated sites.

From km 4.2 to the confluence of the Eureka and Clear Rivers (km 0), recent deposition is evident on the point bars. Some meander migration is also apparent, though such migration could be expected in the 9-year period (between 1989 and 1998) even without the landslide effects.

3.7.6 Fluvial Geomorphic Effects of the Landslide and Dam at the Landslide

Along the length of the new stream (km 10.6 to 11.5), streambed armour is mostly absent. Due to the absence of the bed armour, stream incision into the dam has been rapid (20 m in 9 years at km 11.4). As of August 1999, the new channel was near the elevation of the old channel, at km 11.4 (end of surveyed transect). Upstream of km 11.4, another 5 m of incision is required to completely drain the reservoir. Between km 11.0 and 11.1, and 11.4 and 11.5, instability at the toe of the landslide has consumed much of the pre-landslide channel, causing the reintroduction of the old channel's alluvium into the new channel. This alluvium was subsequently washed downstream. Until armour is re-established, the streambed will remain susceptible to erosion.

3.8 Discussion of Possible Triggers for the Landslide

3.8.1 Introduction

The conditions for the Eureka River landslide were created by streambed incision in response to a lowering of the base level, the Peace River. Accompanying the streambed incision was a gradual softening of the slope in response to the lateral and vertical unloading (Imrie, 1991; Matheson and Thomson, 1973). The landslide showed signs of movement prior to June 1990 (the trace of the main scarp was evident in 1989 Alberta aerial photograph AS3867#94), but the highest velocities occurred during June of 1990. Within this section I explore possible triggers for the June 1990 event; including seismic triggers (3.8.2), and hydrologic triggers (3.8.3). This is not an exhaustive list but, rather, includes the most likely candidates.

3.8.2 Seismic Triggers

Information from the Canadian National Seismological Database, via their interactive web site, revealed that there were no earthquakes near the time of the 1990 Eureka River landslide. The inputs for this query, were as follows: date: 28 April 1989 to 06 October 1992 (pre and post-landslide aerial photographic survey dates); latitude: 55° to 58° N; longitude: -121 to -117° W.

Other queries were performed, using progressively expanded geographical areas; the results were also negative.

3.8.2 Hydrologic Triggers

The possible hydrologic triggers discussed are a decrease in slope toe support due to streambed incision, or an increase in the slope pore water pressure due to an elevation of the water table.

Keegan (1992) and Lu et al., (1998) attribute the triggers for Saddle River and Hines Creek landslides, respectively, to stream incision during a major storm, in mid June 1990. Keegan calculated a return period of 50 years for the flow in the Saddle River, during this storm. Maximum instantaneous and maximum daily stream discharge data, from the Eureka River near Worsley gauge (Environment Canada, Water Survey of Canada, Eureka River near Worsley, 1998) (Figure 3.2), has April 15 as 1990's extreme values. The maximum instantaneous discharge, of 16.7 m^3/s, on April 15 ranks as the 13th largest flow out of 21 records, between 1976 and 1998, mean being 27.2 m^3/s (also see Figures 4.8 and 4.13). At the Clear River, near Bear Canyon gauge (Environment Canada, Water Survey of Canada, Clear River near Bear Canyon, 1998) (Figure 3.2) the maximum instantaneous discharge for 1990 occurred on June 12 (98.2 m^3/s, rank 8/23 (1972-1998), mean 114.7 m^3/s) indicating that the June storm might have affected the lower Eureka River watershed; although, the maximum daily discharge occurred on April 26.

Precipitation data from the town of Eureka River (Environment Canada, Climate Service, Eureka River, 1998) show above average rainfalls for June 1990 (94.4 mm, mean being 63.9 mm, rank 7/36 (1962-1997)). The Clear Hills Lookout (Environment Canada, Climate Service, Clear Hills Lookout, 1993) shows above average rainfalls for May (rank 5/29 (1961-1991)) and June 1990 (rank 4/29 1961-1991)). Neither of these stations indicates a storm equivalent to that that affected the Saddle River watershed (Keegan, 1992), during this time.

The effects of above average precipitation on the water table are likely minimal. There is evidence of a near surface water table in both pre and post-landslide aerial photographs (Alberta, AS3867#93 (1989), AS4333#76 (1992), AS4917#45 (1998)), including ponds on the uplands and valley slopes, and mottled surface tone. In the field, a puddle located 1000 m north of the main scarp, was observed to decrease in depth by only about a decimeter in 22 days (July 21 to August

91

12), despite little rainfall. However, as the landslide velocity increase is concurrent with the wet spring of 1990, elevated pore pressure as a trigger cannot be discounted.

An examination of longer-term hydrologic trends was performed to see if land cover changes, due to human occupation, have affected stream discharge, following the work of Laycock (1990) (Section 4). He suggested that agricultural practices in the Peace River Lowlands have increased the flow, and hence erosive potential, of streams. Laycock (1990) attributed the flow increases to decreased transpiration, due to the replacement of the natural forests with grain crops, coupled with agricultural land drainage. He calculated that there was a five-to ten-fold increase in water surpluses, between 1971 and 1987, in agricultural areas near Grande Prairie, due to agriculture. A comparison of land cover (Canada, Energy Mines and Resources. 1977; Alberta, Forests, Lands and Wildlife, 1991), stream flow (Environment Canada, Water Survey of Canada, 1998) and precipitation data (Environment Canada, Climate Services, 1998) was carried out to test Laycock's (1990) hypothesis (Section 4.0). There is no evidence of an anthropogenic increase in streamflow.

3.9 Conclusions

1. Three surficial units were recognized in the field at the Eureka River landslide, a postglacial lacustrine unit, till, and a preglacial lacustrine unit. The rupture surface of the 1990 landslide was within the preglacial lacustrine unit. Similar stratigraphy was seen at the Saddle River and Montagneuse River landslides. The Eureka River is likely incising into a preglacial channel at the site of the 1990 landslide.

2. Aerial photographs show evidence of large prehistoric landslides in the lower Eureka River watershed, to km 15.2 on the south (left) bank, and 18.2 on the north (right) bank. Here, valley slopes are gentler in this area, and the channel is straight – an exception to this being below km 4.2, where the river meanders. Upstream of this lowest reach, valley slopes steepen and the river meanders. Further upstream (km 32.9 to 42.8), the valley slopes lessen and the channel is mostly straight.

3. The interval between large landslides in the watershed is at least 55 years, and likely substantially longer.

92

4. The June 1990 Eureka River landslide was an enlarged, multiple, wet, earth slide. The estimated volume of the landside is between 18.9 and 54.4 Mm^3 (for Ψ_p of $11°$ and $2°$ respectively). The friction angle of the landslide was estimated to be between $13.1°$ and $22.2°$. To better determine the friction angle, the rupture surface slope might be determined and material strength tests might be done. Between October 6, 1992 and May 1, 1998, the main body of the landslide moved a further 25 to 30 m. Instability at the crown and toe (due to river incision) is ongoing.

5. The 1990 Eureka River landslide dammed the Eureka River between km 10.7 and 11.7. The landslide dam was a class 6 dam. At its maximum, the dam was 20 to 23 m high and created a reservoir exceeding 8 km in length (km 11.5 to 19.8). By August 1999, the reservoir regression was 6.3 km (to km 13.5), which corresponds to reduction in depth of about 16 m. The Eureka River has to incise into the landslide dam about another 5 m to completely drain the reservoir.

6. Fluvial geomorphic effects of the landslide and dam are greatest at the landslide, as the streambed armour was broken, leaving the streambed susceptible to erosion. The re-establishment of the armour is a slow process. Downstream and upstream effects are minimal and include sedimentation.

7. The most probable trigger for 1990 Eureka River landslide is above average precipitation in June 1990. Triggering by an earthquake or changes in land use appear unlikely.

References:

Alberta, Forests, Lands and Wildlife. 1991. Forest Management Unit Map Area, 1:1,000,000, Edmonton.

Alberta, Environment. 1999. Provincial base map 84D/4NE. 1:20,000, Edmonton.

Alberta, Environment. 1999. Provincial base map 84D/5NE. 1:20,000, Edmonton.

Alberta, Environment. 1999. Provincial base map 84D/5SE. 1:20,000, Edmonton.

Alberta, Environment. 1999. Provincial base map 84D/6NW. 1:20,000, Edmonton.

Alberta, Environment. 1999. Provincial base map 84D/6NE. 1:20,000, Edmonton.

American Society for Testing and Materials. 1998. Standard test methods for liquid limit, plastic limit, and plasticity index for soils (D4318-95a). 04.08: 519-529.

American Society for Testing and Materials. 1998. Standard test methods for particle-size analysis of soils (D422-63). 04.08: 10-19.

Benn, D.I. and Evans, D.J.A. 1998. Glaciers and glaciation. John Wiley, New York: 387-394.

Bidwell, A.K. 1999. The Engineering Geology of the Fort St. John Area. Master of Engineering. Report, Department of Civil and Environmental Engineering, University of Alberta, Edmonton.

Bobrowsky, P.T., Catto, N., and Levson, V. 1990. Reconnaissance Quaternary Geological Investigation in Peace River District, British Columbia (93P, 94A). British Columbia Geological Survey, Victoria, British Columbia, Paper 1991-1.

Bruce, I.G., Cruden, D.M., and Eaton, T.M. 1989. Use of tilting table to determine the basic friction angle of hard rock samples. Canadian Geotechnical Journal, 26: 474-479.

Canada, Centre for Remote Sensing. 2000. Website, http://www.ccrs.nrcan.gc.ca/.

Canada, Energy Mines and Resources. 1977. Clear Hills, Alberta. Map 84D, 1:250,000, Ottawa.

Canada, Energy Mines and Resources. 1977. Many Islands, Alberta. Map 84D/6, 1:50,000, Ottawa.

Canada, Environment Canada, Climate Services. 1993. Canadian Monthly Climate Data CD, Clear Hills Lookout.

Canada, Environment Canada, Climate Services. 1998. Canadian Monthly Climate Data CD, Eureka River.

Canada, Environment Canada, Water Survey of Canada. 1998. HYDAT CD. Clear River Near Bear Canyon.

Canada, Environment Canada, Water Survey of Canada. 1998. HYDAT CD. Eureka River Near Worsley.

Canada, Geological Survey. 2000. Canadian national seismological database. Website, www.seismo.nrcan.gc.ca/.

Catto, N.R. 1991. Quaternary geology and landforms of the eastern Peace River region, British Columbia NTS 94A/1,2,7,8. British Columbia Ministry of Energy, Mines and Petroleum Resources, Open File 1991-11, Victoria.

Catto, N.R., Liverman, D.G.E., Bobrowsky, P.T., and Rutter, N. 1996. Laurentide, Cordilleran and montane glaciation in the western Peace River – Grande Prairie Region, Alberta and British Columbia, Canada. Quaternary International, 32: 21-32.

Costa, J.E. and Schuster, R.L. 1988. The formation and failure of natural dams. Geological Society of America, Bulletin 100: 1054-1068.

Cruden, D.M. 2000. Some forms of mountain peaks in the Canadian Rockies controlled by their rock structure. Quaternary International, in press.

Cruden, D.M., Keegan, T.R., and Thomson, S. 1993. The Landslide Dam on the Saddle River near Rycroft, Alberta. Canadian Geotechnical Journal, 30: 1003-1015.

Cruden, D.M., Hofmann, B.A., and Thomson, S. 1991. Observations of Graben Geometry in Landslides. Institute of Civil Engineers, Proceedings of International Conference of Slope Stability Engineering, London: 33-35.

Cruden, D.M., Lu, Z-Y., and Thomson, S. 1997. The 1939 Montagneuse River landslide, Alberta. Canadian Geotechnical Journal, 34: 799-810.

Cruden, D.M. Ruel, M., and Thomson, S. 1990. Landslides along the Peace River, Alberta. Proceedings, 43rd Canadian Geotechnical Conference, 1: 61-67.

Cruden, D.M. and Thomson, S. 1987. Exercises in terrain analysis. University of Alberta.

Cruden, D.M. and Varnes, D.J. 1996. Landslides Types and Processes. In Landslides: Investigation and Mitigation. Transportation Research Board, National Academy of Science, Special Report 247, Washington, D.C.

Evans, S.G. 1986. Landslide Damming in the Cordillera of Western Canada. In Landslide Dams: Processes, Risk and Mitigation. American Society of Civil Engineers, Geotechnical Special Publication No. 3, New York.

Evans, S.G., Hu, X.Q., and Enegren, E.G. 1996. The 1973 Attachie Slide, Peace River Valley, near Fort St. John, British Columbia, Canada: A Landslide with a high-velocity flowslide component in Pleistocene sediments. Proceedings, 7th International Symposium on Landslides, Trondheim, Norway. A.A. Balkema, Rotterdam, 2: 715-720.

Imrie, A.S. 1991 Stress-induced responses from both natural and construction-related deepening of the Peace River valley, B.C. Canadian Geotechnical Journal, 28: 719-728.

Jones, J.F. 1966. Bedrock Geology of the Peace River district. Research Council of Alberta, Bulletin 16, Edmonton.

Hackbarth, D.A. 1977. Hydrogeology of the Grande Prairie Area. Alberta Research Council, report 76.4, Edmonton.

Hardy, R.M., Brooker, E.W., and Curtis, W.E.- 1962. Landslides in over-consolidated clays. Engineering Journal, 45.6: 81-89.

Keegan, T.R. 1992. The Rycroft landslide dam on the Saddle River, Alberta. Master of Science thesis, Department of Civil Engineering, University of Alberta, Edmonton.

Kerr, H.A. 1971. Groundwater study Worsley area. Water Resources Division, Soil Geology and Groundwater Branch, Edmonton.

Laycock, A.H. 1990. Integrated Land Use and Water Management to Limit Erosion in the Peace River Region. In, Smith, P.J., and Jackson, E.L. (editors), A World of Real Places, Studies in Geography, University of Alberta, Edmonton: 115-132.

Liverman, D.G.E. 1991. Sedimentology and history of a Late Wisconsinan glacial lake, Grande Prairie, Alberta, Canada. Boreas, 20: 241-257.

Liverman, D.G.E., Catto, N.R., and Rutter, N.W. 1988. Laurentide glaciation in west-central Alberta: a single (Late Wisconsinan) event. Canadian Journal of Earth Science, 26: 266-274.

Lu, Z.Y., Cruden, D.M., and Thomson, S. 1998. Landslides and Preglacial Channels in the Western Peace River Lowland. Proceedings, 51st Canadian Geotechnical Conference, Edmonton, Alberta, 4-7 October, 1: 267-274.

Matheson, D.S, and Thomson, S. 1973. Geological implications of valley rebound. Canadian Journal of Earth Sciences, 10: 961-978.

Nasmith, H. 1964. Landslides and Pleistocene Deposits in the Meikle River Valley of Northern Alberta. Canadian Geotechnical Journal, 1: 155-166.

Ozoray, G. 1982. Hydrogeology of the Clear Hills-Chinchaga River area, Alberta. Alberta Research Council, Edmonton, Earth Sciences Report 82-4.

Pawlowicz, J.G. and Fenton, M.M. 1995. Bedrock topography of Alberta. Alberta Geological Survey, Map226, Edmonton.

Radarsat International. 2000. Website, http://www.rsi.ca/.

Reeder, S.W. and Odynsky, W.M. 1965. Reconnaissance soil survey of the Cherry Point and Hines Creek area. Research Council of Alberta, Report Number 85, Edmonton.

Schuster, R.L. and Costa, J.E. 1986. A Perspective on Landslide Dams. In Landslide Dams: Processes, Risk and Mitigation. American Society of Civil Engineers, Geotechnical Special Publication No. 3, New York.

Selby, M.J. 1993. Hillslope materials and processes. 2nd ed. Oxford. New York: 111, 270.

Skempton, A.W. 1985. Residual strength of clays in landslides, folded strata and the laboratory. Geotechnique, 35,1: 3-18.

Thomson, S. and Hayley, D.W. 1975. The Little Smoky Landslide. Canadian Geotechnical Journal, 12: 379-392.

Thurber Engineering Ltd. 1997. Eureka River Crossing (of highway 726) Site 1. Survey and drill core data (97-2, 97-3). Thurber Engineering, Edmonton.

Thurber Engineering Ltd. 1998. Eureka River Crossing (of highway 726) Site 2. Survey and drill core data (98-1, 98-2). Thurber Engineering, Edmonton.

4.0 Land Clearing and Tributary Streamflow in the Peace River Lowlands

4.1. Introduction

Since 1990, there have been at least five major landslides in the Peace River Lowlands, Alberta. Ranked by volume, these landslides are amongst the largest that have been recorded in Alberta. These landslides include the 1990 Eureka River landslide (Chapter 3), the 1990 Hines Creek landslide (Lu et al., 1998), the 1990 Saddle River landslide (Cruden et al., 1993), the 1995 Spirit River landslide (Chapter 2), and the Vessall Creek landslide (between 1993 and 1997) (Figure 4.1). The Eureka River, Hines Creek, Saddle River, and Spirit River landslides are the only major landslides, visible on aerial photographs, within each of these watersheds since aerial photographic coverage began (ca. 1945). An inspection of historical aerial photographs of the Saddle River and Vessall Creek watersheds for landslides has yet to be carried out.

Laycock (1990) provided one possible explanation for the occurrence of the recent landslides. He suggested that in the Peace River Lowlands, land clearing for agriculture has increased water excess, which in turn, has increased streamflow and induced streambed erosion. The 1980's saw the Alberta government's Accelerated Land Sales initiative, which actively encouraged agricultural expansion in the Peace River Region, despite extensive tracts of land having being cleared in the recent past (Fox and Mecenko, 1985).

Laycock (1990) attributed the increases in excess water to agriculturally related reductions in transpiration. He calculated that there was a five-to ten-fold increase in water surpluses, between 1971 and 1987, in agricultural areas near Grande Prairie, due to agricultural land clearing. This argument of less transpiration from crops versus forests is challenged by Oke (1987). Laycock (1990) did not support his argument with long-term hydrologic data.

The following will explore whether Laycock's (1990) thesis can be supported with available hydrologic, meteorologic, and land cover data. The Saddle River and Eureka River watersheds were selected for this study, as recent landslides have occurred within these watersheds, and historical hydrologic, meteorologic, and land cover data are available.
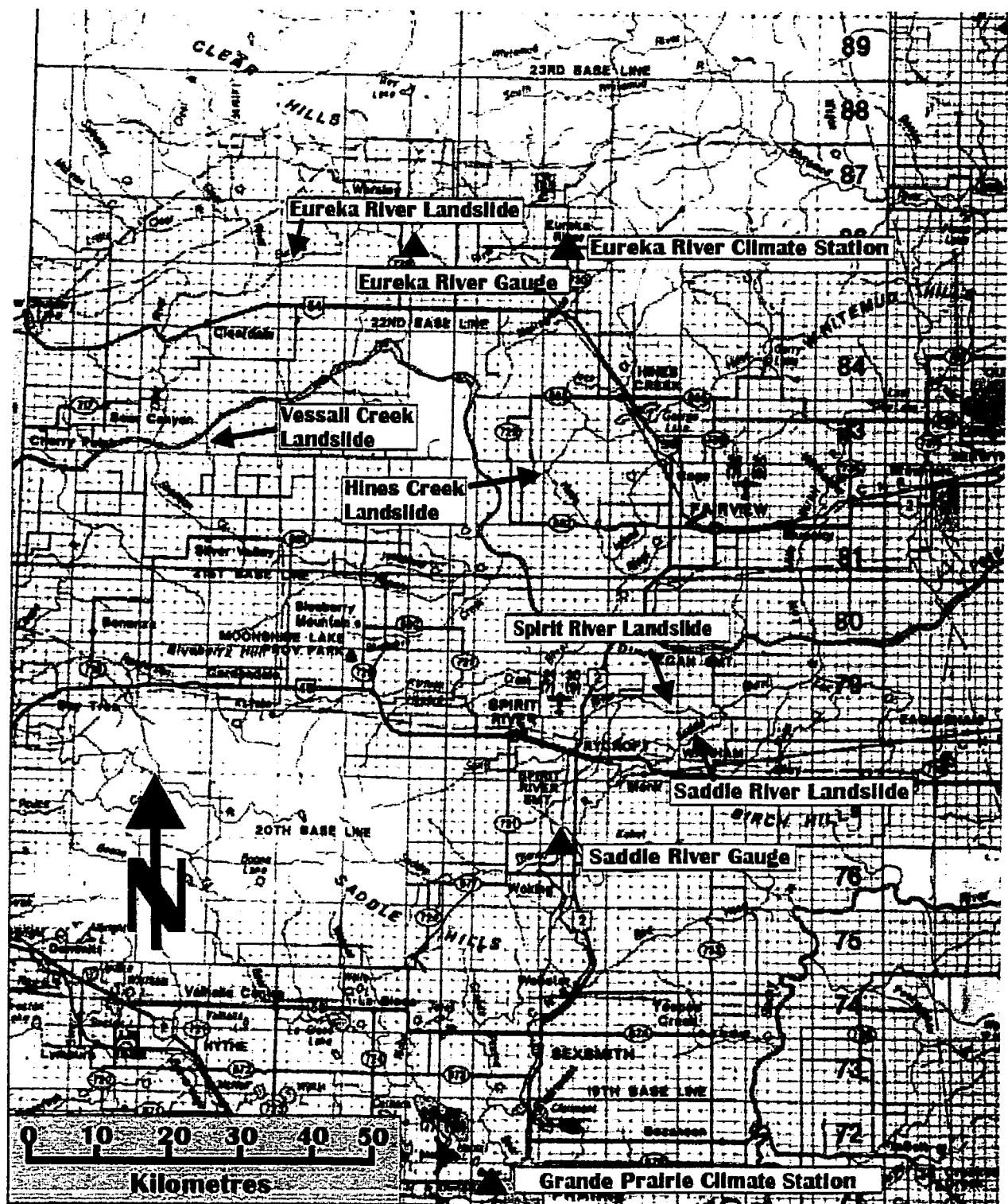
Figure 4.1: Location of landslides, climate stations, and stream gauges (scale 1:800,000; Alberta, 1992).

4.2 Background

4.2.1 Saddle River Watershed

The headwaters of the Saddle River watershed are located in the Saddle Hills, which confine the watershed to the south and to the west. The Saddle Hills rise abruptly from the Peace River Lowlands – a topographically gentle expanse, which constitutes the majority of the watershed's area, and into which the Saddle River has deeply incised. The Saddle River flows in a northeasterly direction, and enters the Peace River on the right bank at 55°50'N, 118°08'W. The maximum relief of the watershed is 690 m (1050 to 360 m.a.s.l.). The Saddle River gauge, operating annually from March to October, is located at 55°38'39"N, 118°41'51"W, near Woking, Alberta (Figure 4.1) (Environment Canada, Water Survey of Canada, Saddle River Near Woking, 1998). The local relief between the headwaters and the gauge is 330 m. There are 538 km² of land upstream of the gauge. This study considers only the area upstream of the gauge.

Land cover information for the Saddle River watershed was extracted from topographic maps. In 1963, upstream of the gauge, there were 106 km² of developed and agricultural land (Canada, Department of Mines and Technical Survey, 1964). By 1989, agricultural and developed land, upstream of the gauge had increased to 184 km² (Energy Mines and Resources, Grande Prairie, 1994), or by 173%.

Precipitation data from the Grande Prairie climate station were used in the analyses of the Saddle River, as this is the closest station to the Saddle River watershed with a continuous precipitation record (Figure 4.1). The station, operating since 1942, is located at 55°11'N, 118°53'W, at an elevation of 666 m.a.s.l (Environment Canada, Climate Services, Grande Prairie, 1998).

4.2.2 Eureka River Watershed

The headwaters of the Eureka River watershed are in the Clear Hills, which confine the watershed to the north and east. The Clear Hills rise abruptly out of the Peace River Lowlands – a topographically subtle expanse, into which the Eureka River has deeply incised. The Eureka River flows predominantly in a westerly direction and enters the Clear River at 56°23'N, 119°30'W. The Clear River, in turn, enters the Peace River on the left bank at 56°10'N, 119°42'W. The maximum relief of the Eureka River watershed is 550 m (1080 to 530 m.a.s.l. at the Clear River). The Eureka River gauge, operating annually from March to October, is located

at 56°27'00''N, 119°07'10''W on the left bank (Figure 4.1) (Environment Canada, Water Survey of Canada, Eureka River Near Worsley, 1998). The local relief between the headwaters and the gauge is 425 m. There are 754 km² of land upstream of the gauge. As for the Saddle River, this study considers only the area upstream of the gauge.

Land cover information for the Eureka River watershed was extracted from topographic maps. In 1975, upstream of the gauge, there were 285 km² of developed and agricultural land (Canada, Energy Mines and Resources, Clear Hills, 1977). By 1990, agricultural and developed land, upstream of the gauge had increased to 525 km² (Alberta, 1991), or by 184%.

Precipitation data from the Eureka River climate station were used in the analysis of the Eureka River. This station, operating since 1962, is located at 56°29'N, 118°44'W, at an elevation of 665 m.a.s.l. (Figure 4.1) (Environment Canada, Climate Services, Eureka River, 1998). Precipitation data, from this station are unavailable for April 1972, 1976 and 1982, January 1986, and July 1989.

4.3 Methods

To analyse whether a relationship exists between agricultural land clearing and stream discharge in the Peace River Lowlands, a series of graphs were created, and the following relationships were investigated:

(1) Historical trends of stream discharge and precipitation for the Eureka and Saddle River watersheds.

Specifically the following relationships were investigated:

a. Trends of total annual stream discharge;

b. Trends of annual precipitation at the Grande Prairie and Eureka climate stations;

c. Trends of total annual stream discharge (using five-year moving means); and

d. Trends of April, May, and June total monthly discharge.

These graphs were created to view the data sets prior to any data manipulation. The graphs of the five-year moving means were created to reduce the scatter in the raw annual data. The April, May, and June monthly total discharge graphs were created, as flooding is most common in the spring.

(2) Trends in the ratio of stream discharge to total basin precipitation for the Eureka and Saddle Rivers.

Specifically the following analyses were performed:

a. Trends in the ratio of total annual stream discharge to total annual basin precipitation (November 1 to October 31);

b. Trends in the ratio of April, May and June, monthly total discharge to April, May, and June monthly total basin precipitation;

These graphs were created to investigate discharge trends, irrespective of precipitation. The analyses required that the precipitation data be multiplied by the basin area, upstream of the gauging stations. The assumption that the precipitation will fall evenly throughout the entire basin is a potential source for error.

The rationale behind using precipitation data spanning November 1st to October 31st of the following year (i.e., November 1, 1980 to October 31, 1981), for the annual analyses, is that after October the mean monthly temperature drops below zero degrees. Therefore, any precipitation recorded will be in the form of snow and will not contribute to streamflow until the subsequent spring. It is recognised that some of this precipitation will sublimate, some will infiltrate, and some will runoff in November, or possibly December, rainfall events. It is also recognised that winter precipitation storage may begin before November 1st in any given year.

The April, May, and June monthly analyses were performed as flooding is most common in the spring. Further, the relationship between rainfall and stream discharge will likely be the strongest in the spring, as proportional losses to evaporation, infiltration, and human use will be minimal. Contributions to stream discharge from snowmelt are a source of error, especially in the early spring.

4.4 Results

4.4.1 Historical Trends in Stream Discharge and Precipitation for the Saddle and Eureka River Watersheds

For the Saddle River and the Grande Prairie climate station, and the Eureka River and Eureka River climate station, there has been an apparent trend toward increasing precipitation and an

102

apparent trend towards decreasing total stream discharge (Figures 4.2 and 4.3). These results challenge Laycock's (1990) hypothesis. If his hypothesis was supported by the raw data, then the discharge trend line should exhibit a more positive slope than the precipitation trend line, given that there has been a net increase in agricultural land over time.
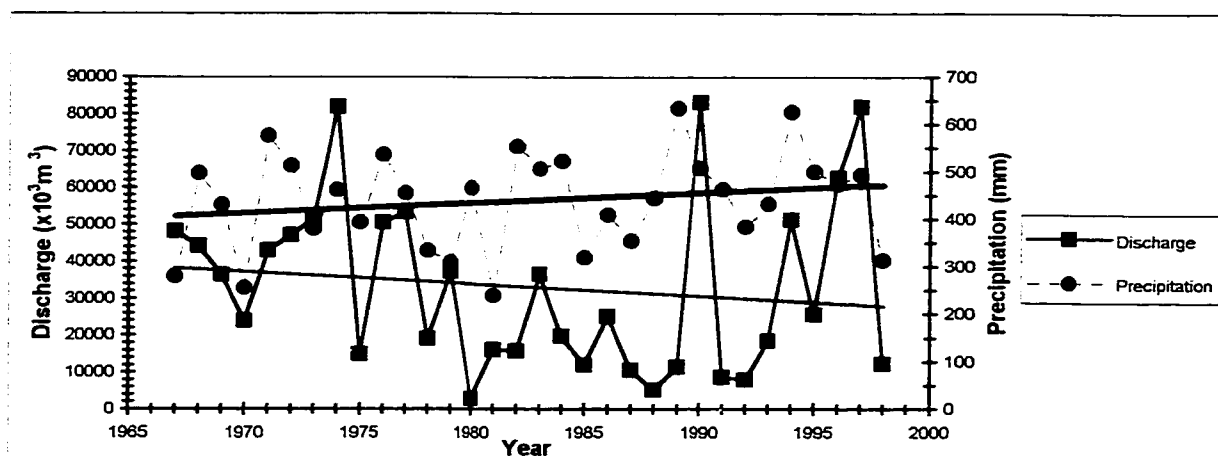
Figure 4.2: Total annual precipitation at the Grande Prairie climate station and total annual streamflow in the Saddle River versus time (x-axis).
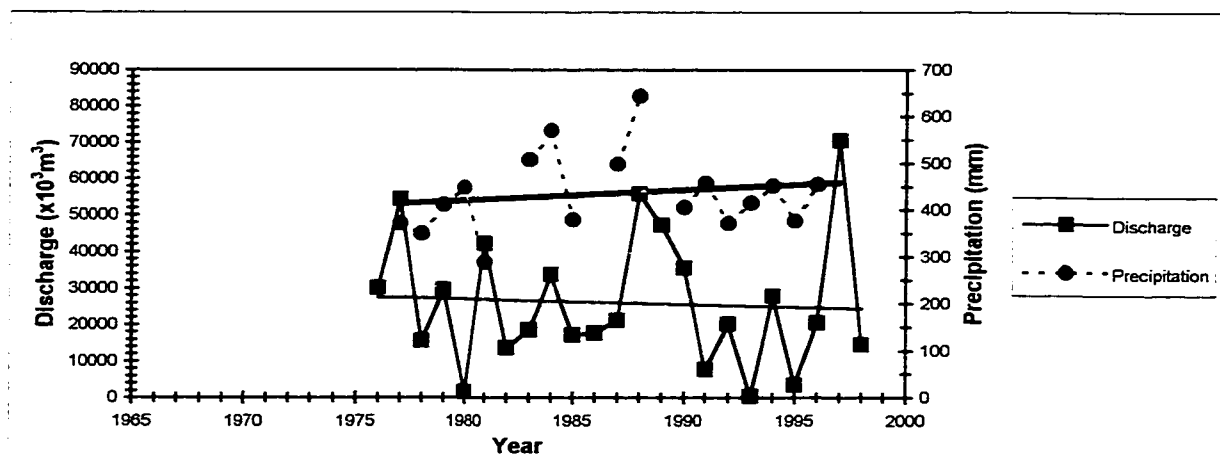
Figure 4.3: Total annual precipitation at the Eureka River climate station and total annual stream discharge for the Eureka River versus time (x-axis).

Figures 4.4 and 4.5 show five-year moving means of the total annual discharge of the Saddle and Eureka rivers respectively. Figures 4.4 and 4.5 are consistent with Figures 4.2 and 4.3, in that the trend lines have negative slopes.

103
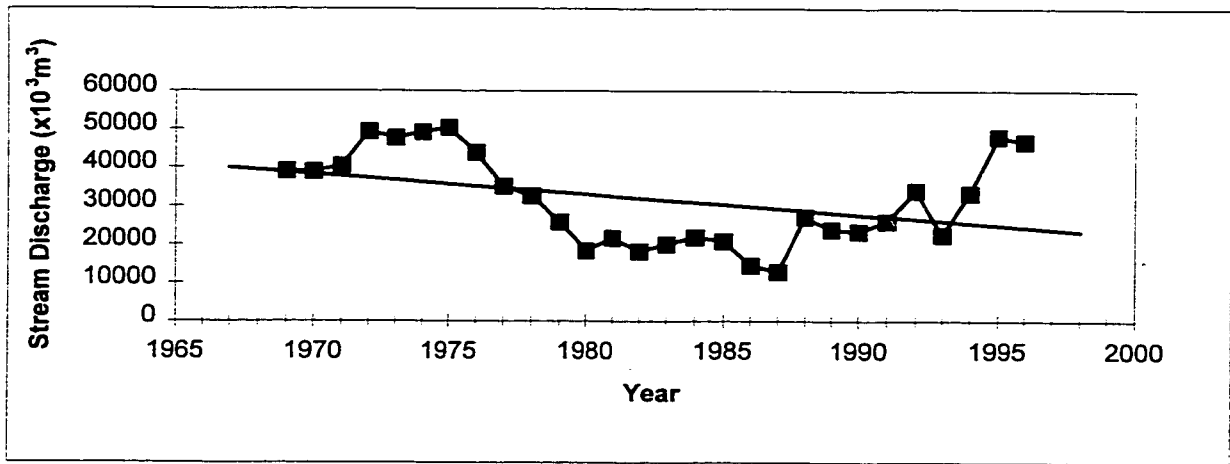
Figure 4.4: Five-year moving mean of Saddle River stream discharge versus time (x-axis).
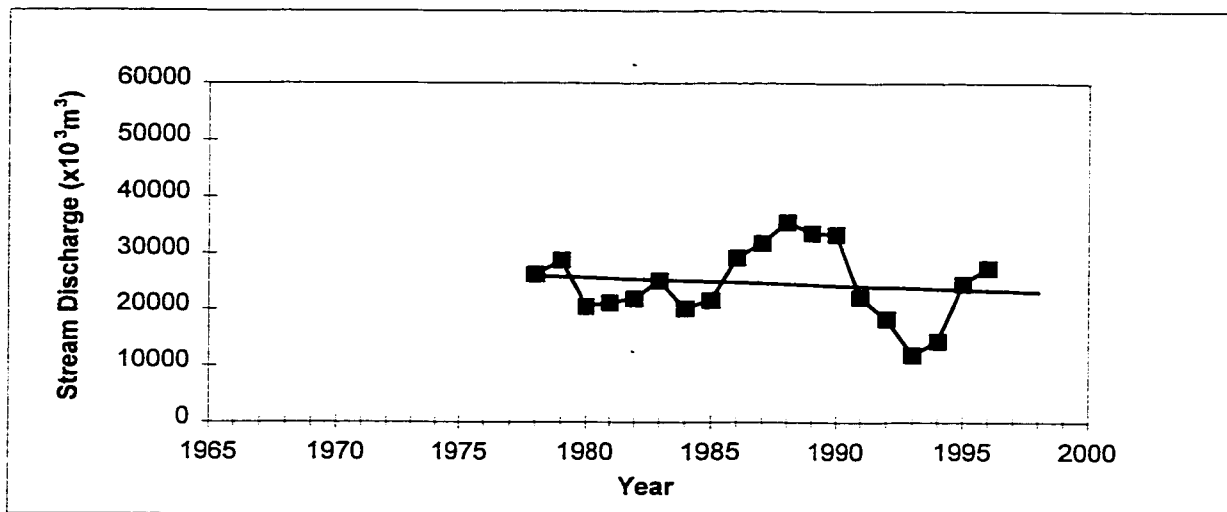
Figure 4.5: Five-year moving mean of Eureka River stream discharge versus time (x-axis).

Figures 4.6, 4.7 and 4.8 show the total monthly stream discharge for April, May, and June (respectively) of the Eureka and Saddle rivers. Generally, the results are consistent with the annual stream discharge data, in that most of the trend lines have negative slopes; the exception being the April streamflow trend line of the Eureka River. The effects of the increased agriculture should be most apparent in these graphs, as the soil will likely be nearly saturated.
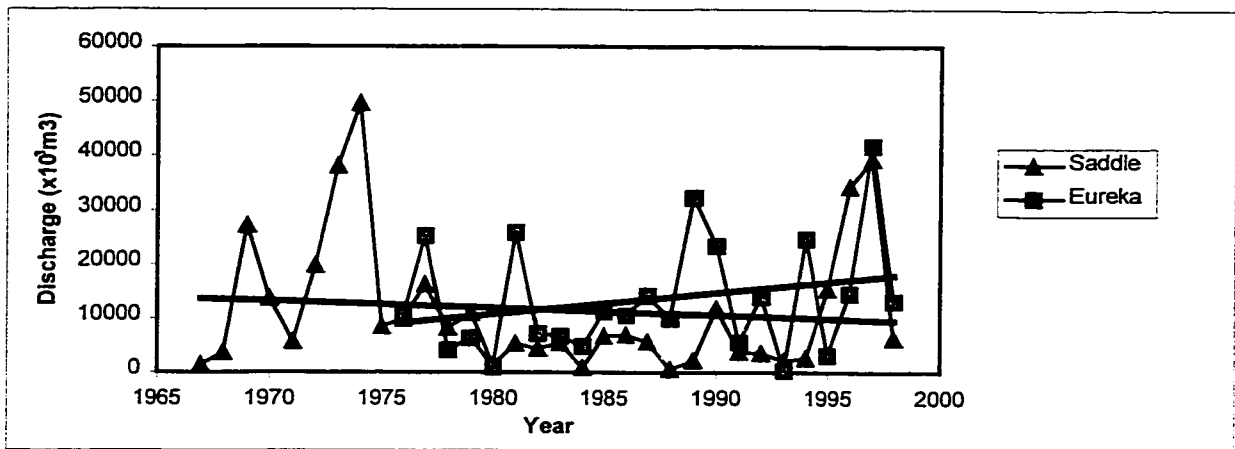
Figure 4.6: April total monthly streamflow in the Saddle and Eureka Rivers versus time (x).
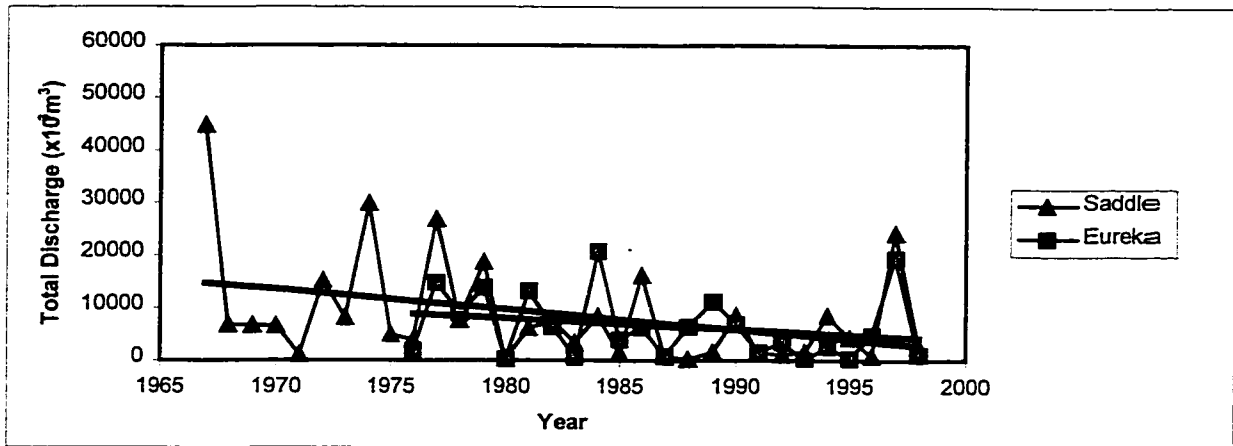
Figure 4.7: May total monthly streamflow for the Saddle and Eureka Rivers versus time (x).
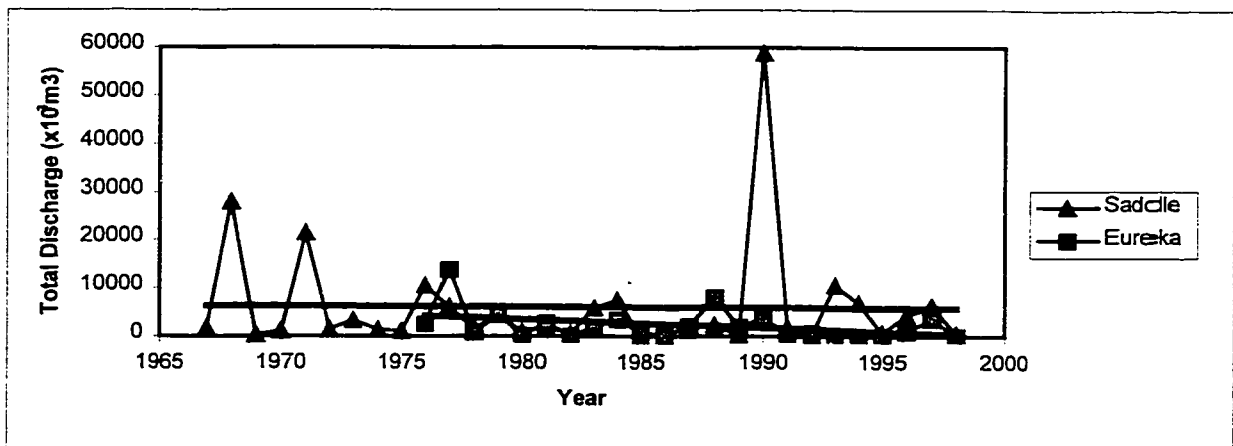
Figure 4.8: June total monthly streamflow for the Saddle River and Eureka River versus time (x axis).

4.4.2 Trends in the Ratio of Stream Discharge to Total Basin Precipitation

Figures 4.9 and 4.10 depict the trend in the ratio of total annual discharge to total annual basin precipitation (November 1 to October 31), for the Saddle River and Eureka River watersheds. The resultant information contains substantial scatter. Scatter is greater in the Saddle River plot (Figure 4.10), possibly due to climatic variability between the Saddle River watershed and Grande Prairie climate station. This climatic variability is most pronounced in the 1990 datum; in that, the high 1990 annual discharge value, for the Saddle River, does not correspond with a higher than average annual precipitation value from the Grande Prairie climate station. Some scatter, in both plots, is expected and can be attributed to wetter than average years having higher relative runoff (to the amount of precipitation) than drier years. Of interest are the low numeric values of the runoff precipitation ratios, indicating that only a very small portion of the total precipitation contributes to stream flow. For the Eureka River the discharge to precipitation ratio averages 7.9% for 1977 to 1997. The linear trend lines in both graphs maintain a negative slope, which suggests that over the interval of the study, the quantity of discharge was decreasing, irrespective of precipitation.
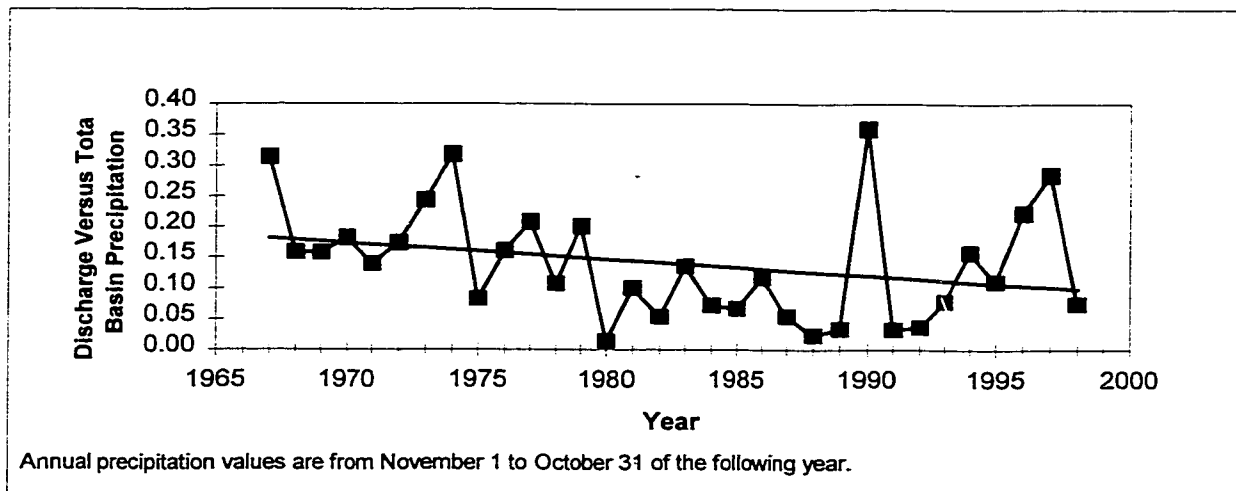
Figure 4.9: Ratio of total annual stream discharge to total annual basin precipitation for the Saddle River, using Grande Prairie precipitation data versus time (x-axis).

106
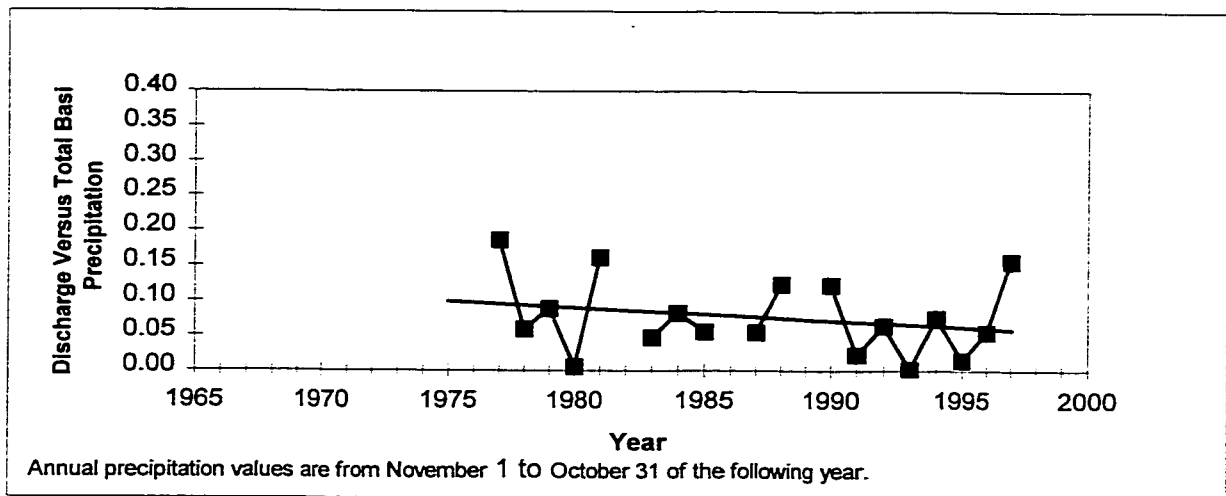
Figure 4.10: Ratio of total annual stream discharge to total annual basin precipitation for the Eureka River using Eureka River precipitation data versus time (x-axis).

Figures 4.11, 4.12, and 4.13 depict the April, May, and June (respectively) total monthly discharge versus total monthly basin precipitation for the Saddle and Eureka rivers. The vertical scale changes between graphs. Both the Saddle and Eureka Rivers report ice conditions in early to mid April. The ice conditions will explain datum values greater than unity in April (Figure 4.11), and the reduction in data variance from the trend line, in subsequent months (Figures 4.12 and 4.13). In Figure 4.12, prior to 1973 the data for the Saddle River have been excluded, as the May 1972 value of 25.7 created an unrealistic trend line slope. The cause of this extraordinary datum value may be due to the use of Grande Prairie precipitation data for the Saddle River analysis. Also of interest is the small proportion of the total precipitation that contributes to stream discharge of the Eureka River in June (average 4.2%). The trend lines in all graphs have a negative slope, which suggests that over the interval of the studies, the quantity of April, May and June monthly discharge was decreasing, irrespective of precipitation.

107
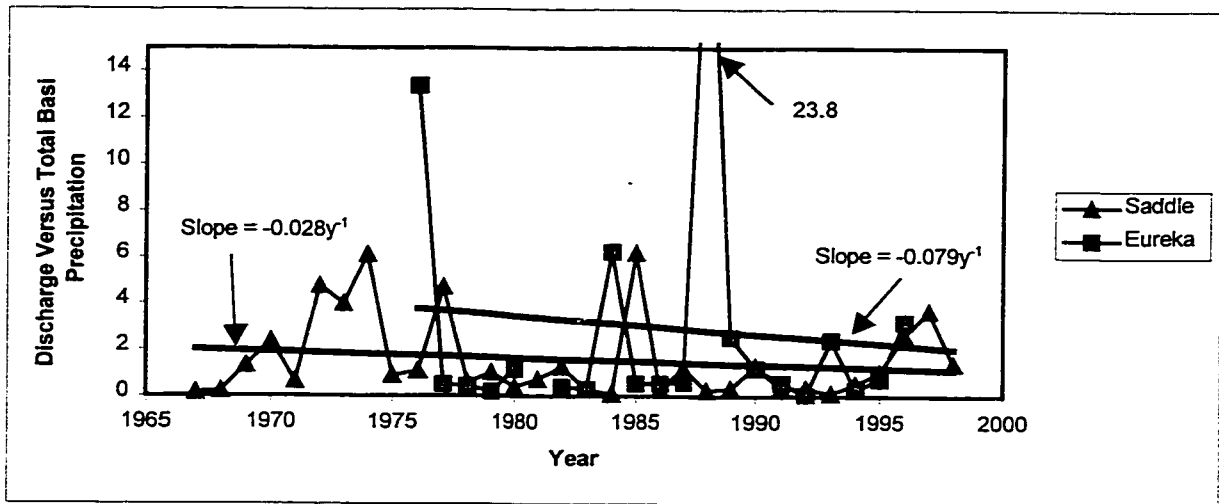
Figure 4.11: Ratio of total April monthly stream discharge to total April monthly basin precipitation for the Saddle and Eureka Rivers (precipitation data for the Saddle River are from the Grande Prairie climate station) versus time (x-axis).
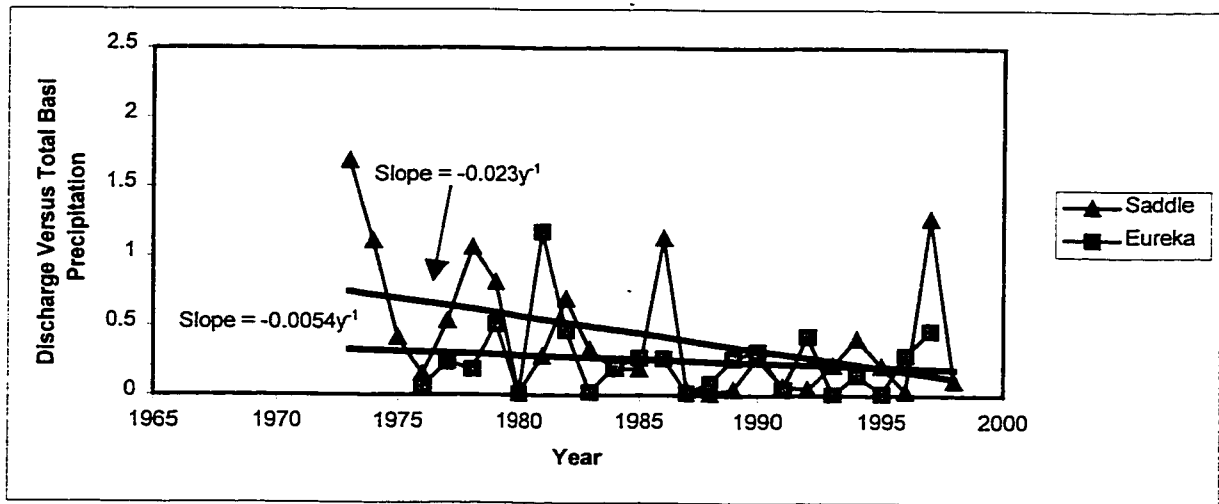
Figure 4.12: Ratio of total May monthly stream discharge to total May monthly basin precipitation for the Saddle and Eureka Rivers (precipitation data for the Saddle River are from the Grande Prairie climate station) versus time (x-axis).
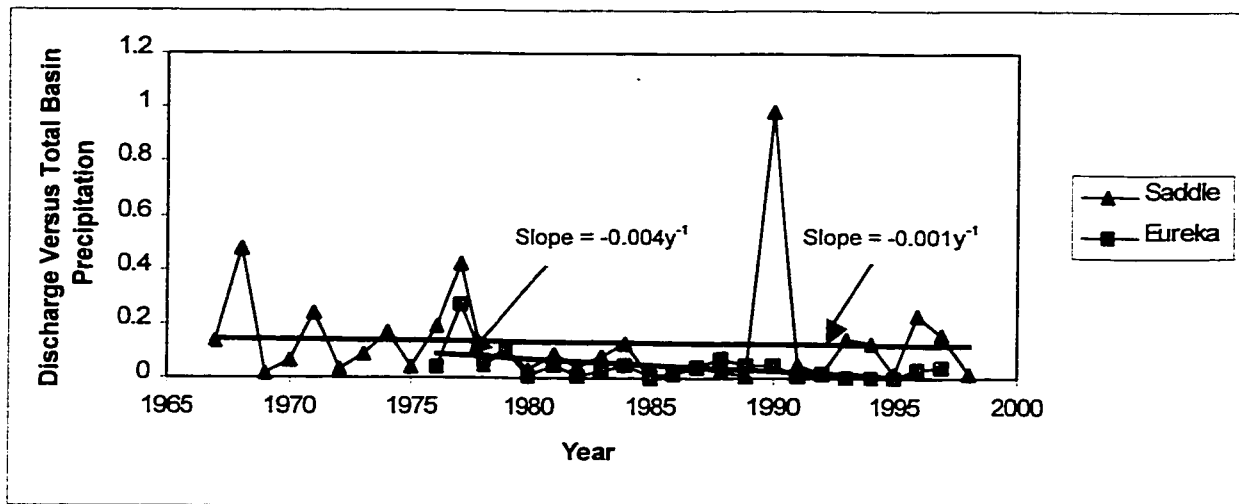
Figure 4.13: Ratio of total June monthly stream discharge to total June monthly basin precipitation for the Saddle and Eureka Rivers (precipitation data for the Saddle River are from the Grande Prairie climate station) versus time (x-axis).

4.5 Conclusions

There appears to be no general trend towards increasing stream discharge for either the Eureka or Saddle Rivers, in annual or April, May and June monthly data, despite substantial increases of agricultural land area within the two watersheds and an apparent increasing annual precipitation trend. The exception to this is in the April total monthly stream discharge trend for the Eureka River (Figure 4.6); although, when precipitation is accounted for, the trend line has a negative slope (Figure 4.11). The April data are strongly affected by snowmelt and ice conditions, thus to draw conclusions from these data requires further analysis. From this preliminary analysis, it is concluded that no tangible positive relationship between agricultural land area and streamflow, is evident.

References

Alberta, Forests, Lands and Wildlife. 1991. Forest Management Unit Map Area, 1:1,000,000, Edmonton.

Canada, Energy Mines and Resources. 1977. Clear Hills, Alberta. Map 84D, 1:250,000, Ottawa.

Canada, Energy Mines and Resources. 1994. Grande Prairie, Alberta. Map 83M, 1:250,000, Ottawa.

Canada, Environment Canada, Climate Services. 1998. Canadian Monthly Climate Data CD, Eureka River. Ottawa

Canada, Environment Canada, Climate Services. 1998. Canadian Monthly Climate Data CD, Grande Prairie. Ottawa.

Canada, Environment Canada, Water Survey of Canada. 1998. HYDAT CD, Eureka River Near Worsley. Ottawa.

Canada, Environment Canada, Water Survey of Canada. 1998. HYDAT CD, Saddle River Near Woking. Ottawa.

Canada, Mines and Technical Surveys. 1963. Grande Prairie, Alberta. Map 83M, 1:250,000, Ottawa.

Cruden, D.M., Keegan, T.R., and Thomson, S. 1993. The Landslide Dam on the Saddle River near Rycroft, Alberta. Canadian Geotechnical Journal, 30: 1003-1015.

Fox, M.F. and Mecenko, S.L. 1985. The agriculture-forest interface: an overview of land use change. Lands Directorate, Environment Canada, working paper 38, Ottawa.

Laycock, A.H. 1990. Integrated Land Use and Water Management to Limit Erosion in the Peace River Region. In, Smith, P.J., and Jackson, E.L. (editors), A World of Real Places, Studies in Geography, University of Alberta, Edmonton: 115-132.

Lu, Z., Cruden, D.M., and Thomson, S. 1998. Landslides and Preglacial Channels in the Western Peace River Lowland. Proceedings, 51st Canadian Geotechnical Conference, Edmonton, Alberta, 4-7 October, 1: 267-274.

Oke, T.R. 1987. Boundary layer climates. 2nd ed. Routledge. New York: 155-156.

5.0 Landslides and Tributary Geomorphology in the Peace River Lowland

5.1 Introduction

The last 60 years have seen at least five major landslides, in natural settings, on tributaries within the western Peace River Lowlands of Alberta. These including the 1990 Eureka River landslide (Chapter 3), the 1990 Hines Creek landslide (Lu et al., 1998), the 1939 Montagneuse River landslide (Cruden et al., 1997), the 1990 Saddle River landslide (Cruden et al., 1993), and the 1995 Spirit River landslide (Chapter 2) (Figure 5.1). A sixth landslide, the Vessall Creek landslide (October 1993 to September 1997), was excluded from this study due to lack of detailed information.

The landslides were entirely composed of Quaternary sediment; the Spirit River and Hines Creek landslides' rupture surfaces are within till and the Eureka, Montagneuse and Saddle River landslides' rupture surfaces are within preglacial lacustrine sediment. Smaller landslides, with rupture surfaces within postglacial sediment, were also recognized in all of these watersheds (except for the Saddle River watershed that was not inspected for this phenomenon).

The following section explores the interrelationship of surficial stratigraphy, landslides, and tributary morphology within the Peace River Lowland. Included are a discussion of the prevalence of landslides within each surficial stratigraphic unit (5.2), a description of how the surficial stratigraphy is revealed in the tributary valley slopes by landslides (5.3), and a discussion on the longitudinal profiles of tributary streams within the Peace River Lowlands (5.4). Finally, a preliminary model of the morphology of a tributary stream, in sediment, within the Peace River Lowlands is suggested (5.5), borrowing from Lu and Cruden (2000).

111
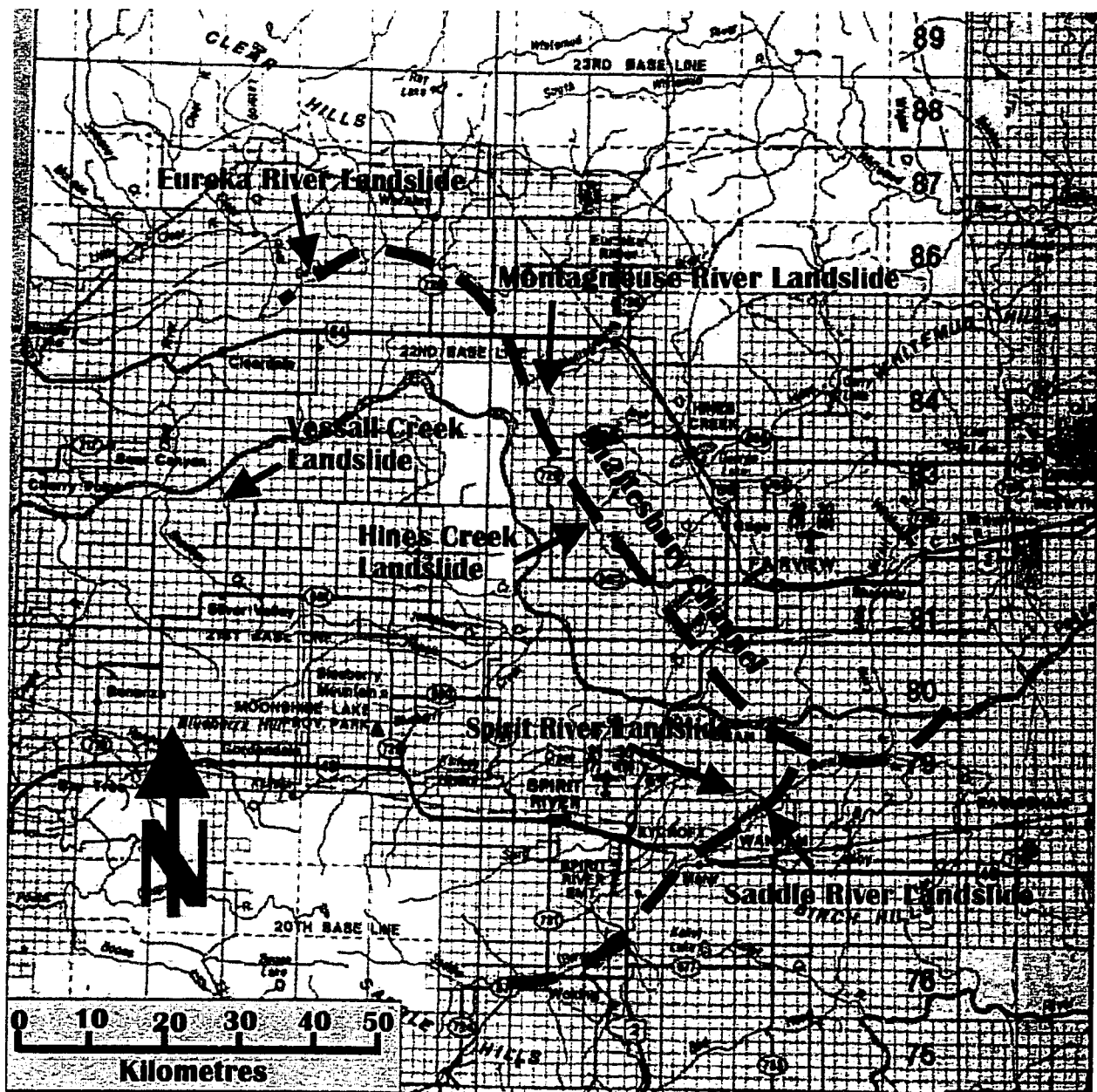
Figure 5.1: The Peace River Lowlands (scale 1:800,000), with the locations of recent large landslides and preglacial valleys (dashed lines) indicated (Pawlowicz and Fenton, 1995).

5.2 Stratigraphy and Landslides

All of the large historic sedimentary landslides being considered occurred within sediment deposited within preglacial valleys (Figures 5.1 and 5.2). The sediments within these preglacial valleys can include preglacial fluvial sediment, overlain by preglacial lacustrine sediment, then

till, and at the surface, postglacial lacustrine sediments (Figure 5.2). In the Peace River Lowlands, outside of the preglacial valleys, sediment typically consist of till with postglacial lacustrine sediments atop (Catto, 1991; Jones, 1966; Ozoray, 1982), and is generally less than 50 m thick (Carlson and Hackbarth, 1974; Hackbarth, 1977; Kerr, 1971; Ozoray, 1982). The thickness of the surficial deposits within the preglacial valleys can exceed 200 m (Carlson and Hackbarth, 1974).
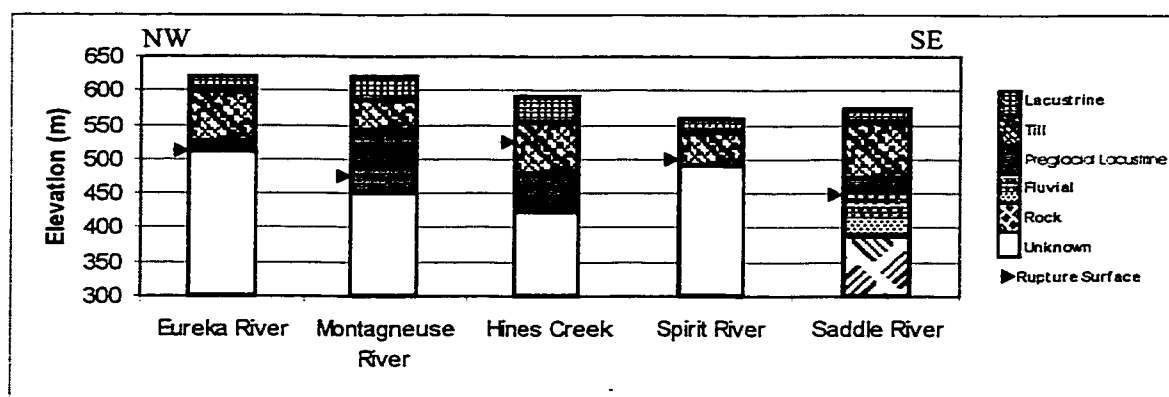
Figure 5.2: Surficial stratigraphy at the Eureka River, Montagneuse River (Cruden et al., 1997), Hines Creek (Lu et al., 1998), Spirit River, and Saddle River (Cruden et al., 1993) landslides.

Each stratigraphic unit is weak and prone to failure upon being exposed by the degrading tributary streams within the Peace River Lowlands. In the Eureka River watershed, abandoned and suspended (last movement within the previous annual cycle) landslides were recognized within the postglacial lacustrine deposits (Thurber Engineering, 1997 and 1998), and dormant and abandoned landslides were recognized within the till and preglacial lacustrine deposit. The 1990 Eureka River landslide was an enlarged earth slide with a rupture surface within the preglacial lacustrine deposit, 120 m below the Lowland plains. In the Montagneuse River watershed, abandoned landslides were recognized within the till and postglacial lacustrine deposits, and dormant landslides were recognized within the preglacial lacustrine deposits (Lu and Cruden, 2000). The 1939 Montagneuse River landslide is a reactivated and retrogressive earth slide with a rupture surface within the preglacial lacustrine deposit (Z. Lu, personal communication, May 2000), 175 m below the Lowland plain (Cruden et al., 1997). In the Hines Creek watershed, abandoned shallow landslides were recognized within the postglacial lacustrine deposits, and dormant landslides were recognized within the till (Lu and Cruden, 2000). The 1990 Hines Creek

113

landslide is a reactivated and retrogressive earth slide with a rupture surface within the till, 76 m below the Lowland plains (Lu et al., 1998). In the Spirit River watershed dormant landslides were recognized within the till and abandoned landslides were recognized within the postglacial lacustrine deposit. The 1995 Spirit River landslide is a reactivated and retrogressive earth slide, with a rupture surface at the bottom of the till, 60 m below the Lowland plains. The 1990 Saddle River landslide is a reactivated and retrogressive earth slide, with a rupture surface within preglacial lacustrine sediment, 125 m below the Lowland plains (Cruden et al., 1993; Keegan, 1992).

As preglacial sediments are concentrated within the preglacial valleys, the distribution of large landslides with rupture surfaces within preglacial sediment is limited to the preglacial valleys. The Eureka River likely follows the Shaftesbury valley to near km 46 (Figures 3.2 and 5.1) (Kerr, 1971), thus landslides within each of the stratigraphic units can be expected, limited eventually by riverbed slope equilibrium. In contrast, the Montagneuse River flows across the Shaftesbury channel at almost a right angle (Cruden et al., 1997). The 1939 Montagneuse River landslide is near the north bank of the Shaftesbury valley, thus near the upstream extent of preglacial sedimentary landslides. Landslides in sediment further upstream will likely have rupture surfaces within the till or the postglacial lacustrine sediment. Reactivated or enlarged landslides in preglacial sediment could occur further downstream of the 1939 Montagneuse River landslide. Like the Montagneuse River, Hines Creek enters the Shaftesbury valley just upriver of the 1990 landslide (Cruden et al., 1997). The creek then follows the Shaftesbury valley for about 20 km, and exits the valley again 6 to 8 km upstream of the Peace River confluence (Carlson and Hackbarth, 1977). Landslides upstream of the 1990 Hines Creek landslides will likely have rupture surfaces within the till or the postglacial lacustrine sediment. The Spirit River parallels the south bank of the Shaftesbury channel, near the valley's rim, from the confluence with the Saddle River to approximately the site of the 1995 landslide (Carlson and Hackbarth, 1977). The depth to bedrock below the bottom of the Spirit River valley, along this section of river, is likely only a few metres. Landslides within preglacial sediment at the site of the 1995 landslide, or further upstream, are unlikely. The Saddle River flows within the its preglacial valley for most of its length until about 15 km from the Peace River confluence, where it flows into the Shaftesbury valley, and out again 7 to 8 km upstream of the Peace River confluence (Carlson and Hackbarth, 1977). Landslides with rupture surfaces within the preglacial fluvial sediment could potentially occur along the entire length of the river, with the exception of the lowest 7 to 8 km. Landslides

within preglacial lacustrine sediment, however, are limited to the upstream extent of preglacial lake flooding.

5.3 Valley Slopes and Landslides

The occurrence of landslides within different stratigraphic units is reflected in the gradient of the valley slopes. Figures 5.3 and 5.4 show the valley slopes of the Spirit and lower Saddle Rivers, and the Eureka and lower Clear Rivers respectively. Slope angles were extracted from topographic maps, where a topographic contour line crossed the stream, using one contour interval (10 m) above the stream (to avoid erroneous values due to the flood plain) to the contour just below the Lowland plain's level. The two graphs (Figures 5.3 and 5.4) are consistent in that the valley slope angles average between 7 and 12° downstream of the recent landslides, to near the Peace River. The slopes in both graphs also abruptly steepen upstream of the landslides, to an average of 18° to 19°. As the rupture surfaces of Spirit and Eureka River landslides are at the bottom of, and below (respectively) the till, the steeper slopes upstream of these landslides might be attributed to the till (i.e. the till can maintain steep valley slopes). Similar increases in the valley slopes were noticed upstream of the Saddle and Montagneuse River landslides (Cruden et al., 1993 and 1997). Upstream of the reach with steeper slope angles, the slope angles lessen in Figures 5.3 and 5.4, and at the Montagneuse River (Cruden et al., 1997). These lower slope angles are at least partially associated with the postglacial lacustrine sediments (i.e. these sediments are unable to maintain slope angles greater than 10°).

An increase in slopes is also seen near the Peace River (Figures 5.3 and 5.4). As the bottom 7 to 8 km of the Saddle River are incising into bedrock (Cruden et al., 1993), the increased valley slopes can be attributed to the rock. The same is also likely true at the mouth of the Clear River. In contrast, near the Peace River, a valley slope increase is not seen in the Montagneuse River, possibly because the Montagneuse River never fully exits the Shaftesbury valley.
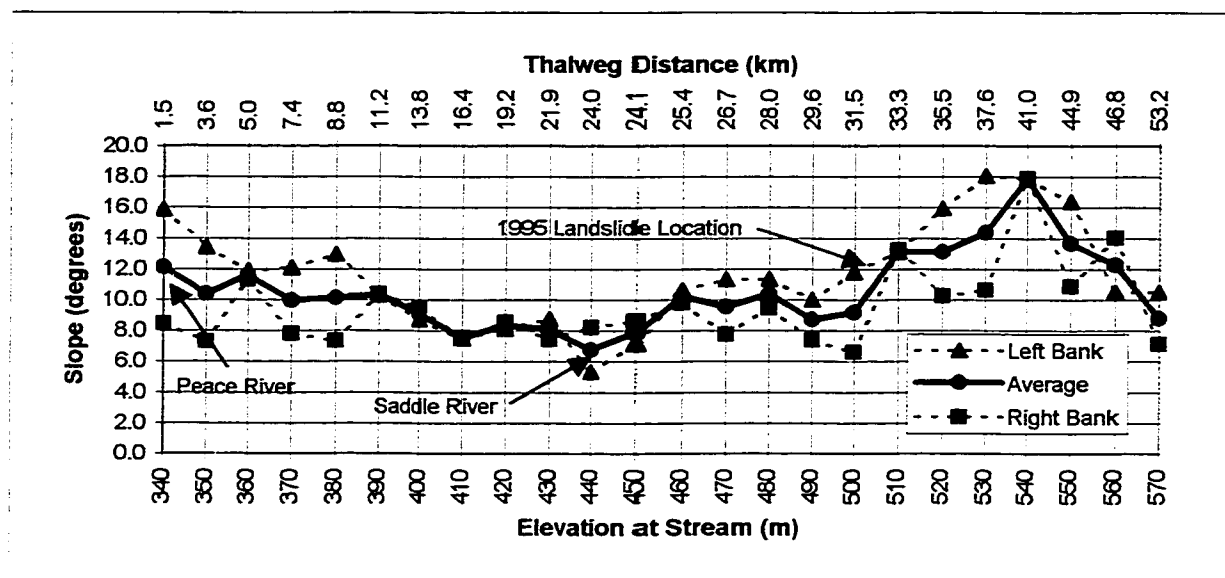
Figure 5.3: Valley slopes of the Spirit River and the Saddle River below the Spirit River confluence.
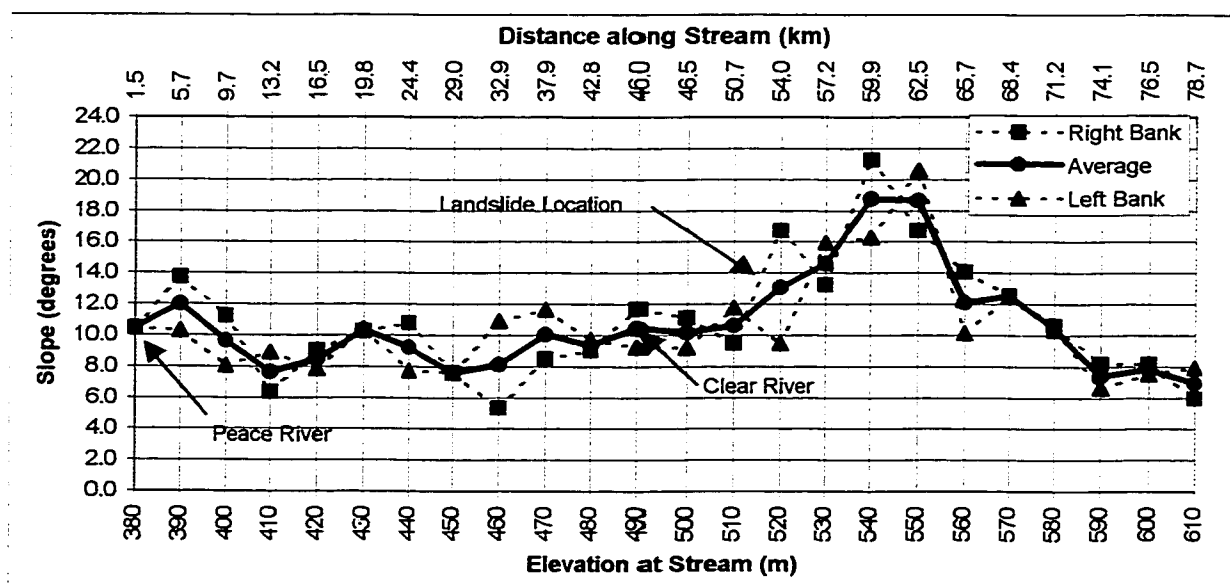
Figure 5.4: Valley slopes of the Eureka River and the Clear River below the Eureka River confluence.

5.4 Longitudinal Profiles and Landslide Activity

Postglacially, the Peace River rapidly incised. The tributaries of the Peace River were unable to keep pace with this rapid incision and thus partially developed convex-upward longitudinal profiles. Begin et al., (1981) showed that longitudinal convexity could develop following base level lowering. Longitudinal convex tributary streams are seen in other parts of Alberta, and also attributed to rapid main stem incision (Rains and Welsh, 1988; Rains et al., 1994).

With a longitudinally convex profile, the steeper downstream reach of the stream will have higher erosive potential, thus inducing over time an upstream migration of the break in slope (knickpoint) (Begin et al., 1981). Accompanying the upstream migration of the knickpoint, in the Peace River Lowlands, is an upstream progression of landslides. Bjerrum et al., (1969, p.535) coined the term "front of aggression" for this phenomenon.

The longitudinal profile of the Spirit River (Figure 5.5) can be characterized as having two contiguous reaches, a steeper lower reach (0.33°) where many large translational slides have occurred, and a gentle upper reach (0.15°) where smaller slides, mostly within postglacial sediment, have occurred. The 1995 landslide is located about 3 km downstream of the knickpoint. Indications of other dormant large landslides are visible on aerial photographs to near the knickpoint. A rise in valley slopes is seen at approximately the same location (Figure 5.5).

The longitudinal gradient of the Spirit River is convex to the Saddle River, indicating the Spirit River is a tributary of the Saddle River, and that the Saddle River is acting as the base level of the Spirit River. The progress of the front of aggression up the Spirit River was therefore delayed until after the front of aggression had reached the Spirit River confluence.

The longitudinal profile of the Saddle River can also be characterized as having two contiguous reaches, a steeper lower reach (0.26°) where many large translational slides have occurred, and a gentle upper reach (0.11°) with no large scale instability. The recent landslide is at least 10 km downstream of the break in slope between the lower and upper reaches (not shown in Figure 5.4).

The longitudinal profile of the Eureka River can also be divided into two contiguous reaches, a steeper lower reach (0.14°), and a gentler upper reach (0.08° dropping to 0.04° at the Lowland plain) (Figure 5.6). The break in slope between the lower and upper reach occurs 41 km upstream of the 1990 landslide, 11 km upstream of a large landslide within the postglacial

lacustrine sediment on highway 726 (Thurber, 1997 and 1998), and well beyond the rise in valley slopes located upstream of the 1990 landslide. The gradient of the Eureka River's steeper lower reach is approximately the same as those of the gentle upper slopes of the Saddle and Spirit Rivers and also the equilibrium lowest reach of the Montagneuse River (see below), suggesting that the profile could be near equilibrium. Large landslides can be seen on aerial photographs for approximately another 8 km upstream of the site of the 1990 landslide (Section 3.5).
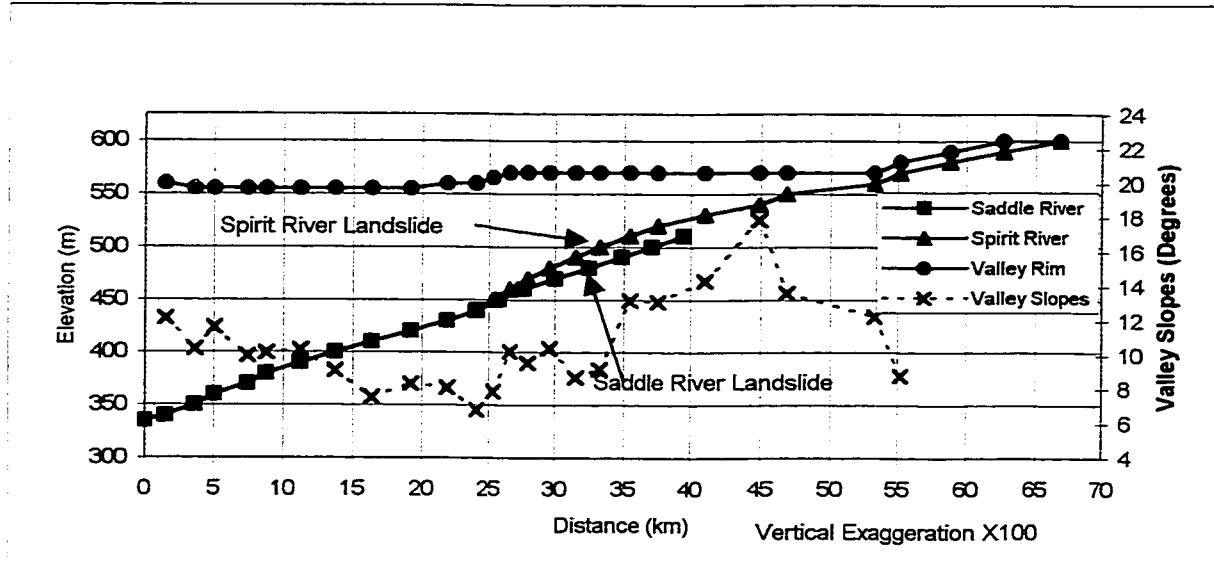
Figure 5.5: Longitudinal profiles of the lower Saddle River and Spirit River with average valley slopes indicated.
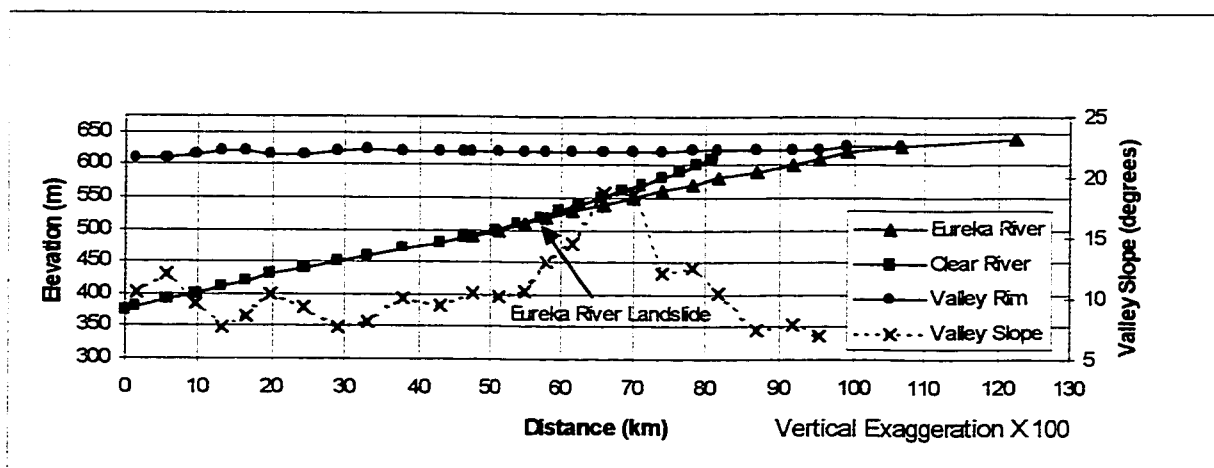
Figure 5.6: Longitudinal profiles of the lower Clear River and the Eureka River with average valley slope indicated.

In contrast, the Montagneuse River's longitudinal profile can be divided into three contiguous reaches: a gentle lower reach (0.1°) in which few or no landslides are presently occurring, a steeper intermediate reach (1.0°) where most of the large recent landslides have occurred, and a gentler upper reach (0.6° reducing to 0.2°) where no large scale instability has occurred (Cruden et al., 1997). "The boundary between ... [reach] two and three corresponds to the boundary of very frequent landsliding" (Cruden et al., 1997, p. 809). An increase in valley gradients is also seen approximately 1 km upstream of this boundary. Bjerrum et al., (1969) noticed a similar profile for the Hynna River, Norway and speculated that the lower reach was in equilibrium with the main channel, the River Romua (i.e. incision has ceased, thus curtailing landslide activity), the middle reach is actively downcutting and is prone to landslides, and the upper reach has yet to experience large scale instability.

An explanation for the three-reach profile of the Montagneuse River, as opposed to the two-reach profiles of the Eureka, Spirit and Saddle Rivers can be found in Begin et al., (1981). They conducted a series of experiments to characterize the development of longitudinal profiles of alluvial channels in response of base level lowering. Begin et al., (1981) found a three-reach profile would develop in flume experiments, as opposed to two-reach profiles when using a Rainfall-Erosion Facility (where the water was distributed to a container filled with sand, by nozzles, and a drainage net developed). The Montagneuse River has only one very small second order tributary, after it leaves the Clear Hills (there are also five very small, likely ephemeral, first order tributaries) thus it is comparable to the flume setting. Whereas the Eureka, Spirit and Saddle Rivers have drainage networks that could be described as dendritic, thus more represented by the Rainfall Erosion Facility experiments.

The stratigraphic heterogeneity present within the Peace River Lowlands complicates the longitudinal profiles of the tributary streams. As each stratigraphic unit is prone to instability, there could potentially be multiple fronts of aggression. The initial front of aggression will be associated with the postglacial lacustrine soil, following this will be a pause in landslide activity giving time for the till to soften, then there will be a second front of aggression associated with the till. The second front of aggression will be expressed as large translational landslides. Any subsequent fronts of aggression, associated with preglacial sediment, may be indistinguishable from the front of aggression associated with the till.

119

The longitudinal profiles are also potentially complicated by bedrock topography and type. The Saddle and Eureka rivers' longitudinal profiles will likely be least impacted by bedrock as both rivers flow mostly within preglacial valleys (Carlson and Hackbarth, 1974; Kerr, 1971). The Spirit River encountered bedrock at about 520 to 530 m.a.s.l. and again at about 610 m.a.s.l., well above the 1995 landslide (Carlson and Hackbarth, 1974). The Montagneuse River and Hines Creek flow across the Shaftsbury valley, thus their longitudinal profiles may be impacted more by bedrock.

5.5 Landslides and Tributary Geomorphology

The development of a tributary stream, within the western Peace River Lowlands that encroaches into the thick sedimentary deposits within the preglacial valleys, will involve a series of landslides of ever increasing volume and of ever increasing effect on stream processes.

Initial instability, within the postglacial lacustrine deposits, occurs when the degrading stream intersects weak layers within the deposit (Lu and Cruden, 2000). Postglacial lacustrine sediments mantle the entire Peace River Lowlands (Jones, 1966), so instability within this deposit will occur in any of the watersheds being considered. Landslides within this deposit are generally in the form of small earth slides and flows, though some larger earth slides were recognized in the Eureka River watershed. Small cuspate shaped scarps, seen in aerial photographs, indicate their occurrence. The depth of the landslides is generally less than 30 m (Lu and Cruden, 2000). Landslides within postglacial lacustrine sediment will likely have little impact on tributary morphology, though some streambed armouring will occur (from dropstones in the glacial lacustrine sediments). Following incision through the postglacial lacustrine deposit, landslides within this deposit become dormant, then abandoned. The postglacial lacustrine material may again be destabilized, if the bank is undercut by river erosion, or when deeper-seated landslides oversteepen the slope (i.e. at a main scarp).

Landslides within the till occur following stream incision into till. The Spirit River and Hines Creek landslides are examples of this phenomenon. The Spirit River and Hines Creek landslides are large translational earth slides, with depth of rupture surfaces of 60 m (Section 2.6.5) and 76 m (Lu et al., 1998) respectively. The till is stiff, and can maintain steep valley slopes (Figures 5.3 and 5.4). The main scarp can be set back some distance from the steeper lower valley slope (maintained by the till), thus a large pre-to post-landslide drop in valley slope angle can be

120

observed. At the Spirit River landslide site, the valley slope angle dropped from 9.2° to 6.9° due to the landslide.

Landslides in till may have a significant impact on stream morphology as landslide dams may form (Lu et al., 1998; Section 2.7). The landslide dam at Hines Creek is a type 6 dam (Lu et al., 1998) (one or more rupture surfaces that extend under the stream or river valley and emerge on the opposite valley side from the landslide (Costa and Schuster, 1988)). Multiple dams were formed by the 1995 Spirit River landslide, most being of type 6. Lacustrine sediments collect behind these landslide dams, which enhances slope toe support (Lu and Cruden, 2000). The longevity of the dams is generally only a few years. In Hines Creek, the stream cut a new channel around the toe of the landslide (Lu et al., 1998), thus potentially destabilizing the opposite valley wall. Lu and Cruden (2000) partially attribute the cause of the 1990 Hines Creek landslide to the slope's toe being undercut following a landslide of the opposite valley wall. The post-landslide channels of Hines Creek and Spirit River avoided the pre-landslide streambed armour, thus enhancing erosion. After the landslide dam has been eroded through, the lacustrine deposits behind the dam are quickly remobilized (Lu and Cruden, 2000). This cycle may be repeated several times until incision into the underlying stratigraphy; upon which, landslides within the till become dormant and then abandoned (Lu and Cruden, 2000). By this time the delivery of a substantial amount of coarse material to the stream can be assumed.

Upon incision into the underlying preglacial sediment, landslides then become associated with these materials. The 1990 Eureka and Saddle River, and 1939 Montagneuse River landslides are examples of this phenomenon. These landslides are all large translational earth slides with rupture surfaces within preglacial lacustrine soil. The residual friction angle of the preglacial lacustrine sediment is low. The residual friction angles from the Montagneuse and Saddle River landslides, for this material, are between 6° and 10° (Cruden et al., 1997 and 1993 respectively). Valley slope angles for rivers incising into the preglacial sediment range between 6° and 12° (Cruden et al., 1997; Figures 5.2 and 5.3).

The rupture surface of the Eureka River landslide extended 20 to 25 m below the valley bottom, creating a type 6 landslide dam. The Saddle and Montagneuse River landslides created dams in much the same manner. The landslide dam at the Eureka River formed a reservoir 8 km in length; the Saddle River's reservoir was 4 km long. Upon overtopping, all three rivers cut new channels around the toes of the landslides, potentially destabilizing the opposite valley walls. As

121

the new channels were free of bed armour, incision was rapid (for example, 20 m in 9 years at Eureka River). Elevated remnants of the original channels can be seen at all three landslides. At the Eureka River landslide, the banks of the new channel are steep, and instabilities (flows and slides) adjacent to the channel are frequent. The instability at the toe of the Eureka River landslide is consuming remnants of the original channel, thus reintroducing coarse alluvium into the new channel. The alluvium is not stable in the channel, and very little remains where it fell. Presumably the alluvium was carried downstream until it encountered undisturbed bed armour, or some other obstruction. This has left the channel very susceptible to erosion, potentially to a lower elevation than before the landslide had occurred. Both the Eureka and Saddle River dams still exist, and a substantial amassment of lacustrine sediments behind the dams can be assumed. Once the reservoirs have drained, a downstream flux of the lacustrine sediments could be expected. This cycle may be repeated.

5.5 Conclusions

1. In the last 60 years, five major landslides within the Peace River Lowlands have occurred, all of which are located within preglacial valleys.

2. The landslides on the Spirit River and Hines Creek had their rupture surfaces within till. The Eureka, Saddle, and Montagneuse River landslides had their rupture surface within preglacial lacustrine sediment. Other large landslides were seen near or downstream of these five recent large landslides. Smaller landslides were seen in the Eureka, Montagneuse, and Spirit River, and Hines Creek watersheds upstream of the recent landslides, most with rupture surfaces within postglacial lacustrine sediment.

3. The valley slope angles increase upstream of the landslide.

4. All five recent landslides occurred in the steepest reach of the convex streams.

5. As each sedimentary unit is eroded through by the river, landslide activity within that unit becomes dormant. Landslide activity then becomes associated with the next lower sedimentary unit.

6. The impact of the landslides on fluvial processes depends on the sedimentary unit in which the landslide's rupture surface is located. Landslides with rupture surfaces in the uppermost postglacial lacustrine unit have little impact on stream processes. Landslides with rupture surfaces in successively lower depositional units have progressively greater impacts on stream processes, as landslide dams form.

References

Begin, Z.B., Myer, D.F. and Schumm, S.A. 1981. Development of longitudinal profiles of alluvial channels in response to base-level lowering. Earth Surface Processes and Landforms, 6: 49-68.

Bjerrum, L., Loken, T., Heiberg, S. and Foster, R., 1969. A field study of factors responsible for quick clay slides. Proceedings, 7th International Conference on Soil Mechanics and Foundation Engineering, Mexico City, 2: 531-540.

Carlson, V.A. and Hackbarth, D.A. 1974. Bedrock topography of the Grande Prairie Area, NTS 83 M, Alberta. Alberta Research Council Map, 1:250,000, Edmonton.

Catto, N.R. 1991. Quaternary geology and landforms of the eastern Peace River region, British Columbia NTS 94A/1,2,7,8. British Columbia Ministry of Energy, Mines and Petroleum Resources, Open File 1991-11, Victoria.

Costa, J.E. and Schuster, R.L., 1988. The formation and failure of natural dams. Geological Society of America Bulletin, 100:1054-1068.

Cruden, D.M., Keegan, T.R. and Thomson, S., 1993. The landslide dam on the Saddle River near Rycroft, Alberta. Canadian Geotechnical Journal, 30:1003-1015.

Cruden, D.M., Lu, Z.Y. and Thomson, S., 1997. The 1939 Montagneuse River landslide, Alberta. Canadian Geotechnical Journal, 34:799-810.

Hackbarth, D.A. 1977. Hydrogeology of the Grande Prairie Area. Alberta Research Council, report 76.4, Edmonton.

Jones, J.F. 1966. Bedrock Geology of the Peace River district. Research Council of Alberta, bulletin 16, Edmonton.

Keegan, T.R. 1992. The Rycroft landslide dam on the Saddle River, Alberta. Master of Science thesis, Department of Civil Engineering, University of Alberta, Edmonton.

Kerr, H.A. 1971. Groundwater study Worsley area. Water Resources Division, Soil Geology and Groundwater Branch, Edmonton.

Lu, Z.Y., and Cruden, D.M., 2000. Fluvial Processes and Landslide Activity in the Western Peace River Lowlands, Alberta, Canada. Proceedings, 8th International Landslide Symposium, Cardiff, Wales. Thomas Telford, 2: 955-960 London.

Lu, Z.Y., Cruden, D.M. and Thomson, S., 1998. Landslides and preglacial channels in the western Peace River Lowland, Alberta. Proceedings, 51st Canadian Geotechnical Conference, Edmonton, Vol.1, pp.267-274.

124

Ozoray, G. 1982. Hydrogeology of the Clear Hills-Chinchaga River area, Alberta. Alberta Research Council, Edmonton, Earth Sciences-Report 82-4.

Pawlowicz, J.G. and Fenton, M.M. 1995. Bedrock topography of Alberta. Alberta Geological Survey, Map 226, Edmonton.

Rains, R.B., and Welsh, J. 1988. Out-of-phase Holocene terraces in part of the North Saskatchewan River basin, Alberta. Canadian Journal of Earth Sciences, 25: 454-464.

Rains, R.B., Burns, J.A., and Young, R.R. 1994. Postglacial alluvial terraces and an incorporated bison skeleton, Ghostpine Creek, southern Alberta. Canadian Journal of Earth Sciences, 31: 1501-1509.

Thurber Engineering Ltd. 1997. Eureka River Crossing (of highway 726) Site 1. Survey and drill core data (97-2, 97-3). Thurber Engineering, Edmonton.

Thurber Engineering Ltd. 1998. Eureka River Crossing (of highway 726) Site 2. Survey and drill core data (98-1, 98-2). Thurber Engineering, Edmonton.

6.0 Conclusions

The June 1990 Eureka River landslide and July 1995 Spirit River landslide are two, of at least five, major landslides that have occurred in natural settings within the Peace River Lowlands of Alberta, in the last 60 years. The other three landslides include the 1990 Hines Creek landslide (Lu et al., 1998), the 1939 Montagneuse River landslide (Cruden et al., 1997), and the 1990 Saddle River landslide (Cruden et al., 1993). A sixth landslide, the Vessall Creek landslide (1993 to 1997), was excluded from this study due to lack of detailed information. All five of the landslides are composed entirely of Quaternary sediment, and are located within preglacial valleys.

The June 1990 Eureka River landslide was an enlarged, multiple, wet, earth slide, with a rupture surface within preglacial lacustrine sediment. The estimated volume of the landside is 18.9 to 54.4 Mm^3. The July 1995 Spirit River landslide was a reactivated and retrogressive, or enlarged, multiple, wet, earth slide, with a rupture surface within the till. The estimated volume of the landside is 10.4 to 31.1 Mm^3.

All of the recent landslides created predominantly class 6 landslide dams (Costa and Schuster, 1989). The most upstream dam on the Spirit River, at km 9.8, was approximately 9 m in height, and created a reservoir approximately 2100 m in length. By July 1999, this reservoir was approximately 700 m length. The landslide dam on the Eureka River was, at its maximum, 20 to 23 m in height, creating a reservoir exceeding 8000 m in length. By August 1999, this reservoir was 1800 m long, which corresponds to reduction in depth of approximately 16 m. The gradual erosion of the landslide dam and subsequent drainage of the reservoir, as opposed to rapid failure, appears usual in the Peace River Lowlands. Thus the hazard to people and structures downstream of the dams, from a dam breach, is mitigated. Nonetheless, as large volumes of water are impounded behind these dams, their condition should be periodically assessed.

Landslides with rupture surfaces within postglacial lacustrine sediment, till, and preglacial lacustrine and fluvial sediments, have been recognised in the Peace River Lowlands. As a tributary stream incises into each subsequent sedimentary unit, landslide activity becomes associated with that unit. Landslides with rupture surfaces within postglacial lacustrine sediment are often small earth slides or earth flows. Landslides with rupture surfaces within till, or preglacial sediments, are mostly large translational earth slides, thus are potentially disastrous to

126

infrastructure traversing the tributaries. Valley slopes steepen and longitudinal slopes lessen upstream of the large translational earth slides, thus infrastructure should be situated some distance upstream of these features. Locating infrastructures in areas that have previously slid is ill advised, as these slopes are prone to reactivation.

With the exception of the 1939 Montagneuse River landslide (Cruden et al., 1993), all of the recent landslides occurred within the last decade. The Spirit River, Saddle River, and Hines Creek landslides consumed valuable farmland. As the Peace River Lowlands have seen continuous growth in agriculture for several decades prior to the landslides, agricultural land clearing as a factor causing the landslides was explored, but no causal relationship was found. Triggering of the recent landslides by earthquakes was likewise rejected. The most likely trigger for the recent landslides is above average precipitation, thus making prevention difficult.

Future work should include locating preglacial valleys thus identifying high risk zones to infrastructure. The geomorphology of tributary streams in the Peace River Lowlands might also be further defined to better anticipate the landslide hazard. Included in this definition, are issues concerning the expression of bedrock topography in the longitudinal profiles of the tributary streams, and the factors controlling the progress of the front of aggression, that need further consideration.

References

Costa, J.E. and Schuster, R.L., 1988. The formation and failure of natural dams. Geological Society of America Bulletin, 100:1054-1068.

Cruden, D.M., Keegan, T.R., and Thomson, S. 1993. The Landslide Dam on the Saddle River near Rycroft, Alberta. Canadian Geotechnical Journal, 30: 1003-1015.

Cruden, D.M., Lu, Z-Y., and Thomson, S. 1997. The 1939 Montagneuse River landslide, Alberta. Canadian Geotechnical Journal, 34: 799-810.

Lu, Z.Y., Cruden, D.M., and Thomson, S. 1998. Landslides and Preglacial Channels in the Western Peace River Lowland. Proceedings, 51st Canadian Geotechnical Conference, Edmonton, Alberta, 4-7 October, 1: 267-274.

Appendix 1: Publicly Available Aerial Photographs of the Spirit River

Date	Project #	Role #	Photo #	Scale	True Scale	Emulsion	Source	Reviewed	Coverage	Comments
95-09-13	95-97A	AS4680	27-35 71-75	40,000	41,105	B/W AFGA	Alberta Air Photo Library	YES	km 0-25	Slide @ 31-33
89-00-00	89-120A	AS3895	92-100	30,000	31,132	B/W 2405	Alberta Air Photo Library	YES	km 0-25	Slide @96-98
88-00-00	88-209	AS3749	69-75	40,000		B/W AFGA	Alberta Air Photo Library	YES	km 0-25	
85-05-09	85-123			60,000		B/W 2405	Alberta Air Photo Library	NO		
84-07-24	84-6	AS3066	35-43	30,000		B/W 2405	Alberta Air Photo Library	YES	km 0-25	
81-08-08	81-50			60,000		PAN 2405	Alberta Air Photo Library	NO		
79-07-04	79-32IR	AS1996	214-229	15,000		IR 2424	Alberta Air Photo Library	YES	km 0-25 South	Slide @ 222-224
		AS1997	62-69	15,000		IR 2424	Alberta Air Photo Library		km 9-19 North	
74-08-25	74-50	AS1346	108-112	50,000		IR 2424	Alberta Air Photo Library Cameron Library	YES	km 0-25	Slide @ 110-111
70-07-16	70-322 83M	AS1112	294-296	80,000		PAN 2405	Alberta Air Photo Library Cameron Library	YES	km 0-28	Slide @ 294-295
67-00-00	6706-26-667	5519-6752	004-001	31,680		UNKNOWN	Cameron Library	YES	km 0-9	Slide @ 1-2
67-00-00	67-83M	AS972 5519	85-89	31,680		UNKNOWN	Alberta Air Photo Library	YES	km 0-25	
61-00-00	C61.18-607	5518 YC 490	59-57 56-53	31,680		UNKNOWN	Cameron Library	YES	km 5-13 km 17-28	Slide @ 58-59
		5519 YC 360	37-33 98-96	31,680		UNKNOWN	Cameron Library	YES	km 8-21 km 0-6	
61-00-00	61-83M	AS802	139-136	31,680		UNKNOWN	Alberta Air Photo Library	YES	km 0-11	Slide @ 136-137
54-00-00		A14251	45-52	40,000		UNKNOWN	Cameron Library	YES	km 0-25	Slide @ 47-48
52-00-00	162A	5532-2367-52	76-68	15,840		UNKNOWN	Cameron Library	YES	km 0-9.5	Slide @ 69-71
51-00-00	51-83M			15,840		SUPER XX	Alberta Air Photo Library	NO		
50-00-00	160	A12899	320-327	40,000		UNKNOWN	Cameron Library	YES	km 0-28	Slide @ 322-323
49-00-00	49-83M			40,000		SUPER XX	Alberta Air Photo Library	NO		
45-00-00		A8765	22-13	15,840		UNKNOWN	Cameron Library	YES	km 0-10.5	Slide @ 14-16
		A8099	79-84 78-75	15,840		UNKNOWN	Cameron Library	YES	km 9-17.5 km 17-22	

130

Appendix 2: **Publicly Available Aerial Photographs of the Eureka River**

Date	Project #	Roll #	Photo #	Scale	True Scale	Emulsion	Source	Reviewed	Coverage	Comments
98-05-01	98-062	AS4917	43-45; 33-37; 23-27	20,000	20,030	KODAK DX	Alberta Air Photo Library	YES	km 0-10	Slide @ 35-36
97-09-01	97-159	AS4892	103-106; 145-150; 171-177	30,000		AGFA 200	Alberta Air Photo Library	YES	km 0-35	Slide @ 146-147
92-00-00	92-158	AS4333	175-184; 101-102; 260-270	20,000		PAN 150	Alberta Air Photo Library	YES	km 0-35	Slide @ 178-179
89-04-27	89-100	AS3867	64-67; 92-99; 121-129	20,000	21,114	PAN 2405	Alberta Air Photo Library	YES	PARTIAL	Slide @ 94-95
89-00-00	89-183			20,000		IR 2424	Alberta Air Photo Library	NO	PARTIAL	
87-05-16	87-094	AS3579	14-16; 65-70; 121-128	30,000		PAN 2405	Alberta Air Photo Library	YES	km 0-35	
84-06-22	84-102	AS3058	8-10; 135-140	60,000		PAN 2402	Alberta Air Photo Library	YES	km 0-35	
83-06-16	83-131			15,000		IR 2424	Alberta Air Photo Library	NO		
80-05-04	80-122	AS 2187	162-164	60,000		PAN 2405	Alberta Air Photo Library	YES		Slide @ 162-164
78-06-00	78-52	AS1815	127-130; 233-237	15,000		IR 2424	Alberta Air Photo Library	YES	km 0-3; km 3-7	
		AS1816	24-28; 195-202	15,000		IR 2424	Alberta Air Photo Library	YES	km 7-12; km 18-28	Slide @ 24-26
		AS1959	185-190	15,000		IR 2424	Alberta Air Photo Library	YES	km 11-18	
74-08-14	74-50IR	AS1349	10-12; 98-103	50,000		IR 2424	Alberta Air Photo Library Cameron Library	YES	km 0-9; km 5-35	Slide @ 98-99
71-06-12	71-89	AS1150	119-120; 171-175; 223-229;	31,680		PAN 2405	Alberta Air Photo Library Cameron Library	YES	km 0-6; km 5-18; km 12-35	Slide @ 171-172
66-09-12	6616	26 966 5609 R145	13-15	31,680		Unknown	Cameron Library	YES	km 0-6	
66-09-12	6616	26 966 5610 R145	14-18; 20-22	31,680		Unknown	Cameron Library	YES	km 5-18; km 30-35**	Slide @ 15-16
66-00-00	66-84D	AS927	84-89	31,680		Unknown	Alberta Air Photo Library	YES		Slide @ 85-86
60-00-00	60-84D			31,680		Unknown	Alberta Air Photo Library	NO		
60-09-12	2908	5608 221 5609 225	107-113; 72-75	31,680		Unknown	Cameron Library	YES	km 0-18; km 17-29	Slide @ 15-16
58-02-06	YC 46		97-100; 85-89; 69-72; 52-56; 39-41; 24,26	31,680		Unknown	Cameron Library	YES	km 0-8; km 5.5-14; km 11-20; km18-27; km 24-32; km 31-35*	Slide @ 85-89; Flown N-S
54-00-00		A14259	13-18; 20-24	40,000		Unknown	Cameron Library	YES	km 0-18; km 27-35	Slide @ 14-15
51-00-00	51-84D	AS246	89-92	15,840		SUPER XX	Alberta Air Photo Library	YES	km 0-3	
		AS244	117-120	15,840		SUPER XX	Alberta Air Photo Library	YES	km 3-11	
		AS239	175-176	15,840		SUPER XX	Alberta Air Photo Library	YES	km 11-18	
50-00-00	160	A13222 or 5608 1987	44*	40,000		Unknown	Cameron Library	YES	km 0-12	
	160	5608/09B 2064	82-89	40,000		Unknown	Cameron Library	YES	km 6-35	Slide @ 82-83
49-00-00	49-84D	AS92-5607	54-57	40,000		SUPER XX	Alberta Air Photo Library	YES	km 0-35	
		AS92-5608	244-252	40,000		SUPER XX	Alberta Air Photo Library	YES	km 0-35	

45-00-00 to 48-00-00		A8348	81-79	15,840		Unknown	Cameron Library	YES	km 0-5	
		A8304	55-52	15,840		Unknown	Cameron Library	YES	km 3-7	
		A8303	53-63	15,840		Unknown	Cameron Library	YES	km 6-17 South	Slide @ 54-56
		A8143	74-65	15,840		Unknown	Cameron Library	YES	km 11-21 North	
		A8142	68-80	15,840		Unknown	Cameron Library	YES	km 18-35 North	
		A8143	60-56	15,840		Unknown	Cameron Library	YES	km 28-35 South	

Notes: * No Stereo Coverage Available
           **Incomplete Coverage

.

.

.

.